

HU ISSN 1785-6892 in print
HU ISSN 2064-7522 online

DESIGN OF MACHINES AND STRUCTURES

A Publication of the University of Miskolc

Volume 10, Number 2 (2020)



Miskolc University Press
2020

EDITORIAL BOARD

- Á. DÖBRÖCZÖNI
Editor in Chief
Institute of Machine and Product Design
University of Miskolc
H-3515 Miskolc-Egyetemváros, Hungary
machda@uni-miskolc.hu
- Á. TAKÁCS
Assistant Editor
Institute of Machine and Product Design
University of Miskolc
H-3515 Miskolc-Egyetemváros, Hungary
takacs.agnes@uni-miskolc.hu
- R. CERMAK
Department of Machine Design
University of West Bohemia
Univerzitní 8, 30614 Plzen, Czech Republic
rcermak@kks.zcu.cz
- B. M. SHCHOKIN
Consultant at Magna International Toronto
borys.shchokin@sympatico.ca
- W. EICHLSEDER
Institut für Allgemeinen Maschinenbau
Montanuniversität Leoben,
Franz-Josef Str. 18, 8700 Leoben, Österreich
wilfrid.eichlseder@notes.unileoben.ac.at
- S. VAJNA
Institut für Maschinenkonstruktion,
Otto-von-Guericke-Universität Magdeburg,
Universität Platz 2, 39106 Magdeburg, Deutschland
vajna@mb.uni-magdeburg.de
- P. HORÁK
Department of Machine and Product Design
Budapest University of Technology and Economics
horak.peter@gt3.bme.hu
H-1111 Budapest, Műegyetem rkp. 9.
MG. ép. I. em. 5.
- K. JÁRMAI
Institute of Materials Handling and Logistics
University of Miskolc
H-3515 Miskolc-Egyetemváros, Hungary
altjar@uni-miskolc.hu
- L. KAMONDI
Institute of Machine and Product Design
University of Miskolc
H-3515 Miskolc-Egyetemváros, Hungary
machkl@uni-miskolc.hu
- GY. PATKÓ
Department of Machine Tools
University of Miskolc
H-3515 Miskolc-Egyetemváros, Hungary
patko@uni-miskolc.hu
- J. PÉTER
Institute of Machine and Product Design
University of Miskolc
H-3515 Miskolc-Egyetemváros, Hungary
machpj@uni-miskolc.hu

CONTENTS

<i>Cabezas, Sebastian – Szilágyi, Attila:</i> Thermal behavior in CNC machine-tools.....	5
<i>Cabezas, Sebastian – Szilágyi, Attila:</i> Thermal and structural simulations of a CNC turning center.....	11
<i>Derekas, Csaba – Kiss, Dániel:</i> Development of desktop 3D printer	20
<i>Ficzere, Péter – Lukács, László Norbert:</i> Examination of possibilities of the strength modification in the case of FDM/FFF manufacturing technology	27
<i>Kapitány, Pálma – Lénárt, József:</i> Designing of a BLDC motor bench.....	35
<i>Kiss, Dániel – Mihályi, Gergő:</i> Conceptual cutting tool design for internal thread turning	41
<i>Kiss, Róbert – Szilágyi, Attila:</i> Analysis of DMU40 machine centre by finite degrees of freedom	49
<i>Kiss, Róbert – Szilágyi, Attila:</i> Analysis of DMU40 machine centre by CAE software	54
<i>Kiss, Róbert – Szilágyi, Attila:</i> Analysis of DMU40 machine centre by vibration measurement.....	59
<i>Kmetz, Barbara – Takács, Ágnes:</i> Demand for recycling filament in 3D printing	65
<i>Kovács, Endre – Saleh, Mahmoud:</i> Drag coefficient calculation of modified Myring- Savonius wind turbine with numerical simulations	73
<i>Mohammad, Al-zgoul – Szilágyi, Attila:</i> Dynamical Simulation Of A Cnc Turning Center (Survey Paper)	85
<i>Mohammad, Al-zgoul – Szilágyi, Attila:</i> Dynamical simulation of a CNC turning center	91
<i>Pintér, Ádám – Sarka, Ferenc:</i> Research into the uses of sandblasting waste	97
<i>Soltész, László – Kamondi, László – Berényi, László:</i> Product development from ecodesign point of view in practice	106

<i>Soltész, László – Kamondi, László – Berényi, László:</i> Project management success factors: in search of product development project specialities.....	114
<i>Szabó, Kristóf – Hegedűs, György:</i> Brief overview of generative design support software.....	123
<i>Szilágyi, Attila – Kiss, Dániel:</i> The methods of numerical mechanics for the improvment of machine-tools	133
<i>Thomas, Wallyson – Fülöp, Zsombor – Szilágyi, Attila:</i> Comparison between a conventional and an antivibrating boring bar in the internal turning of long overhangs	145
<i>Thomas, Wallyson – Fülöp, Zsombor – Szilágyi, Attila:</i> Evaluating CBN tool life in hardened boring operations in long overhangs.....	150
<i>Tóth, Sándor Gergő – Takács, György:</i> Introduction of active and passive control options for hydrostatic pressure chambers	155
<i>Tóth, Sándor Gergő – Takács, György:</i> Examination of machine tool slideway combined with pressure chambers	160
<i>Trautmann, Laura – Piros, Attila – Rádics, János Péter – Jakab, Ivett – Badak-Kerti, Katalin:</i> A new method for production development.....	165

THERMAL BEHAVIOR IN CNC MACHINE-TOOLS

SEBASTIAN CABEZAS – ATTILA SZILÁGYI

University of Miskolc, Department of Machine Tools
3515 Miskolc-Egyetemváros
sebascabezas1@gmail.com

Abstract: This article describes errors in machine-tools focusing on thermal errors. The internal and external heat sources in machine tools. The basic concepts of heat transfer and an introduction to Finite Element Method FEM applied to heat transfer.

Keywords: *machine-tools, heat sources, heat transfer, manufacturing errors, Finite Element Method*

1. INTRODUCTION

Thermal behaviors in machine tools are from many years the case of study in universities and manufacturing companies. Effects related with thermal deformation in machine tools can influence the accuracy of the manufactured pieces. It lays on how precise are the movements between the machine tool and the workpiece. If the deformations overlap the established tolerances, the workpieces will require more machining process and it will increase the cost of production.

The most relevant part of disturbance in the production systems and production processes are related with the loss of energy, which is transformed in heat energy. Part of this energy will be transferred to the machine-tool and workpiece and the other part to the surroundings. The transfer of energy provokes the thermal deformations in the process.

The machine tool's heat behavior is determined by the output of the heat sources, primarily shown as power losses in the friction nodes and electric motors located within the structure, the increase in the temperature of the machine tool components at certain points, the temperature distribution, the thermal deformations of the load bearing system, and the mutual displacements of the assemblies [1].

2. ERRORS

The deviation of the measured value (assumed) from its true value is called error. There are two kinds of errors:

- Random errors.
- Systematic errors.

Random errors have a relation with the precision of results and are treated statistically. The magnitude of the random error is analyzed from the results of a set of

repeated measurements. Systematic errors occur at every measurement in the same way and cannot be analyzed by examining the results.

Theoretically, the measured value $x_{measured}$ from an instrument must be identical to the true value x_{true} [1].

$$X_{true} = X_{measured} + Error \quad (1)$$

2.1. Main errors related with machine tools

Errors in machine tools that are described in this section are studied and analyzed in the field of precision engineering manufacturing due to the importance in the performance of the machine and in the final results in the products created in different kind of machine tools.

Motion errors

Usually a machine-tool, depending on the application can perform movements in 3D space. Three translational movements along the axis x, y, z and three rotational movements pitch, yaw and roll respectively about x, y, z.

Translational errors

Generated by geometric deformations, design or physical properties that can produce the next effects:

- Positioning errors.
- Straightness of each axis in ITS perpendicular axes.
- Abbé error.
- Reversal errors.
- Backlash errors.
- Flatness error.
- Orthogonality error between two axes.
- Friction and stick slip motion errors.
- Parasitic movements.
- Inertia force errors in transient movements (braking/accelerating).

Rotational errors

In spindles and chucks can occur deviation from the datum point. Angular deviation and radial displacements can occur about x, y and z axis.

Associated errors with rotational motion are:

- Out-of-round.
- Eccentricity.
- Radial throw of an axis at a given point.
- Spindle radial deviation.
- Spindle axial deviation.

- Spindle inclination.
- Pitch, roll, yaw angular errors.

Geometric errors

Constitute a large source of inaccuracy, due to design, built-in during assembly, tolerance of components used on the machine.

Thermal errors

Thermal errors of machine tools are one of the main contributors for geometrical inaccuracies of machined workpieces and deformations [1].

Thermal errors account for 70% of the total dimensional and shape errors in machines. This type of errors have either a dynamic or quasistatic behavior. Related with cost, it is more effective to compensate thermal errors rather than using expensive and high-precision components for the machine construction.

3. INTERNAL AND EXTERNAL HEAT SOURCES IN MACHINE TOOLS

Internal heating sources are related with the inner machine components that belong to the part of the machine such as:

- Bearings.
- Linear electric motors.
- Servomotors.
- Belts and chains.
- Hydraulic systems.
- The material used for the construction of different parts of the machine.
- Linear and rotational rail guides.
- Caged ball motion blocks.

External heating sources are related with the environment and the surrounding influences exerted over the machine-tool. These external heating sources are:

- Temperature distribution (vertical/horizontal).
- Temperature fluctuations (day, night, seasons of the year).
- Air conditioning systems inside the workshops.
- Air currents.
- Thermal memory for a previous environment.
- The shop floor environments where the machine is located.
- Meteorological factors.

Temperature controlled environments require high capital investments and running costs. Which are undesirable and impractical in some cases [2].

4. HEAT TRANSFER IN MACHINE TOOLS

The thermal behavior of a machine tool during its operating condition and the influence on machining accuracy depends on the heat exchange between the machine tool and the environment, the heat transfer within the housings and the load-bearing structure of the machine tool.

Accumulation of large quantities of heat close to intensive heating sources in the machine tool may affect its geometrical accuracy. This means that heat transfer conditions should be rationally shaped during the design. Using a heat model based on FEM and running numerical simulations of the heating up and deformation of the machine tool, one can design optimum heat transfer model by selecting materials with favorable thermal conductivity and creating proper conditions of heat transfer through the joints between the machine tool components and housings, through natural convection or forced convection by the linear or rotary motion elements, and through controlled heat abstraction by cooling overhead places [1].

4.1. Heat transfer modes

Heat transfer studies the energy transport between material bodies due to temperature difference [3]. The three modes of heat transfer are:

- Conduction.
- Convection.
- Radiation.

Conduction occurs due to the exchange of energy from one molecule to another without motion of the molecules, or it can be due to the motion of free electrons. This mode of heat transport depends on the properties of the medium and takes place on solids, liquids and gases. Molecules that are present in liquids and gases can move freely from hot to a cold region. During the motion, the molecules carry energy with them.

The transfer of heat from one region to another due to the macroscopic motion in liquids and gases is called heat transfer by convection. Convection may be free, forced or mixed. Natural or free convection occurs due to a density variation caused by temperature differences. Forced convection occurs when energy is transferred to the fluid by an external force (fans, pumps, blowers, etc.). Mixed convection occur when natural and forced convection are present.

Radiation does not require a material medium for heat transfer to occur. The propagation of energy is carried out by electromagnetic waves. When the electromagnetic waves strike other body surface, one part is reflected, another part is transmitted and the other part is absorbed.

All the materials can emit thermal radiation at all temperatures [2].

4.2. Heat transfer laws

To quantify the energy transferred per unit time is needed to apply rate equations. For heat conduction the heat transfer equation known as the Fourier's equation quantifies the amount of energy transferred per unit time per unit area.

$$q_x = -k \frac{dT}{dx} \quad (2)$$

Where:

- q_x Represents the heat flux in one dimension (W/m^2).
- k The thermal conductivity that is a material property of the body (W/mK).
- dT/dx The temperature gradient (K/m).

Heat convection follows Newton's law of cooling.

$$q = h(T_w - T_\alpha) \quad (3)$$

Where:

- q Represents the heat flux (W/m^2).
- $(T_w - T_\alpha)$ Temperature difference between the surface of a body and the fluid.
- h Heat transfer coefficient (W/m^2K).

In heat conduction through solids, the heat transfer coefficient appears as a boundary condition in the solution of heat conduction through solids.

Flux that can be emitted by radiation from a black surface is given by the Stefan–Boltzmann Law.

$$q = \sigma(T_w^4) \quad (4)$$

Where:

- q Represents the radiative heat flux (W/m^2).
- σ Stefan–Boltzmann constant 5.669×10^{-8} (W/m^2K^4).
- T_w Surface temperature.

The increase of energy in a system is equal to the difference between the energy transfer by heat to the system and the energy transfer by work done on the surroundings of the system.

$$E = dQ - dW \quad (5)$$

- Q Total heating entering the system.
- W The work done by the surroundings.

The rate of energy transfer is expressed by the equation:

$$\frac{dE}{dt} = \frac{dQ}{dt} - \frac{dW}{dt} \quad (6)$$

5. FINITE ELEMENT METHOD FOR HEAT TRANSFER

The finite element method is a numerical tool for determining approximate solutions to a large class of engineering problems. In the finite element method, the actual continuum or body of matter (solid, liquid, or gas), is represented as an arrangement of subdivisions called finite elements.

Elements are interconnected at specified joints. Since the variation of the field (displacement, stress, temperature, velocity, pressure) inside the continuum is not known, assuming that the variation of the field variable inside a finite element can be approximated by a simple function. These functions known as interpolation functions are defined in terms of the values of the field at the joints. By solving the field equations, the nodal values of the field variable will be determined.

FEM has received considerable attention in engineering education and in industry because of its diversity and flexibility. Although it is possible to derive the governing equations and boundary conditions from first principles, it is often difficult to obtain any form of analytical solution due to the fact that either the geometry is irregular or boundary conditions are complex [3].

ACKNOWLEDGMENT

The described article/presentation/study was carried out as part of the EFOP-3.6.1-16-2016-00011 *Younger and renewing University – Innovative Knowledge City – institutional development of the University of Miskolc aiming at intelligent specialization* project implemented in the framework of the Szechenyi 2020 program. The realization of this project is supported by the European Union, co-financed by the European Social Fund.

REFERENCES

- [1] Mekid, S. (2009). *Introduction to precision machine design and error assessment*, Boca Raton, FL, Taylor & Francis Group.
- [2] Mian, N. S., Fletcher, S., Longstaff, A. P., Myers, A. (2012). *Efficient estimation by FEA of machine tool distortion due to environmental temperature perturbations*. Huddersfielsd, UK: Elsevier.
- [3] Zhao, H., Yang, J., Shen, J. (2006). *Simulation of thermal behavior of a CNC machine tool spindle*. Shanghai, Elsevier.
- [4] Nithiarasu, P., Lewis, R. W., Seetharamu, K. N. (2016). *Fundamentals of the finite element method for heat and mass transfer*. Chichester, UK, John Wiley & Sons.

THERMAL AND STRUCTURAL SIMULATIONS OF A CNC TURNING CENTER

SEBASTIAN CABEZAS – SZILÁGYI ATTILA

University of Miskolc, Department of Machine Tools
3515 Miskolc-Egyetemváros
sebascabezas1@gmail.com

Abstract: This article shows the application of Finite Element Analysis FEA using Siemens NX 12 Nastran for thermal and structural simulations of a CNC turning center CTX Alpha-500 Gildemeister. The simulations were performed under steady state conditions, stationary system, the heat generated by the workpiece and the machine is neglected and the control volume remains constant.

Keywords: *FEA, steady state, control volume*

1. INTRODUCTION

When it comes to determine the thermal distribution temperatures, the thermal gradient and the displacements occasioned due to heating in a complete system, it is not suitable to make numerical calculations, because the machine is treated as a three dimensional element. Moreover, the machine has many individual components that has a non-determined geometrical shape that cannot be assumed as one-dimensional element.

The use of FEM software is a powerful tool that provides approximate solutions with high accuracy in less time. By computer simulations, the task which by traditional methods will take some days, with these software's the results can be obtained in a few hours and it is possible to make changes and perform more simulations.

2. PROCEDURE

The procedure has been divided into two main parts, 3D modelling and thermodynamical model in which the main aspects to create the 3-dimensional model and the required characteristics to make thermal and structural analysis have been described.

2.1. 3D modelling of the turning center

This section describes the steps that were followed to create the 3D model of the turning center CTX-Alpha 500 GILDEMEISTER using CAD software SIEMENS NX 12.

Measurements:

The dimensions were obtained with a flexible meter *ELLIX 573 522 ECII 2m* for large distances, and a caliper Mitutoyo for small components.

3D CAD Model:

The machine was modelled with the software Siemens NX 12 Modelling. The CAD model of the machine was described in chapter 4. The parts of the machine were divided in subassemblies named: X Axis, Xs Axis, Y Axis, Chuck N1, Chuck N2 and Main Table (see *Figure 1*).

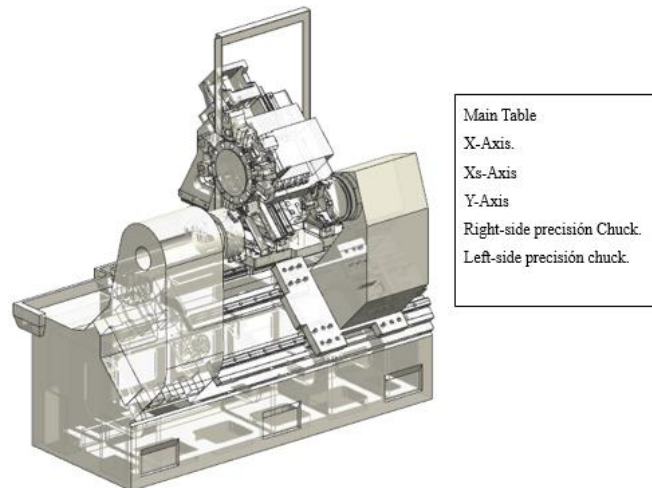


Figure 1
3D Assembly turning machine CTX-Alpha 500

2.2. Thermodynamical model

This section describes the steps followed to create the finite element model for thermodynamical analysis of the turning center in which the fundamentals of heat transfer has to be applied. Moreover, it is needed to stablish thermal conditions and analyze the type of solution, the location of the heat sources in the 3D model, the boundary and initial conditions, restrictions, topology of mesh and the thermal loads.

Finite element method

The finite element method is a numerical tool for determining approximate solutions to a large class of engineering problems. In the finite element method, the actual continuum or body of matter (solid, liquid, or gas), is represented as an arrangement of subdivisions called finite elements.

Elements are interconnected at specified joints. Since the variation of the field (displacement, stress, temperature, velocity, pressure) inside the continuum is not

known, assuming that the variation of the field variable inside a finite element can be approximated by a simple function. These functions known as interpolation functions are defined in terms of the values of the field at the joints. By solving the field equations, the nodal values of the field variable will be determined [1].

To determine the thermal distribution temperatures, the thermal gradient and the displacements due to heating in a complete system, it is not suitable to make numerical calculations. The turning center CTX Alpha 500 is treated as a three dimensional component. Moreover, the machine has many individual components that has a non-determined geometrical shape and cannot be assumed as one-dimensional element.

Type of elements

Engineering systems may be simplified by subdividing them in elements. The elements can be analyzed by first principles. By assembling the elements together, the analysis of a full original system can be reconstructed. These systems are called discrete systems. The turning machine was divided in three dimensional elements called tetrahedrons. This procedure establishes the most accurate approximations compared to one-dimensional or two-dimensional elements.

The temperature distribution in a tetrahedron element is given by the equation:

$$T(x, y, z) = \alpha_1 + \alpha_2 x + \alpha_3 y + \alpha_4 z \quad (1)$$

The number of subdivisions of the turning center obtained by the software was 597210 elements.

Type of solution

Here the steady state solution occurs when there is no accumulation of mass and energy within the control volume, and the properties at any point within the system are independent of time. In this project the system was considered as a steady state for the following reasons: the heat loads will be constant and won't vary with time, the heat sources are independent of time, the temperature distribution is considered as function of time, there is no variation of mass in the control volume, there is no variation of energy in the control volume, the materials of the machine are considered to be isotropic and are the same at any point in the machine.

Heat Sources and location

To perform the thermal simulation is necessary to identify the energy losses produced by the heat sources in the turning center. Heat sources are servomotor loads, linear rail guides and bearings. These heat loads are located in the Axis of rotation and in the linear guides who are used to slide the systems in the machine. Convective heat sources are not considered in this analysis as loads but are considered as initial and boundary conditions. In the simulation the heat dissipated between the work-piece and the machine is not considered.

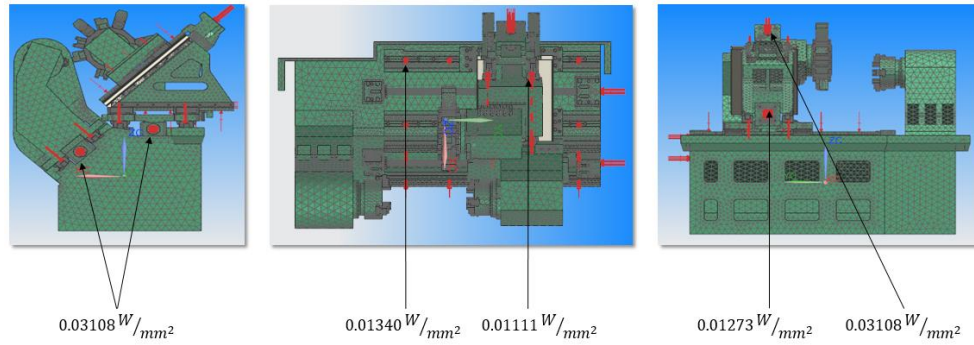


Figure 2
Heat sources and location

Table 1
Heat Sources

Heat sources	Q [watts]
Servomotors S-1FK7060-5AF71-1FH0. (x4)	25
Linear Motion blocks HSR-35A (x8)	31.74
Linear Motion blocks HSR-35LA (x8)	38.28

Boundary Conditions

Convective flow of the air is considered in the analysis as a boundary condition. The media where the machine is surrounded is natural air and the natural convective coefficients are considered.

Initial Conditions

The temperature of the air in the workshop is considered as constant and it is used as the initial condition at any time. $T(t = 0) = T(t)$

Restrictions

The restrictions considered for this analysis are:

- Seasons of the year are not taken into account. The values considered for simulation are said to be the same in spring, summer, fall and winter.
- The operational speeds of the motors are taken from catalogues and considered as nominal speeds.
- The heat generated by the workpiece and the machine is neglected.

- The time operation of the machine is not considered because the system will be treated as steady state.

Thermal Loads

The available thermal loads in NX Nastran environment are:

- QVECT Directional heat flux from a distant source.
- QVOL Volumetric internal heat generation.
- QHBDY Heat flux applied to an area defined by grid points.
- QBDY1 Heat flux applied to surface elements.
- QBDY2 Heat flux applied to grid points associated with a surface element.
- QBDY3 Heat flux applied to surface elements with control node capacity.
- SLOAD Power into a grid or scalar point.
- NOLIN1 Nonlinear transient load as a tabular function.

The heat dissipation produced by the electric motors connected to the shafts, the linear motion blocks rolling on the surfaces of the rail guides and bearings is treated as heat conduction. For the simulation the required loads dealing with heat transfer by conduction are QBDY1 and SLOAD.

Geometric surface element mode

Surface element geometries are associated with surface types. NX Nastran classifies in three forms:

- CHBDYE deals with the geometry type implicitly by reference to the underlying conduction element.
- CHBDYG identifies the radiation surface geometry and material.
- CHBDYP this specification is identified on the CONVM entry as the element identification number.

In this analysis the geometric surface element mode was CHBDYE dealing with heat transfer by conduction.

Material components

The material for simulations were obtained from the catalogues and manuals of the turning center and from the manufacturers of different components of the machine e.g. bearings, linear rail guides, linear motion blocks.

Mesh generation

The domain discretization is classified under different categories such as topology, method of generation, element type, conformity, body alignment. Structured and unstructured meshes are widely classified by topology. The mesh topology used and performed by NX Nastran for this experiment is non-uniform structured mesh.

3. THERMAL SIMULATIONS

After defining, the thermal loads, the mesh generation, boundary and initial conditions into the software is possible to run the thermal simulation of the turning center obtaining the results shown in *Table 2*.

- CHBDY Geometry types 180598.
- CONV Constraint points 179092.
- CTETRA Number of elements 597210.

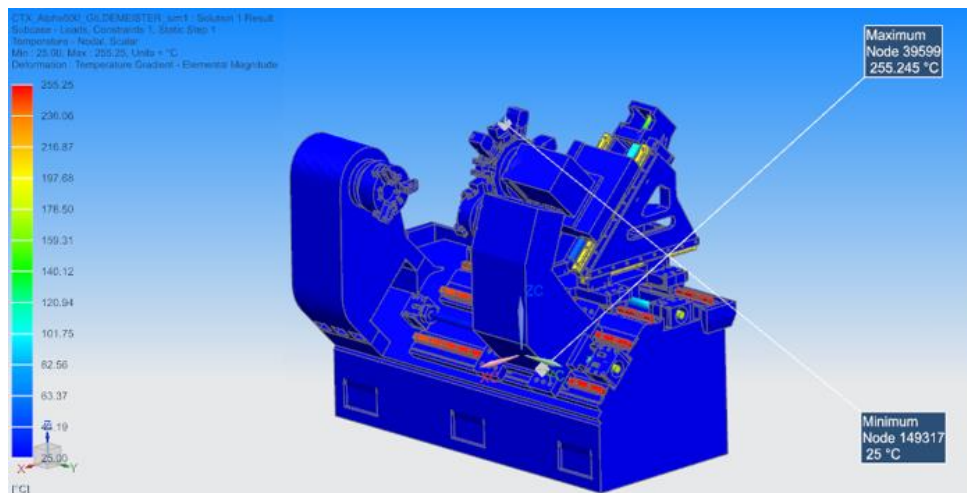


Figure 3
Temperature distribution

Table 2
Temperature distribution results

	Node	Value [°C]
Minimum scalar temperature	149,317	25
Maximum scalar temperature	39,599	255.245
MtAxis1	95,567	175.952
MtAxis2	102,085	175.95
XsAxis	88,075	114.564
Xaxis	149,820	177.371
Linear rail guides Main table	36,478	250.984
Linear rail guides XsAxis	34,667	203.685
Linear rail guides XAxis	33,762	201.887

4. STRUCTURAL SIMULATIONS

Applying the results obtained during the thermal simulation as temperature loads, to find the displacements which will cause inaccuracies in the precision of the turning center.

Displacement in X direction:

Table 3
X-Direction deformation

X- Direction	Node	Deformation [mm]	Deformation [μm]
Minimum	87,681	0.00558361	5.58361
Maximum	39,162	-0.0125772	-12.5772

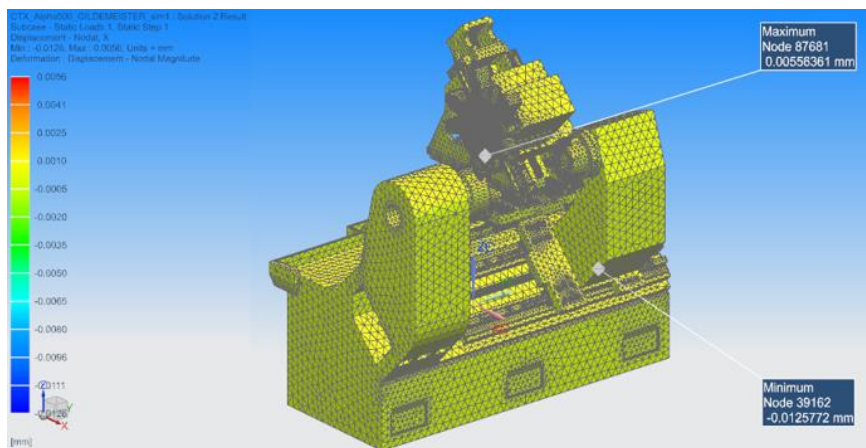


Figure 4
Displacement in X-direction

Displacement in Y direction:

Table 4
Y-Direction deformation

Y- Direction	Node	Deformation [mm]	Deformation [μm]
Minimum	33,239	0.00397778	3.97778
Maximum	89,884	-0.00621152	-6.21152

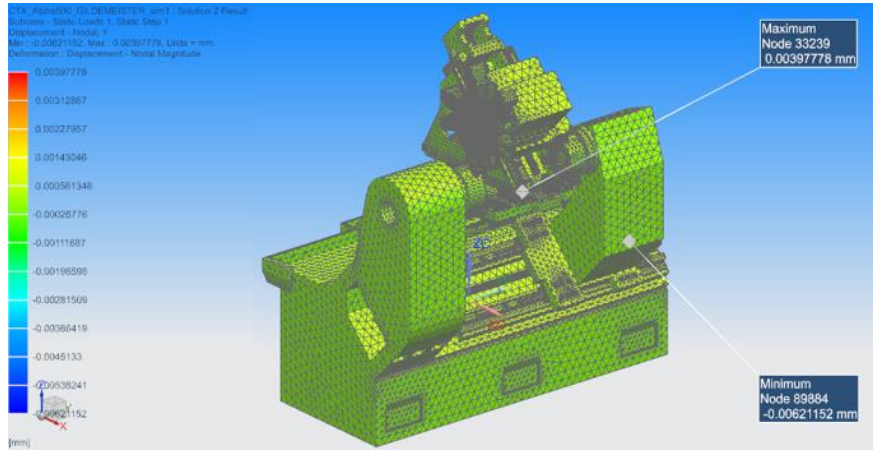


Figure 5
Displacement in Y-direction

Displacement in Z direction:

Table 5
Z-Direction deformation

Z- Direction	Node	Deformation [mm]	Deformation [μ m]
Minimum	35,395	0.0102213	10.2213
Maximum	36,178	-0.0125486	-12.5486

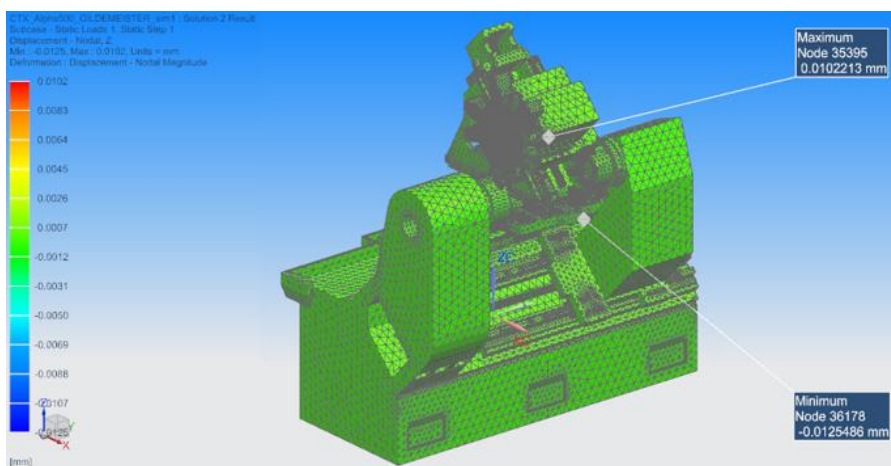


Figure 6
Displacement in Z-direction

5. SUMMARY

The turning machine was analyzed by FEM simulations dividing into small 3D tetrahedrons with four nodes each one of them, the size of the tetrahedrons were defined in order to improve the time of the interactions in the simulations that was around 20 minutes for thermal analysis and 23 minutes for structural analysis.

The workshop environment where the turning machine is located can be of significant importance for accuracy of manufacturing. Temperature controlled environments require a big amount of investment, which in the majority of the cases are undesirable and impractical. For the simulation analysis of the turning machine, the temperature environment established was 25 °C, due to the fact that the workshop where the machine is located possesses air conditioning system which can be regulated independently of the seasons of the year.

The maximum temperature estimated in steady state with the established parameters of the heat sources was $T_{max} = 255.205$ °C, node 39,599, located in the rail guides of the main table and Chuck N2. No cooling and lubricant factors were considered during the simulation. The increase of the temperature in the rail guides occur due to the friction if the system is not properly aligned, lubrication is not appropriate or the bearings are failing. To avoid this problem is needed to take preventive maintenance to check the state of the linear rail guides and the bearing components.

ACKNOWLEDGMENT

The described article/presentation/study was carried out as part of the EFOP-3.6.1-16-2016-00011 *Younger and renewing University – Innovative Knowledge City – institutional development of the University of Miskolc aiming at intelligent specialization* project implemented in the framework of the Szechenyi 2020 program. The realization of this project is supported by the European Union, co-financed by the European Social Fund.

REFERENCES

- [1] Nithiarasu, P., Lewis, R. W. Seetharamu, K. N. (2016). *Fundamentals of the finite element method for heat and mass transfer*. Chichester, UK: John Wiley & Sons.
- [2] Mekid, S. (2009). *Introduction to precision machine design and error assessment*. Boca Raton, FL, Taylor & Francis Group.
- [3] Zhao, H., Yang, J., Shen, J. (2006). *Simulation of thermal behavior of a CNC machine tool spindle*. Sanghai, Elsevier.
- [4] Mian, N. S., Fletcher, S., Longstaff, A. P., Myers, A. (2012). *Efficient estimation by FEA of machine tool distortion due to environmental temperature perturbations*. Huddersfielsd, UK, Elsevier.
- [5] SIEMENS (2014). *Thermal Analysis User's Guide*.

DEVELOPMENT OF DESKTOP 3D PRINTER

CSABA DEREKAS – DÁNIEL KISS

University of Miskolc, Department of Machine Tools
3515 Miskolc-Egyetemváros
kiss.daniel@uni-miskolc.hu

Abstract: In this paper, we present the design and construction of a rapid prototyping machine based on FDM (Fused Deposition Modeling) technology and the results of the test pieces made with it. The design basis of the machine was provided by an existing ISEL 5D milling machine, from which the two axes realizing the orientation movements were removed, and then the motion control of the three axes realizing the linear movements was realized with an Arduino Uno microcontroller. With the completed 3D printer, we printed test pieces from different raw materials and printing parameters during the testing, the results of which are reported.

Keywords: 3D printer, FDM, microcontroller

1. INTRODUCTION

The idea of 3D printing has been assumed in the 1970's, but the first experiments are dated from 1981. *Dr. Hideo Kodama* was the first to describe a layer by layer approach for manufacturing, creating an ancestor for *SLA (StereoLithoGraphy)*, where a photosensitive resin was polymerized by an ultraviolet light. In 1984 *Alain Le Méhauté, Olivier de Witte* and *Jean-Claude André*, was interested by the stereolithography but abandoned due to a lack of business perspective. This 3D printing attempt was also using a stereolithography process.

Charles Hull was also interested in the technology and submitted a first patent for stereolithography in 1986. He founded the *3D Systems Corporation* and in 1988, released the SLA-1, their first commercial product.

In 1988 Carl Deckard at the University of Texas brought a patent for the *SLS (Selective Laser Sintering)* technology, another 3D printing technique in which powder grains are fused together locally by a laser.

In the meantime, Scott Crump, a co-founder of *Stratasys Inc.* filed a patent for *FDM (Fused Deposition Modelling)* [1].

The recent years have been very important for 3D Printing. With the FDM patent expiration, the first years of the decade have become the years of 3D printing. Additive manufacturing is then becoming a real and affordable prototyping and production technique for businesses, opening new possibilities. Due to these reasons, the 3D printing processes that can be used for hobby purposes have become widely

available, so these devices can be built from simple and cost-effective parts. The Institutional Department of Machine Tools of the University of Miskolc made proposals for the design of several devices using the design methodology guidelines [2]. These include measuring station concepts for welded earthmoving machine arms [3], industrial measuring machine [4], mechatronic systems design [5], bearing wear and testing equipment for determining the remanent life of rolling bearings [6], and chip removal design for milling machines [7]. Using the above experience and design methodology principles, a 3D printer using fused deposition modeling technology was built. Due to the size of the machine, its workspace allows you to print small parts.

2. STEPS OF THE DEVELOPMENT PROCESS

In this section the brief description of the steps of the development process is shown. The base of the new desktop 3D printer was an *ISEL 5D* milling machine, the analysis of its structure discussed in the next subsection.

2.1. Analyzing the machine structure

The 5D milling machine has three linear axes (X , Y , Z) and two rotational axes (A , C). Each of the linear axes are driven by a stepper motor and a ball screw drive mechanism, while the rotational axes have a stepper motor drives with timing belt. The motion range of the axes are controlled by limit switches and the drives are controlled by *ISEL* five-axis controller (*Figure 1*).

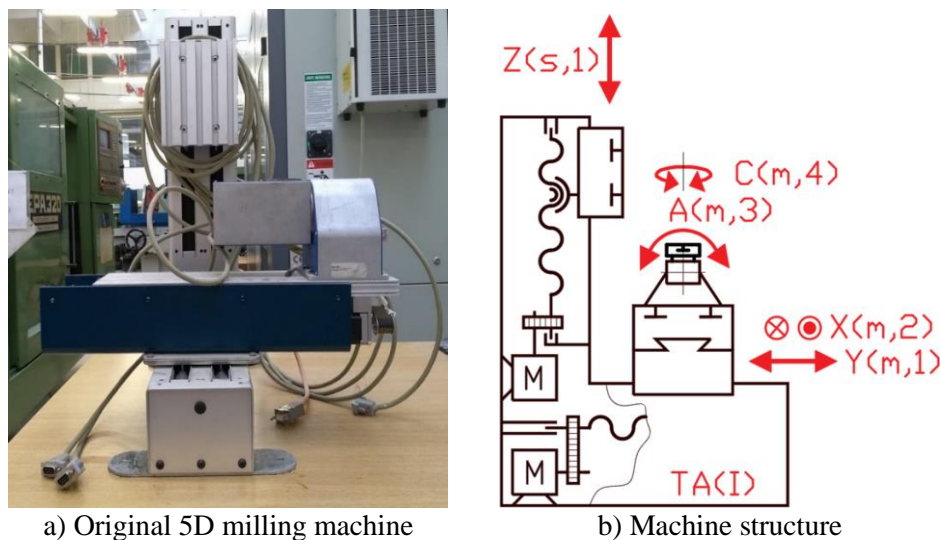


Figure 1
Machine structure

Identification of machine structure components:

- TA(I) base,
- Z(s,1) Z axis, linear movement for the tool, priority 1,
- Y(m,1) Y axis, linear movement for the part, priority 1,
- X(m,2) X axis, linear movement for the part, priority 2,
- A(m,3) A axis, rotation around X axis for the part, priority 3,
- C(m,4) C axis, rotation around Z/Y axis for the part, priority 4.

A value analysis method was used to find the new functions of the 3D desktop printing machine. The main points were the price, the complexity of the control system and the time of the development process. At the end of the method find out, that the best new functions are the three-axis 3D printer and the three axis CNC milling machine (*Table 1*). The five-axis CNC milling machine, three-axis laser cutting engraving machine, five-axis 3D printer were too difficult to realize.

Table 1
Value method to find the best solution

	viewpoint			Σ
	price	complexity	need of work	
importance of the viewpoint	40	30	20	
points of 5 axis milling machine	4	3	7	
point*importance	160	90	140	390
points of 3 axis milling machine	6	8	8	
point*importance	240	240	160	640
points of laser engraving machine	3	6	5	
point*importance	120	180	100	400
points of 3 axis 3D printer	6	8	6	
point*importance	240	240	120	600
points of 5 axis 3D printer	3	3	4	
point*importance	120	90	80	290
points of turret cnc machine	2	2	3	
point*importance	80	60	60	200

2.2. Computer aided design of the equipment

After the value analysis the next milestone was the computer aided design of the 3D desktop printer. The 3D geometric modeling of the components and the overall assembly modeling of the product was performed in *Siemens NX PLM 11* software. Engineering analyses were executed, such as kinematic simulations, collision detection during the moving of the different axes. *Figure 2* shows the 3D assembly model of the designed 3D desktop printer.

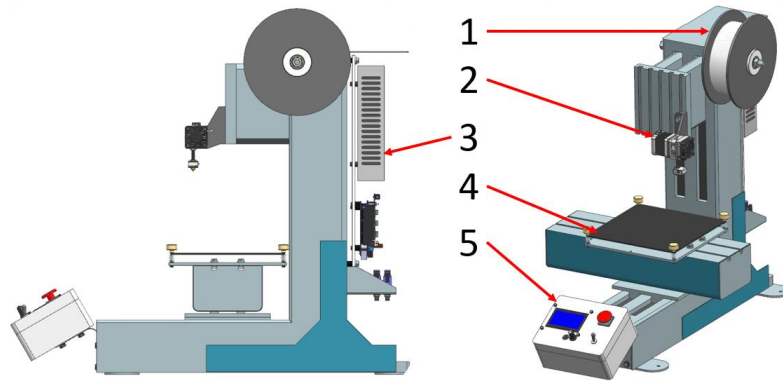


Figure 2
The final design of the 3D desktop printer

The new equipment on the final design (Figure 2):

- 1 filament feeder,
- 2 extruder,
- 3 power supply,
- 4 heated bed,
- 5 controller.

These new components are commercial and standard products. The cost calculation of the purchased items is listed in the Table 2.

Table 2
Cost calculation of commercial components

<i>name</i>	<i>quantity</i>	<i>piece price [HUF]</i>
MK8 extruder	1	12700
MK3 ALU-heated bed	1	5080
ABS-Filament 1.75	1	6700
Thermistor	2	65
Jumper, red, RM=2.54mm	30	5.08
Krimp. Connector	200	4.74
Connector cover 1p NSR-01	50	8.62
Connector cover 2p NSR-02	50	10.19
Connector cover 3p NSR-03	50	4.5
Connector cover 4p NSR-04	20	6.45
D-SUB connector, lengő, 9p, female	5	36
Shrink-on tube, blue 4/2mm BL	3	28
Shrink-on tube, blue 6/3mm BL	3	38.1
Shrink-on tube, blue 10/5mm BL	3	91.44
RepRap Graphic Smart Controller 12864	1	5842
Arduino Mega+Ramps 1.4+ A4988 pack	1	10795
PSU 360W 12V 30A S-360-12	1	8200
		52494.52

3. TESTING OF THE ASSEMBLED EQUIPMENT

The newly assembled components compose the 3D desktop printer. The hardware controller based on an Arduino Uno microcontroller, which has an open source software development platform. It is connected with a Ramps 1.4 shield, which helps to control the stepper motors, through A4988 stepper motor controllers.



Figure 3
The assembled 3D desktop printer

The machine was made to be independent of the computer with a 12864 type graphic smart controller. The data can be uploaded through a secure digital (SD) card to the machine. The Marlin 1.1 open source software was applied to communicate with the hardware. After the testing of the drives and fine-tuning, the three-axis 3D desktop printer was available to printing different sample parts. For the machine the code from the 3D STL model is generated by the software *Cura 4.0*. During the testing process *ABS (Acrylonitrile-Butadiene-Styrene)* and *PLA (Poly Lactic Acid)* filaments were used as well. The construction of the machine is not optimal to print with *ABS*, due to the material is sensitive for the small airflows. Some *ABS* parts cracked during the printing process. The test results were much better with *PLA* filament. After the 3D printing the strength of the parts were higher, the surface was smoother, and the bonding of the layers was stronger.



Figure 4

3D desktop printed parts with different raw material



Figure 5

3D printed part from PLA

Some small parts printed by *ABS* material resulted suitable products (*Figure 4*) without any problem. However, when the printed parts dimensions have reached a critical dimension limit they started to crack after printing process. Parts printed by *PLA* filament resulted better products, due to its one of the material properties, which is less sensitive for the air flow during printing process (tendency to crack did not appear after printing). *Figure 5* shows a 3D printed part with *PLA* filament.

4. SUMMARY

In recent years the 3D printers using *FDM* technology have exploded, due to the state of the art. These devices have already appeared in everyday use. In this article, we examined the possibility of converting an available *ISEL 5D* milling machine to be suitable for building a 3D desktop printer. Prior to the process, a value analysis

was performed, which confirmed that the available tools provide the optimal starting point for building the printer. The 3D design and analysis of the printer was followed by the assembly of the missing components, then the examination of the printing parameters and their effects, and the testing of the 3D desktop printer. It can be stated that the current results confirmed the pre-design assumption that the constructed printer can print parts comparable to the accuracy of the FDM process used in mechanical applications.

ACKNOWLEDGEMENT

The described study was carried out as part of the EFOP-3.6.1-16-00011 *Younger and Renewing University – Innovative Knowledge City – institutional development of the University of Miskolc aiming at intelligent specialization* project implemented in the framework of the Szecsenyi 2020 program. The realization of this project is supported by the European Union, cofinanced by the European Social Fund.

REFERENCES

- [1] *The Ultimate Guide to Stereolithography (SLA) 3D printing*. White paper, Marc 2017, www.formlabs.com.
- [2] Takács, Gy., Zsiga, Z., Makó, I., Hegedűs, Gy. (2011). *Methodical design of production equipment*. Budapest, Hungary, Nemzeti Tankönyvkiadó, 187 p. (in Hungarian).
- [3] Jakab, E., Takács, Gy., Hegedűs, Gy. (2002). Measuring station concepts for welded earthmoving-machine arms. *GÉP*, 53, 6–7, pp. 45–48, 4 p. (in Hungarian).
- [4] Hegedűs, Gy. (2003). Application of methodical machine design in the development of an industrial measuring machine. *PhD Students Conference 2002*, Section publication of the Faculty of Mechanical Engineering, Miskolc, Hungary: University of Miskolc Innovation and Technology Transfer Center, pp. 98–103, 6 p. (in Hungarian).
- [5] Takács, Gy., Patkó, Gy., Csáki, T., Szilágyi, A., Hegedűs, Gy. (2006). Development of Mechatronic Systems at the Institute for Mechatronics at the University of Miskolc. *2006 IEEE International Conference on Mechatronics*, pp. 326–331.
- [6] Hegedűs, Gy., Barak, A., Barna, B., Demeter, P., Simon, G., Szilágyi, A., Takács, Gy. (2010). Development of analyzing equipment of the remanent lifetime on roller bearings. *MicroCAD 2010: XXIV. microCad International Scientific Conference*, Section L, Machine and structure design, Miskolc, Hungary: University of Miskolc, pp. 47–52.
- [7] Szabó, K., Takács, Gy., Hegedűs, Gy., Tóth, S. G. (2019). Examination of Design Methodology of Screw Conveyors. *Design of Machines and Structures*, 9, 1, pp. 58–63.

EXAMINATION OF POSSIBILITIES OF THE STRENGTH MODIFICATION IN THE CASE OF FDM/FFF MANUFACTURING TECHNOLOGY

PÉTER FICZERE – NORBERT LÁSZLÓ LUKÁCS

Budapest University of Technology and Economics,
Department of Vehicle Elements and Vehicle-Structure Analysis
1111 Budapest, Sztoczek u. 2.
ficzere@kge.bme.hu

Abstract: In many situations the result of the topology optimization or generative design can be manufactured only by additive manufacturing technologies. It is also important to know how the optimised shape behaves from the mechanical stiffness, the manufacturing technology and beneficial point of view. These two different goals can be combined and just the infill properties can be changed and optimised within the main body of 3D printed part.

Keywords: *Hybrid infill, FDM, Additive Manufacturing, Generative Design*

1. INTRODUCTION

Additive manufacturing technologies has become increasingly widespread in many fields. Nowadays 3D printed products can be found in many different environments like health care service, where the individual orthoses and prostheses can be 3D printed. One of the new fields of application is jewellery where AM technologies are also a widely used [1], [2], [3]. In numerous cases the 3D printed products must be loadbearing. For this reason, the application of simulations is inevitable, where a proper 3D geometry, the environment and structural constraints, the loads and material characteristics must be well known [4], [5], [6]. In the light of these circumstances the weak and overdesigned points of structure can be found by using numerical simulations, then the 3D model can be modified based on the results. This step can be automated by CAD and FEM software and topology optimisation also can be performed [7]. Engineering design software like Fusion 360 by Autodesk or Solid Edge by Siemens use artificial intelligence (AI) for generative design which can provide lighter and stronger parts. *Figure 1* shows an axle stub designed with generative design.

In this figure the complex geometry can be seen. It is easily observable that the geometry is inproducible by conventional technologies and an AM technology must be applied. The complexity of geometry requires support structures to achieve precise dimensions and it can highly raise the production time and material cost [8]. Besides increased costs the remove of supports can also be a difficulty therefore the small details can increase price directly and make the production more difficult. The

small parts can easily brake during the support removal process. For this reason, the customisation of infill features for more sufficient mechanical properties can be easier and cheaper.

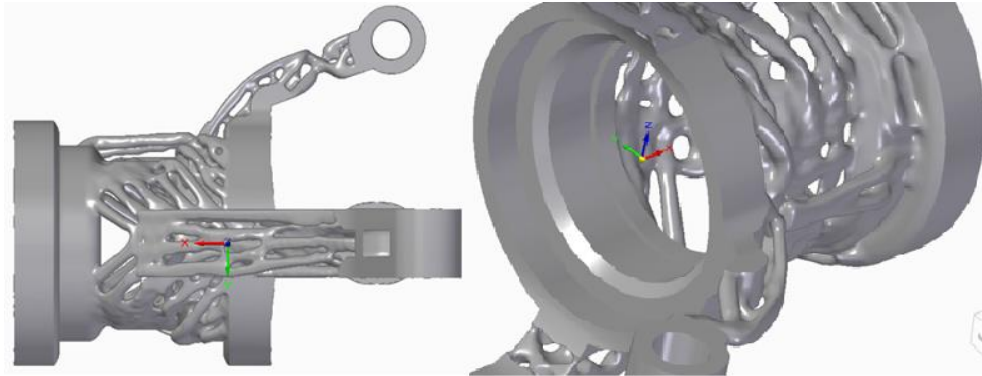


Figure 1
Axle stub produced by the help of generative design

2. METHOD

In case of a simple bending specimen it is easily visible that the stress is much higher in the sides of the specimen, while the neutral axis is exactly in the middle of the specimen where the stress is nearly zero (*Figure 2*).

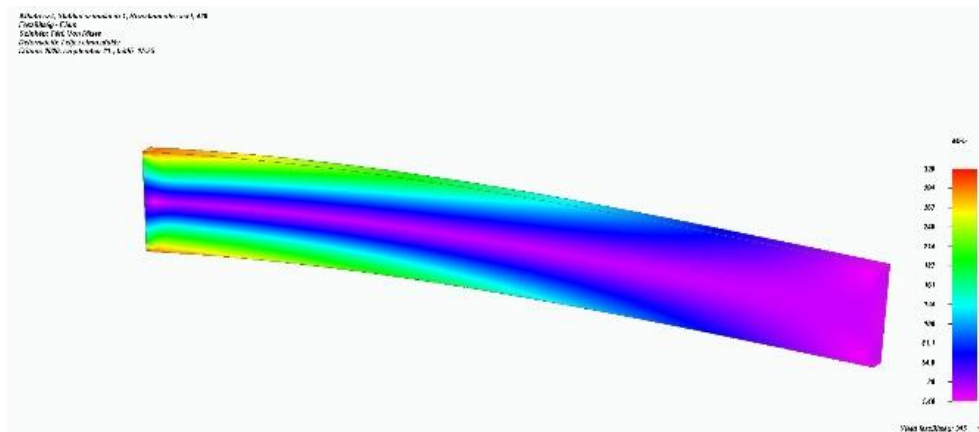


Figure 2
Stress distribution in a bent beam

For this reason, it is logical if the unladen parts are hollowed and the loaded parts are filled with material, but infill properties can be optimised as well.

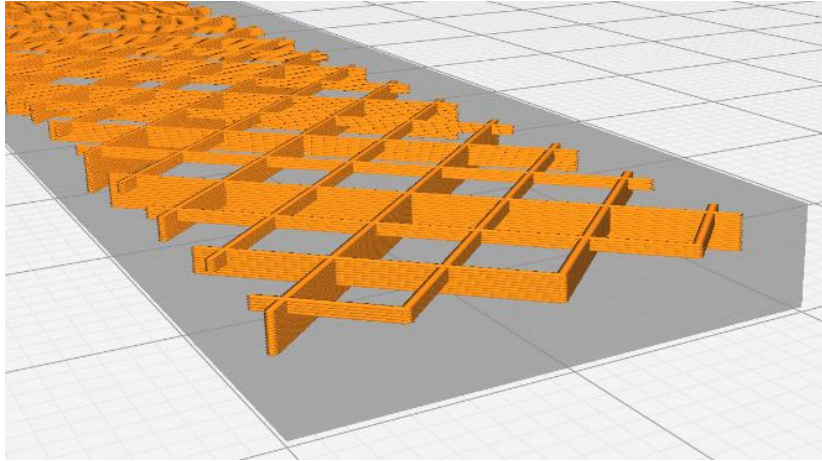


Figure 3
Gradual infill

Furthermore, there are many options to change infill pattern, direction and dense.

Important to notice that these parameters can be modified just in the production simulation software – slicer software – like Cura, Simplify, etc. For this reason, mechanical strength can be just estimated.

For the proper simulations the infill must be generated by a CAD software than the validation could be done by numerical simulations.

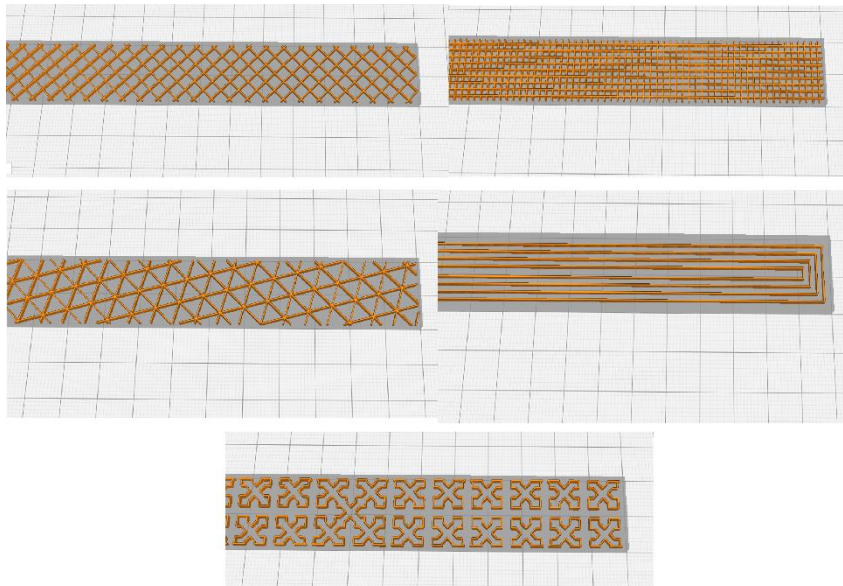


Figure 4
Infill types with same density but with different line directions

In light of mechanical properties of infill patterns there is a possibility to use a special gradual infill to provide an optimised filling. For optimised mechanical properties a Finite Element Method needed wherefrom the results (iso surfaces) can define the exact infill borders.

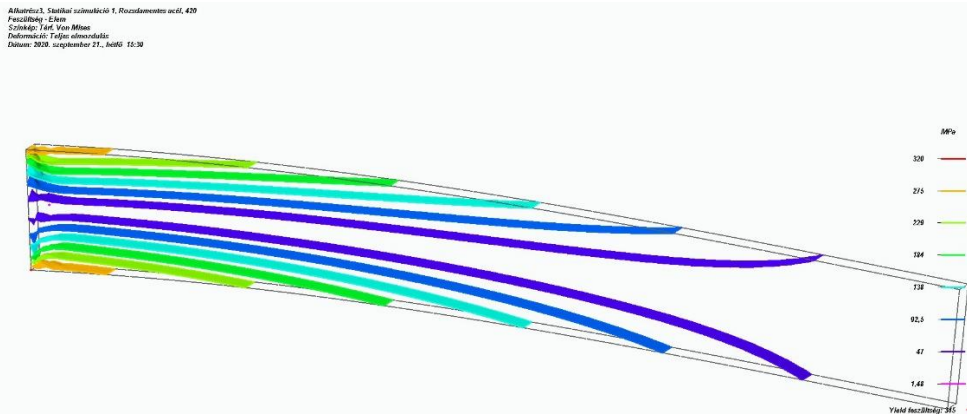


Figure 5
Iso surfaces within a test specimen

An advantage of mechanical strength optimisation by infill variation can be highlighted such as the small details can be avoided therefore the support extraction can be much easier and material costs can be lower [9]. Another way to increase the strength of composite-based manufacturing, but it is much more expensive and requires more consideration [10]

3. RESULTS

The shape of the specimen made by generative design can be seen in *Figure 6*.



Figure 6
Geometry produced by generative design

In *Figure 6* it is easily observable that the geometry is more sufficient from mechanical perspective, but it is relatively hard to produce even with 3D printing. The small

details require more support structures which can make the production expensive (more time and material) and the removal of support structure is also can be difficult, the small details can easily brake during the process.

In *Figure 7* some infill variations can be seen.

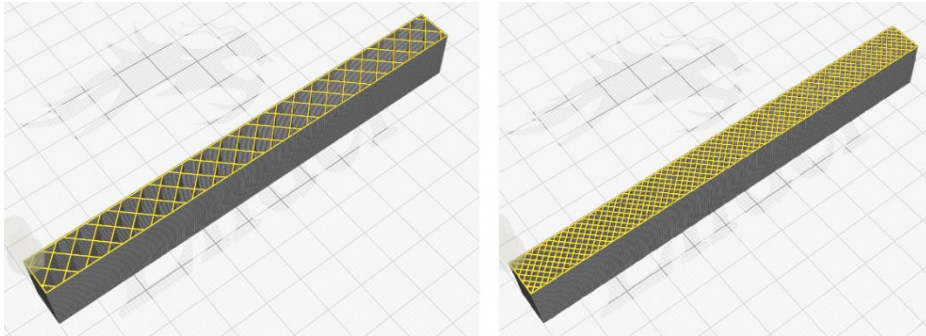


Figure 7
Different infill densities

Based on *Figure 2* it is easy to notice the consistent infill is unnecessary since the middle of the specimen is not loaded. For this reason, a hybrid solution can be applied where the infill is changed based on the stress volume.

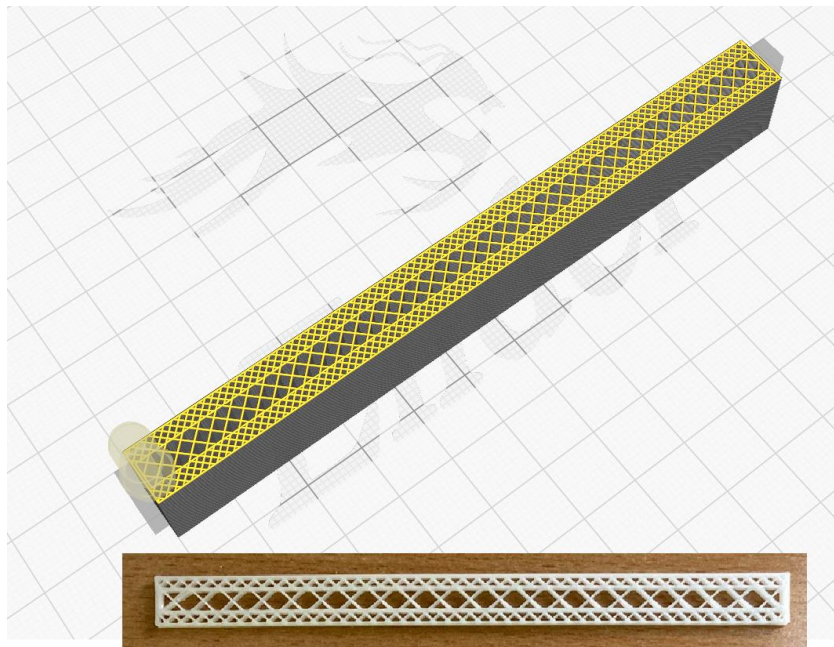


Figure 8
Hybrid infills

Infill is dense in the sides of the specimen while near to the neutral axis it is more diffuse. This easy solution provides lighter and stronger 3D printed parts (*Figure 8*). Based on *Figure 5* – where the result of bending test is – an infill modifier body can be used in slicer software which can provide optimised infill modifications. This solution can be seen in *Figure 9*.

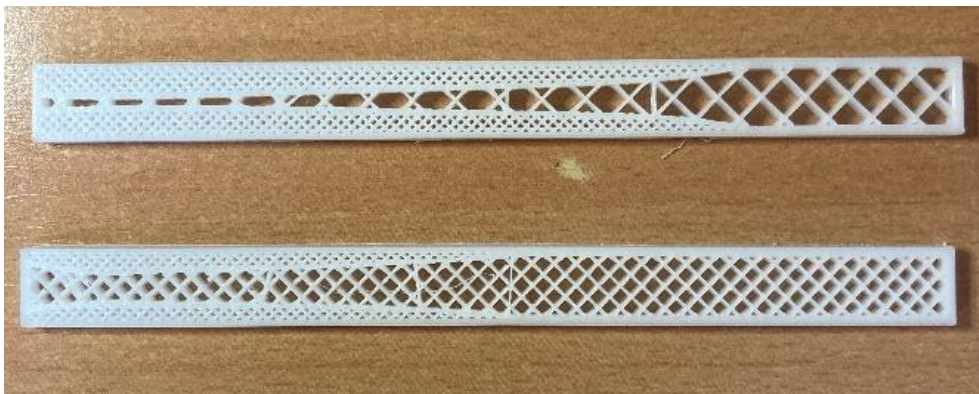


Figure 9
Modified specimens based on iso surfaces

4. ANALYSIS

Based on the results it is easy to notice the infill properties can be changed properly which has a huge effect on mechanical properties. Therefore, this feature can be optimised and the production can be cheaper and faster. The removal of supports can also be easier. For this reason, the exact effects of infill properties on mechanical strength must be well known.

Furthermore, some important source of errors can appear, for example if there are not walls between the different infills. *Figure 10* shows a pair of specimens with and without walls between infill transitions.

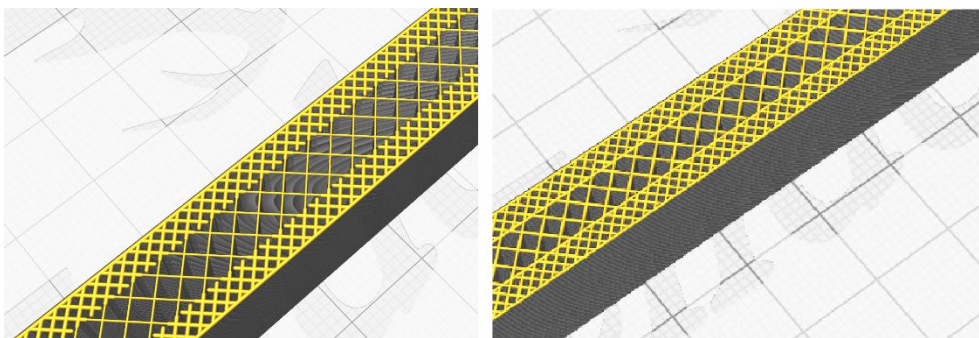


Figure 10
Infill connections without and with walls

It is worth highlighting that if there is not wall between infills the lines of different infills cannot connect to each other which can cause the 3D printed parts to lose strength. This phenomenon can be the issue of a new investigation.

5. CONCLUSION

Due to the popularity of 3D printing the technology has a good progression therefore new features are available for users. Nowadays the individual or low volume production require advanced solutions and AM technologies are good options. The goal is the best and the strongest product on the cheapest and faster way as possible. For this reason, the affect of the different infill parameters has been investigated. There are a huge number of different infill settings which can help the production of better products. For the proper use numerical simulations and experimental validation are required. Furthermore, the application and education of new thinking method are needed.

REFERENCES

- [1] Ficzer P., Horváth Á. M., Sipos T. (2020). Elalvások balesetek csökkentési lehetősége additív gyártási eljárással fejlesztett kapszulák segítségével. *Közlekedéstudományi Szemle*, 70, 1, pp. 77–85., <http://doi.org/10.24228/KTSZ.2020.1.3>.
- [2] Ficzer, P. (2018). Design Questions of the Individual Medical Implants. In: Háber, István Ervin, Bogdán, Csaba, Szőke, András (eds.). *Proceedings of the 4th International Interdisciplinary 3D Conference*, Engineering Section, Pécs, Hungary: October 5–6, 2018, University of Pécs, pp. 57–67.
- [3] Ficzer P., Borbás L., Falk Gy. (2018). Csont anyagtulajdonságainak megfelelő anyagmodellek előállítása additív gyártástechnológiákkal. *Biomechanica Hungarica*, 11, 2, pp. 77–83., doi.org/10.17489/2018/2/1.
- [4] Ficzer, P., Borbas, L., Falk, Gy., Szebenyi, G. (2018). Experimental determination of material model of machine parts produced by Selective laser sintering (SLS) technology. *Materials Today: Proceedings*, 5, 13, pp. 26489–26494., <https://doi.org/10.1016/j.matpr.2018.08.104>.
- [5] Ficzer, P. (2020). Experimental Dynamical Analysis and Numerical Simulation of the Material Properties of Parts Made by Fused Deposition Modelling Technologies. *Periodica Polytechnica Transportation Engineering*, 48 (3), pp. 221–225., <https://doi.org/10.3311/PPtr.13947>.
- [6] Ficzer, P., Lukács, N. L. (2020). Influence of 3D printing parameters. *IOP Conference series: Materials Science and Engineering*, 903 p. 012008, 7 p., doi.org/10.1088/1757-899X/903/1/012008.

- [7] Győri, M., Ficzeré, P. (2017). Use of Sections in the Engineering Practice. *Periodica Polytechnica Transportation Engineering*, 45 (1), pp. 21–24., doi.org/10.3311/PPtr.9144.
- [8] Ficzeré, P., Borbás, L., Török, Á. (2013). Economical Investigation of Rapid Prototyping. *International Journal for Traffic and Transport Engineering*, 3, 3, pp. 344–350., doi.org/10.7708/ijtte.2013.3(3).09.
- [9] Ficzeré P. (2019). Alkatrészek munkatérben történő elhelyezésének a gyártási költségekre gyakorolt hatása additív gyártástechnológiák esetén. *GÉP*, 70, 3, pp. 26–29., 4 p.
- [10] Tóth Cs., Kovács N. K. (2020). Additív gyártástechnológiával készült, politejsav mátrixú kompozitok vizsgálata. *Polimerek*, 6/5., pp. 926–930.

DESIGNING OF A BLDC MOTOR BENCH

PÁLMA KAPITÁNY – JÓZSEF LÉNÁRT

University of Miskolc, Robert Bosch Department of Mechatronics
3515 Miskolc-Egyetemváros
kapitanypalma@gmail.com, lenart.jozsef@uni-miskolc.hu

Abstract: This paper deals with designing and development of a bench for the test of a brushless DC motor. The bench contains a hydraulic circuit, which provides a controllable load for the motor. The hydraulic system is equipped with a hydraulic pump and choke valve and a manometer. The mechanical connection between the hydraulic pump and the BLDC motor is designed with two clutches and structure of two sheet plates. The bench contains a torque meter, which is built between the two shafts of the motor and pump. The system can determine rotational speed, torque, current and voltage with respect of the load.

Keywords: *BLDC motor, hydraulic circuit, measurement of motor characteristics*

1. INTRODUCTION

Nowadays Brushless DC (BLDC) motors [1] are even used for hobby tools, e.g., lawn and garden devices. The main benefit of this motor that it has not commutator slices, which wear and generate sparks and noises. The commutation is provided by Hall sensors and FETs. The characteristics of the current is varying not with a harmonic function but as a square wave signal. Permanent magnets are mounted onto the rotor and the coils are wired onto the stator. This type of motor even if the voltage source is a battery pack can provide high torques and power.

The characteristics of electric motors are measured usually with such a system, in which the load is provided by another electric motor controlled by computer. This motor is equipped with load cells to determine the torque with respect the rotational speed. The measurement of the voltage and current is performed parallelly.

The authors of this paper have only bench for different type of motors but for small torque and power intervals [2], [3]. Due to this drawback a new measurement system should be designed and developed. Designing of the measurement system for a high-power rate BLDC motor requires caution from engineers.

This paper is organized as: Section 2 deals with the geometrical design process of the clutches and the structure of the sheet metals. Section 3 contains the set-up of the test bench. Section 4 shows the result of a test measurement.

2. DESIGNING THE ELEMENTS OF THE BENCH

Measuring the characteristics of a BLDC motor requires an adjustable load unit, which in our case is a hydraulic pump. A torque measuring cell between the motor

and the pump shafts measures the transmitted torque. The design of the two couplings and the mounting structure required to achieve the mechanical connection. The available items are shown in *Figure 1*.

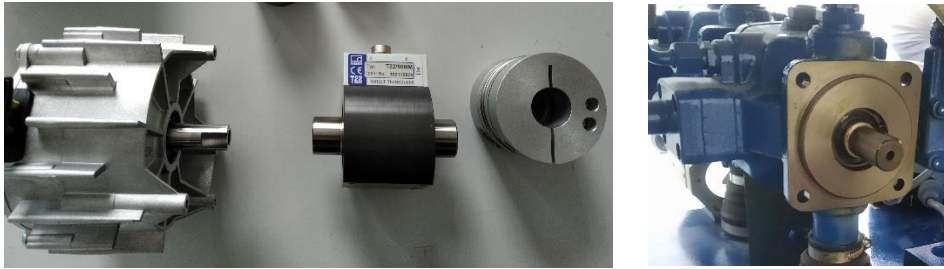


Figure 1

The existing elements: BLDC motor, torque measuring cell, clutch, and hydraulic pump

Additional machine elements have been designed in Autodesk Inventor 2020 software. The coupling of the BLDC motor and the torque measuring cell clutch requires the design of an intermediate clutch, which is illustrated in *Figure 2*.

Between the hydraulic pump and the torque measuring cell there is also a clutch necessary, which ensures force-locking connection at one side, and at the other side there is a locking groove (see *Figure 3*).

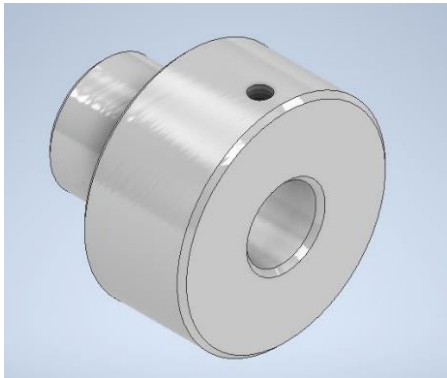


Figure 2

The intermediate clutch

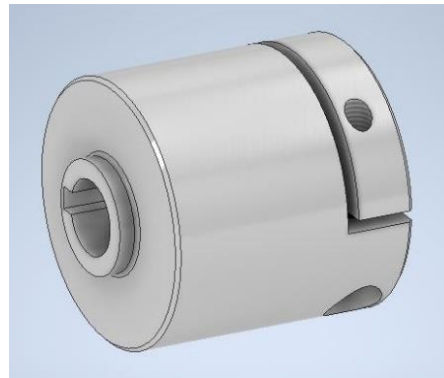


Figure 3

The clutch between the pump and the torque measuring cell

The hydraulic pump and the BLDC motor are mounted on sheet metal structure. The 3D drawing of the pump support element with the corresponding holes is shown in *Figure 4*. The thickness of the plate is 5 mm.

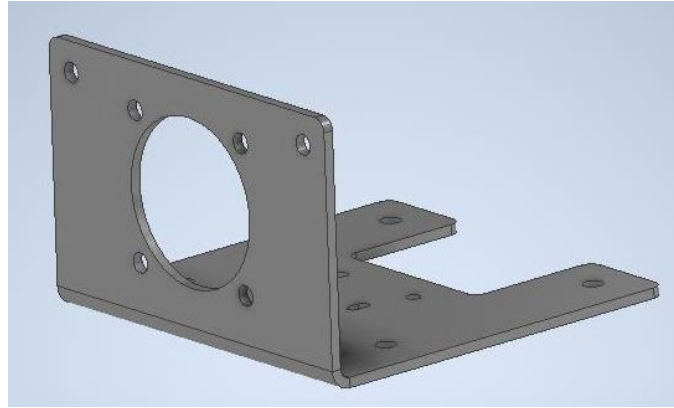


Figure 4

The drawing of the pump supporting sheet metal

A bent plate was also designed to mount on the BLDC motor (see *Figure 5*), which has 3 mm thickness. It is noted that for the sake of mountability, stretched holes are designed for the bolts.

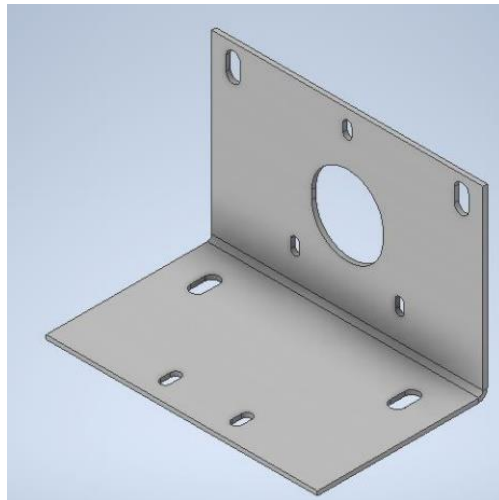


Figure 5

The 3D drawing of the BLDC supporting sheet metal

The designed elements have been manufactured, which are shown together with available ones (see *Figure 6*). The aluminum clutches shown in *Figure 2* and *3* are produced by turning-machine at the Institute of Machine Tools and Mechatronics. The steel sheet metals were formed by laser cutting and edge bending at AR-Robotics Ltd.



Figure 6
The designed and available elements

3. SET UP OF THE TEST BENCH

The picture of the test bench is displayed in *Figure 7*. Standard machine elements are used to fix the metal structure to mount on the hydraulic system.

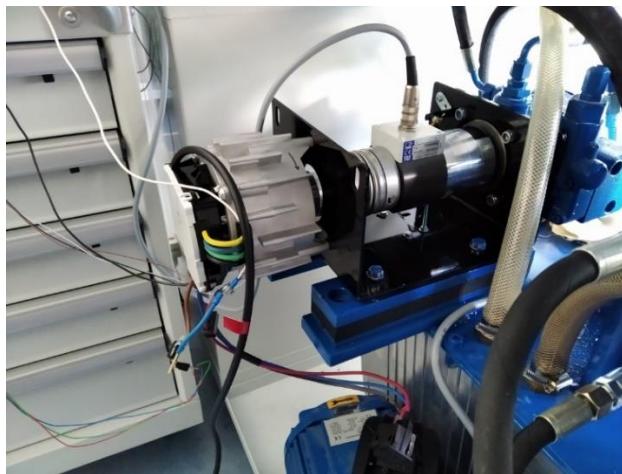


Figure 7
The test bench

The test bench is capable to measure the current, voltage, torque, and rotation speed (RPM). The scheme of the measurement system is shown *Figure 8*. The measured signals are digitized by an Atmega328 microcontroller, which are transmitted to a Personal Computer (PC). The sampling frequency of the microcontroller is set to 10 Hz. The available voltage source is about 20 V, therefore a voltage divider is required to provide the voltage TTL logic level. The type of the current sensor is ACS758ECB-200B-PFF-T, which has 200 A upper limit. The torque sensor is HBM T22/50 Nm.

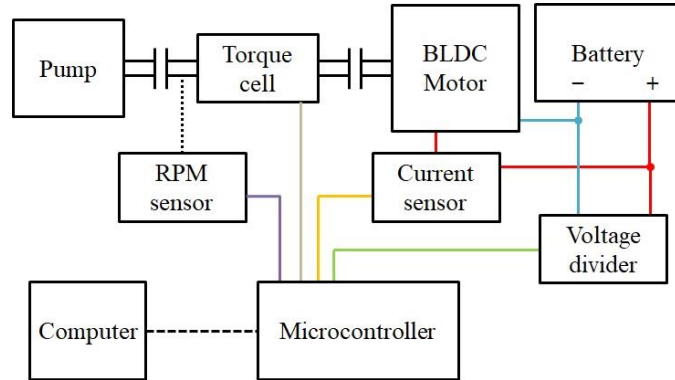


Figure 8
Block diagram of the measurement system

4. MEASUREMENT

A test measurement has been performed for 5 bar load produced by the hydraulic circuit. The signals of one of the measurements are shown in *Figure 9*, where the voltage, the current, the RPM and the torque are denoted by green, purple, red and orange curves, respectively. The vertical axis represents the quantized values between 0–1,023 due to the 10-bit A/D converter, while the horizontal axis shows the elapsed time in ms.

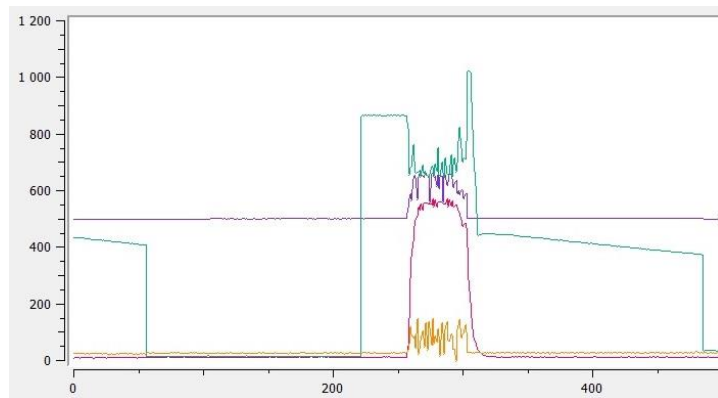


Figure 9
The results of a test measurement

The BLDC motor is started with two pushbuttons, one button enables, while the other actually provides voltage to the system. As *Figure 9* shows, the first button is pressed at 220 ms, i.e., the voltage ramps up, while the second button is pressed at 250 ms when the voltage drops somewhat and shows an oscillating character in

the course of rotation. It can be seen that the current is also showing oscillations at the same time. The operating RPM is achieved suddenly and almost constant during the operation. The measured torque also shows oscillations due to the flexible clutch.

The presented measurement demonstrates that the system works properly but postprocessing the digitized signals need to be postprocessed.

5. SUMMARY

This paper dealt with design of a BLDC motor test bench. The required machine elements were designed in Autodesk Inventor 2020 CAD system. The elements were manufactured, and the system was assembled. A test measurement was performed to demonstrate its functionality. The system can determine the current, voltage, RPM and torque of a BLDC motor controlled under hydraulic loads. The advantage of the system that the load can be adjusted up to 50 bar hydraulic pressure.

ACKNOWLEDGEMENT

The described article was carried out as part of the EFOP-3.6.1-16-2016-00011 *Younger and Renewing University – Innovative Knowledge City – institutional development of the University of Miskolc aiming at intelligent specialisation* project implemented in the framework of the Szechenyi 2020 program. The realization of this project is supported by the European Union, co-financed by the European Social Fund.

REFERENCES

- [1] Krause, P. C., Wasynczuk, O., Sudhoff, S. D. (2002). *Analysis of Electric Machinery and Drive Systems*. New Jersey, USA, John Wiley & Sons, second edition.
- [2] Schultz, G. (2004). *Gleichstrommaschinen*. Lehrerausgabe, Hürth, Germany, Leybold Didactic GmbH.
- [3] Schultz, G. (2004). *Wechselstrommaschinen*. Lehrerausgabe, Hürth, Germany, Leybold Didactic GmbH.

CONCEPTIONAL CUTTING TOOL DESIGN FOR INTERNAL THREAD TURNING

DÁNIEL KISS¹ – GERGŐ MIHÁLYI²

¹University of Miskolc, Institutional Department of Machine Tools,
3515 Miskolc-Egyetemváros
kiss.daniel@uni-miskolc.hu

²BekoMold Kft.

Abstract: This article describes the different machining methods of the ball nut thread. One of the disadvantages of machining high pitch ball nuts by grinding process is to produce a modified tool profile to avoid collisions between the tool holder and the workpiece. However, by using profiled lathe inserts, it is possible to produce the thread profile of the ball nut using turning technology. The applicability of the technology is verified by tooling and experimental machining based on conceptual designs, the results of which are described at the end of the article.

Keywords: *turning, tool, ball nut*

1. MACHINING METHODS OF BALL NUTS

In recent decades, very narrow machining technology has become suitable for machining ball nuts, depending on the heat treatment condition of the workpiece [1], [2]. When cutting in the softened state, turning (*Figure 1*) and milling (*Figure 2*) technologies are applied, in hardened and case-hardened state grinding technology is used for finishing of ball nuts.

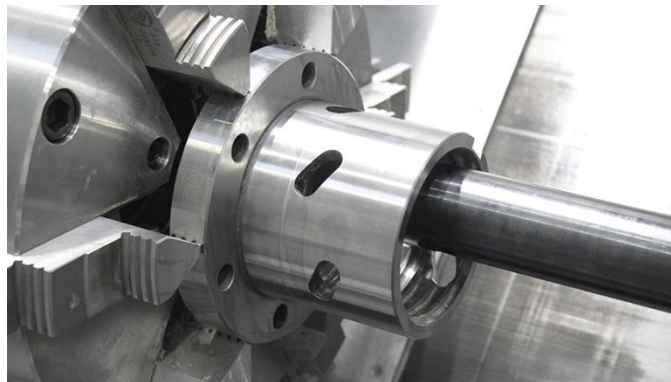


Figure 1
Internal threading of a ball nut [3]

Considering the lifespan of the ball nut, the martensitic tissue structure is widespread. The advantage of the martensitic fabric structure is the high hardness and wear resistance; however, this makes cutting difficult. For this reason, profile grinding is used as a finishing machining in conventional manufacturing operations, which can be used very well within certain technological constraints (nut inner diameter, thread length). The aim of this study is to investigate the possibility of hard turning for machining gothic-arc profile nuts in hardened or case-hardened condition.

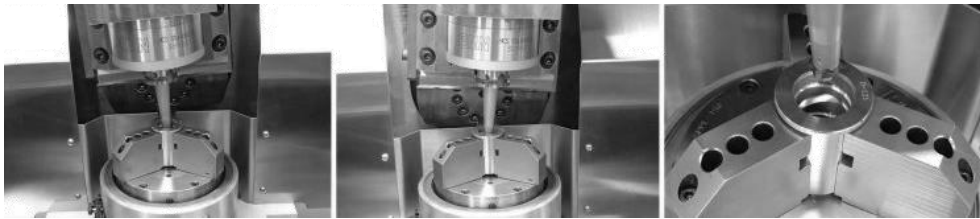


Figure 2
Internal thread milling of a ball nut [4]

For ball nuts with high pitch, a tool with a modified profile due to the pitch angle must be designed. To avoid profile distortion, turning and milling tools also solve this problem with back angle compensation. The size of the applied (working) back angle is obtained as the sum of the minimum back angle required for cutting the material quality and the angle of inclination calculated for the smallest diameter of the ball nut.

For this reason, milling technology cannot be applied to machining in a hardened state without effective tilting of the tool, as the result of large back angles adversely affects the edge environment of the tool. A further disadvantage is that only one-edge milling cutter can be considered without tilting, as the additional milling edges would chip the unmachined surfaces in the feed direction. If the milling tool can be tilted without collision during machining, a multi-edged tool is also suitable for cutting. One of its advantages is that more edges mean higher productivity, but the profiles of the edges cannot be precisely synchronized, thus it is not suitable for producing high-precision threads. This method can only be used productively for roughing, because when smoothing a profile, the contact ratio is less than 1, therefore only one edge can cut at a time.

The technological limitation of grinding is the internal diameter of the ball nut, the diameter of the grinding wheel and the thread length of the ball nut, since the grinding tool must be tilted in the axial direction according to the pitch angle [5]–[7]. In contrast to low- and medium-pitch nut versions, hardened profile grinding is not feasible in case of high thread lengths, for two main reasons. The pitch angle resulting from the long thread length and the large thread pitch results in a collision of the tool holder on the core hole diameter. The other main problem stems from the pitch angle, the greater the degree to which a profile tool must be tilted, the greater the degree of profile distortion. The value of the wheel tilt angle is also affected by

the diameter of the grinding wheel, which affects the speed of the tool. The disadvantage of the smaller grinding disc diameter is that it can operate technologically well at high speeds and reduces the disc tilt angle. *Table 1* lists specific technologies for ball screws production in the 20–80 mm range. In the table, it can be clearly seen that the preforms made by rolling are most prevalent in the left and lower table regions of the table. The main reason for this may be the force required for plastic forming, as the depth of the ball raceways also increases with increasing diameter. The technological limitations of grinding are limited by the pitch and the associated pitch angle, as the grinding wheel must be tilted according to the pitch angle.

For ball nuts which have at most 6° lead angle parameter, turning, milling and grinding technologies are also suitable for machining due to the negative effects of the previously mentioned geometrical and technological parameters.

Based on the experience gained in the industry, the upper limit of turning in the production of a ball nut is approximately $P/D \approx 0.63$ (where P is pitch, D is nominal diameter of ball nut). This ratio of 0.63 resulted in a high feed demand. In the case under study, this proportion is approximately 0.48, but in contrast to previous experience, cutting must be performed at a much greater depth of cut.

Table 1
Applied technologies on ballscrew depending on its sizes

		Nominal diameter (D) [mm]						
		20	25	32	40	50	63	80
Nominal pitch (P) [mm]	5	●○	●○	●○	●○			
	10	○	●○	●○	●○	●○	●○	●○
	15			○	○		○	
	20	●	●	●	●○	●○■	●○■	○■
	25					■	○■	○■
	30							○
	32			●				
	40			●	●			
	50	●	●					

●Rolled ○ Ground/Whirled ■ Heavy Duty Ground/Whirled

The individual technological limitations can be linked not only to the need for strength and power of the machining, but also to the manufacturability of the tool. The tiltability of the cutting inserts is not a particular problem, as such inserts are not produced in a tool body belonging to its position in cutting, but in a tool body with a so-called tiltability of $\gamma_{radial} = 0^\circ$ or $\gamma_{axial} = 0^\circ$, so the tool inserts are made with a distorted profile. The grinding limit for the primary back angle is approximately 30°, but can be higher with electrical discharge machining (EDM) and a suitable device. The manufacturing technology limitation is also limited by the tilting angle γ_{axial} of

the insert, as the useful profile width of the insert decreases with tilting, which limits the manufacturability of the required profile.

The literature differs in the definition of hard cutting technology, but it can be stated that steels with hardness 55–64HRC can be considered hard cutting. Inherent in the technology is that due to the high hardness, the shear plane does not form and the chip elements tear off the surface of the workpiece at the onset of a crack, while significant forces are exerted compared to the machining in the softened state.

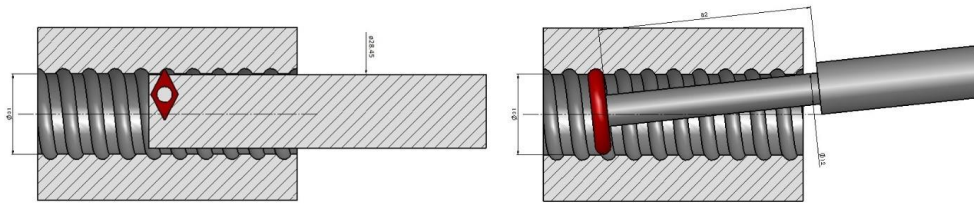


Figure 3
Hard turning (left) and profile grinding (right) of a ball nut [8]

Figure 3 shows the machining process of a ball nut in case of hard turning and grinding process. The different machining parameters and the achievable accuracies are listed in Table 2 (according to thread turning and thread grinding processes).

Table 2
The differences between hard turning and grinding

	Thread turning	Thread grinding
<i>Metal rate removal</i>	150–1,500 mm ³ /min	10–60 mm ³ /min
<i>Possible tool rigidity</i>	15–100 N/μm	0.1–8 N/μm
<i>Pitch errors</i>	0.5–2 μm	0.5 μm*
<i>Roughness Ra</i>	0.2–0.5 μm	0.1–0.4 μm*
<i>Accuracy class</i>	IT 1–2	IT 1–5

*According to the bibliographical references

Grinding was used for finishing in the early stages of hard turning. One of the environmental disadvantages of using grinding is that during grinding a so-called “grinding mud” is formed from the workpiece material and the components of the grinding wheel. Therefore, the material quality of CBN/PCBN has been purposefully developed, which, when applied with WIPER geometry, results in surface and microtopographic characteristics characteristic of the ground surface in hard turning. CBN technology also has limitations, such as hardness, i.e. it is not economical to use CBN below 48HRC. The CBN tool material is recommended for large series above 60HRC where the chance of payback is higher. To produce the ball nut, CBN technology causes several technological problems. In the case of the tested part, the profile of the ball nut is too wide, so due to the large temperature difference during soldering

of the *CBN* insert, the carbide bed can crush the *CBN* insert, so it would be expedient to use *CBN* coating layers, if any. However, there are boron-containing coatings which also show high hardness e.g. Ti_2B_2 or $TiBN$ [9].

Another problem that arises from the threading technology itself is that *CBN* inserts can be used at high cutting speeds as opposed to threading technology. Thus, thread cutting cycles are not possible due to low cutting speeds and high feeds. Another solution could be the type of coating with the fancy name *OERLIKON BALZERS ALDURA*, which is specifically recommended for machining high-hardness material grades. Ceramic insert tools can be included in the field of hard turning. The use of two known ceramics is widespread in industrial practice. Silicon nitride (Si_3N_4) is one of the known ceramics which is very advantageous for intermittent cutting, as its breaking strength is even higher than that of *CBN*. Silicon nitride also has a high oxidation resistance and is economical to use at higher cutting speeds. Ferrous metals are especially suitable for roughing strategies and are more economical to use at high cutting speeds and medium volume production. The proposed workpiece hardness limit is $50-55HRC$, located in terms of cost between carbide inserts and *CBN* insert inserts.

Alumina (Al_2O_3) ceramics are used for cutting continuous surfaces (smoothing technologies) and should be used in an even higher cutting speed range than silicon nitride. Similar to silicon nitride ceramics, alumina also has high oxidation resistance. Both ceramics are only recommended for dry cutting, as the tool material snaps upon cooling. With its high oxidation resistance compared to other tool materials, it is specifically used in higher temperature ranges.

Conventional carbide insert grades can also be used for hard cutting, but at low cutting speeds and up to $55HRC$ hardness. It is worth applying when talking about low-volume production, as the service life of carbide is significantly reduced during hard cutting.

2. DESIGN OF CUTTING TOOL FOR BALL NUT THREAD TURNING PROCESS

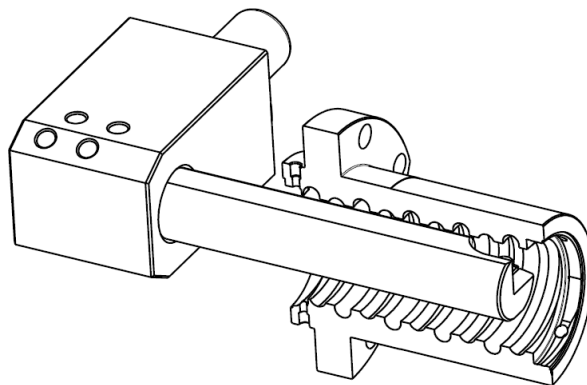


Figure 4

Conceptional design of cutting tool for ball nut thread

The conceptional design of the shank and the insert was performed for a ball nut with dimensions $D = 50 \text{ mm}$ nominal diameter and $P = 25 \text{ mm}$ nominal pitch. *CATIA V5R19* software was used for conceptual design. The schematic diagram of the developed conceptual tool is illustrated in the *Figure 4*.

For the test cutting, it was necessary to manufacture the previously designed cutting insert and tool shank (*Figure 5*).



Figure 5

The manufactured cutting insert (left) and shank (right)

Test conditions for experimental machining of the thread surface:

- machine tool: *DMG CTX Alpha 500* (controller: *SINUMERIK 840D*),
- coolant lubricant was applied,
- spindle speed: $n = 180 \text{ min}^{-1}$ (cutting speed: $v_c \approx 30 \text{ min}^{-1}$),
- feed rate: $f = 25 \text{ mm}$.

The self-excitation phenomenon of the elements involved in the cutting be a function of the distance from the end plate, which also requires further tests as a function of the depth of cut.



Figure 6

Result of an experimental machining of the ball nut thread

In the initial stage of cutting, when even the insert is not working in the full cross-section of the profile, the vibrations are not significant. With the full operation of the profile section (moving towards the workpiece gripper), the vibrations are amplified, and the phenomenon of self-excitation can be sensed from the fact that the grooves gradually deepen on the workpiece surface along the thread length. In the left part of the *Figure 6*, both the beginning and the end of the run can be observed for comparison. The thread surface is smooth at the beginning of machined surface; however, the surface roughness becomes rougher with increasing thread length. This type of self-excitation can also be a defect on the tool carriage.

3. SUMMARY

The article provides a brief summary of the manufacturing technology options for machining the inner thread surface of ball nuts. Based on the literature and previous experience, soft turning and thread milling are primarily suitable for rough cutting of ball raceways. Suitable tooling was designed for experimental machining to make the thread surface of a ball nut of a given size, where the evaluation of machining results shows that conventional thread grinding and hard turning should be chosen to achieve adequate dimensional accuracy and surface roughness if a machine tool with stiffness and stability is available.

ACKNOWLEDGEMENT

The article was carried out as part of the EFOP-3.6.1-16-00011 *Younger and Renewing University – Innovative Knowledge City – institutional development of the University of Miskolc aiming at intelligent specialization* project implemented in the framework of the Szechenyi 2020 program. The realization of this project is supported by the European Union, cofinanced by the European Social Fund.

REFERENCES

- [1] Rech, J., Moisan, A. (2003). Surface integrity in finish hard turning of case-hardened steels. *International Journal of Machine Tools and Manufacture*, 43 (5), pp. 543–550.
- [2] Bartarya, G., Choudhury, S. (2012). State of the art in hard turning. *International Journal of Machine Tools and Manufacture*, 53 (1), pp. 1–14.
- [3] <https://danobatgrinding.com/en/balls-screw-nut-machining> (accessed: 8 September 2020).
- [4] *Introducing Drake GS: VTM-LM* (brochure).
- [5] Harada, H., Kagiwada, T. (2004). Grinding of high-lead and gothic-arc profile ball-nuts with free quill-inclination. *Precis Eng.*, 28 (2), pp. 143–151., doi.org/10.1016/j.precisioneng.2003.07.003.
- [6] Hegedűs, Gy., Patkó, Gy., Takács, Gy. (2012). Determination of Tool Profile for Ballnut Grinding by Numerical Methods. *Proceedings of the 13th International Conference on Tools*, ICT 2012, ISBN:978 963 998835 4.
- [7] Hegedűs, G. (2015). Newton's method-based collision avoidance in a CAD environment on ball nut grinding. *The International Journal of Advanced Manufacturing Technology*, doi. org/10.1007/s00170-015-7796-5.
- [8] Why hard turning is up to three times faster than grinding. *Article- Hembrug Machine Tools*, <https://www.hembrug.com/hardtturningballscrewnuts/>.

- [9] More, A., Jiang, W., Brown, W., Malshe, A. (2006). Tool wear and machining performance of cBN–TiN coated carbide inserts and PCBN compact inserts in turning AISI 4340 hardened steel. *Journal of Materials Processing Technology*, 180 (1–3), pp. 253–262., doi.org/10.1016/j.jmatprotec.2006.06.013.

ANALYSIS OF DMU40 MACHINE CENTRE BY FINITE DEGREES OF FREEDOM

RÓBERT KISS – ATTILA SZILÁGYI

University of Miskolc, Department of Machine Tools
3515 Miskolc-Egyetemváros
robert.kiss9405@gmail.com, szilagyi.attila@uni-miskolc.hu

Abstract: This article is part of a longer research-analytical work, because it outlines the results and conclusions of the study according to the main topic of the research and the applies method. The central theme of the research is the dynamic stiffness of machine tools and the various methods for their determination. The first such (finite element) method is modal analysis, which allows for an analytical test. The purpose of this article is to approach this study from the practical side through a specific example.

Keywords: *analytical method, dynamic stiffness, modal analysis, natural frequency, FEM*

1. INTRODUCTION

During the test, the primary goal was to set up the mechanical and mathematical model of the DMU40 machine centre, in order to achieve more realistic results. Machine tools always form a vibrating system due to the generated vibrations and following this line the machine tools can be considered as a multi degree of freedom, damped, linear vibration systems which containing excited vibration [1] [3]. The mathematical model based on the mentioned systems and on the vibration model. After sketching the mechanical model, the mathematical model can be written in the form of a differential equation system, which provides the deformation of each component (machine base, x-slide, y-slide, z-slide) in different directions as a function of time (amplitude-time diagrams).

Dynamic stiffness is basically influenced by the following factors: static stiffness, oscillation frequency, natural frequency and the Lehr-damping. Moreover, the dynamic stiffness and the magnitude of the damping at the local frequencies can be considered as dynamic characteristics of a vibrating system.

Because of the precision, shape accuracy and surface roughness are all important criteria in the production and whereas these are greatly influenced by vibrations, so first of all the above-mentioned natural frequency locations should be determined and this can improve the precision and quality of the manufacturing.

2. MECHANICAL MODEL

Figure 1 is shown the examined catalog image of a 5-axis CNC controlled machine centre (without cover) which can be found in the department's workshop and aligns it with the mechanical model of the same machine.

On the vibration model beside the four main building units, there are linear guideways, ball screw-ball nut systems which are connecting to the main units. These items have been replaced by springs and dampers on the mechanical model. Later, based on catalog data, these spring stiffness values and damping factors became determinable.

The structure equation of the machine centre:

$$A_I \mathbf{0}_F(s, 4) X(s, 1) Y(s, 2) Z(m, 1) R_y(s, 3) R_z(m, 2)$$

The following picture (Figure 1) contains the examined machine tool (without cover) and this machine's vibration model (with replacement models in case of the linear guideways and the ball screw-ball nut systems):

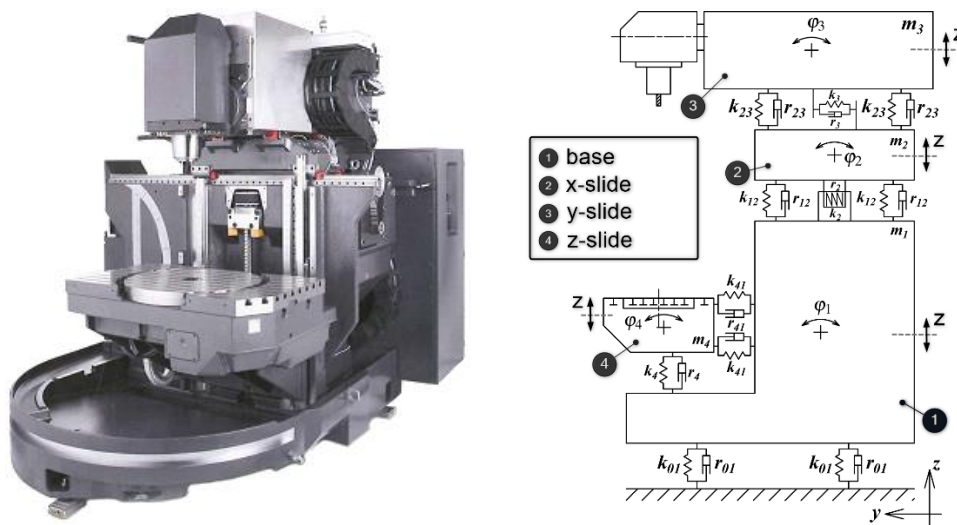


Figure 1
Catalog image and mechanical model of the machine tool [2]

Where each parameter meaning:

- k [N/m] – spring stiffness
- r [Ns/m] – damping factor
- φ – angle of rotation
- z – linear displacement

3. MATHEMATICAL MODEL

The above mechanical model (*Figure 1*) can be used to describe the system's motion equation using the Lagrange's Equations of Motion of Second Kind [4]. This allows both linear displacements and angle of rotations to be taken into account. Taking the damping into account, the basic context can be written as:

$$\frac{d}{dt} \left(\frac{\partial \alpha}{\partial \dot{q}_i} \right) - \frac{\partial \alpha}{\partial q_i} + \frac{\partial Q_f}{\partial \dot{q}_i} = Q_f \quad (1)$$

By writing the (1) Lagrange-function and performing the mathematical operations in the above context, we obtain the following differential equation system:

$$\begin{aligned} \ddot{z}_1 &= \frac{1}{m_1} \left[-\frac{z_1}{c_{01}} - \frac{z_1 - z_2}{c_{12}} - \frac{z_1 - z_4}{c_{41}} - \frac{(l_{12} - l_{11})\varphi_1}{2c_{01}} - \frac{(l_{21} - l_{22})\varphi_2}{2c_{12}} + \frac{(l_{42} - l_{41})\varphi_4}{2c_{41}} \right] \\ \ddot{\varphi}_1 &= \frac{1}{J_1} \left[-\frac{(l_{12} - l_{11})z_1}{2c_{01}} - \frac{(l_{12}^2 + l_{11}^2)\varphi_1}{2c_{01}} \right] \\ \ddot{z}_2 &= \frac{1}{m_2} \left[-\frac{z_2 - z_3}{c_{23}} - \frac{z_2 - z_1}{c_{12}} - \frac{(l_{31} - l_{32})\varphi_3}{2c_{23}} - \frac{(l_{22} - l_{21})\varphi_2}{2c_{12}} \right] \\ \ddot{\varphi}_2 &= \frac{1}{J_2} \left[-\frac{(l_{21} - l_{22})z_1}{2c_{12}} - \frac{(l_{22} - l_{21})z_2}{2c_{12}} - \frac{(l_{21}^2 + l_{22}^2)\varphi_2}{2c_{12}} \right] \\ \ddot{z}_3 &= \frac{F_g}{m_3} + \frac{1}{m_3} \left[-\frac{z_3 - z_2}{c_{23}} - \frac{(l_{32} - l_{31})\varphi_3}{2c_{23}} \right] \\ \ddot{\varphi}_3 &= \frac{1}{J_3} \left[-\frac{(l_{31} - l_{32})z_2}{2c_{23}} - \frac{(l_{32} - l_{31})z_3}{2c_{23}} - \frac{(l_{31}^2 + l_{32}^2)\varphi_3}{2c_{23}} \right] \\ \ddot{z}_4 &= \frac{1}{m_4} \left[-\frac{z_4 - z_1}{c_{41}} - \frac{(l_{42} - l_{41})\varphi_4}{2c_{41}} \right] \\ \ddot{\varphi}_4 &= \frac{1}{J_4} \left[-\frac{(l_{42} - l_{41})z_4}{2c_{41}} + \frac{(l_{42} - l_{41})z_1}{2c_{41}} - \frac{(l_{42}^2 + l_{41}^2)\varphi_4}{2c_{41}} \right] \end{aligned} \quad (2)$$

This (2) DE system was solved using the Maple (this is a mathematical software), based on the Runge-Kutta method. The diagram in *Figure 2* shows the degree of deformation in the z-direction for each component, for the above mechanical system. In the undamped case, oscillatory motion of the mass is observed, while in the damped case (*Figure 2*) the damping absorbs energy, causing the vibration of the system to disappear after a certain period of time [5].

The maximum displacement is related to the y-slide and its magnitude $z \approx (-2 \div 2) \mu m$.

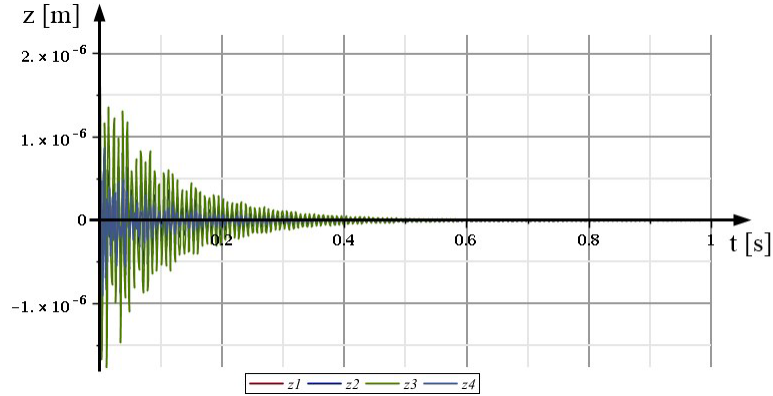


Figure 2

Amplitude-time diagram – in damped case

Modal analysis deals with the study of vibration characteristics and allows the determination of the natural frequencies of any physical system.

The basic equation of the modal analysis [6]:

$$\underline{\underline{M}} \cdot \underline{\dot{q}} + \underline{\underline{K}} \cdot \underline{q} = \underline{f} \quad (3)$$

Modifying the above *Equation (3)*, the resulting relation can be traced back to an eigenvalue task, which problem is the next:

$$\underline{\underline{M}}^{-1} \cdot \underline{\underline{K}} = \alpha^2 = \lambda \quad (4)$$

If we solve this *Equation (4)*, we will get the following natural frequencies, which based on the above-mentioned eight degree of freedom vibration system (*Figure 3*):

mode	$\lambda \left[\frac{\text{rad}^2}{\text{s}^2} \right]$	$\alpha \left[\frac{\text{rad}}{\text{s}} \right]$	T [s]	f [Hz]
1	$4.553 \cdot 10^5$	674.740	0.0093	107.3882
2	$7.112 \cdot 10^5$	843.328	0.0075	134.2199
3	$1.011 \cdot 10^6$	1005.586	0.0062	160.0439
4	$1.932 \cdot 10^6$	1389.829	0.0045	221.1982
5	$3.955 \cdot 10^6$	1988.684	0.0032	316.5089
6	$5.662 \cdot 10^6$	2379.484	0.0026	378.7066
7	$1.153 \cdot 10^7$	3396.107	0.0019	540.5072
8	$1.716 \cdot 10^7$	4142.302	0.0015	659.2678

Figure 3

A summary of the results obtained

4. SUMMARY

In this article we have presented a possible method for determining the dynamic stiffness (natural frequencies) of a machine centre. This method is extremely time consuming due to the high computing and work requirements of multi degree of freedom systems. However, in simpler cases it may be faster and easier than other methods. The results obtained were approximately the same as for other methods.

ACKNOWLEDGEMENT

The described article/presentation/study was carried out as part of the EFOP-3.6.1-16-2016-00011 *Younger and Renewing University – Innovative Knowledge City – institutional development of the University of Miskolc aiming at intelligent specialisation* project implemented in the framework of the Szechenyi 2020 program. The realization of this project is supported by the European Union, co-financed by the European Social Fund.

REFERENCES

- [1] Kiss, R., Szilágyi, A. (2019). Analysis of the dynamic behaviour of the CNC machine centre by FEM. *DMS Journal*, Miskolc, Vol. 9, No. 1, pp. 24–28.
- [2] *DMU monoBLOCK Series catalogue*. <https://www.dmg.com>, downloaded: 2018. 01. 26.
- [3] Kiss R. (2019). *CNC megmunkáló központ dinamikai viselkedésének vizsgálata végelem-módszerrel*. Diplomaterv, Miskolc.
- [4] Csernák G., Stépán G. (2012). *A műszaki rezgésstan alapjai*. Egyetemi jegyzet, Budapest, BME.
- [5] Dömötör F.: *Rezgésdiagnosztika I*. Dunaújváros, Dunaújvárosi Főiskola.
- [6] Pascal, M. (2012). *Parallelization of Design and Simulation: Virtual Machine Tools in Real Product Development*. Doctoral Thesis, ETH Zürich.

ANALYSIS OF DMU40 MACHINE CENTRE BY CAE SOFTWARE

RÓBERT KISS – ATTILA SZILÁGYI

University of Miskolc, Department of Machine Tools
3515 Miskolc-Egyetemváros
robert.kiss9405@gmail.com, szilagyi.attila@uni-miskolc.hu

Abstract: This article is part of a longer research-analytical work, because it outlines the results and conclusions of the study according to the main topic of the research and the applied method. The central theme of the research is the dynamic stiffness of machine tools and the various methods for their determination. After analytical testing, we will deal with another method, because we also use CAE software (ANSYS Workbench R19.1) to perform previous tests in the form of simulations. The results obtained are compared with the values previously determined analytically.

Keywords: ANSYS R19.1, CAE, dynamic stiffness, modal analysis, natural frequency, FEM

1. INTRODUCTION

One of the most commonly used finite element method (FEM) for mechatronic problems is a structural analysis [1] [3]. In mechanical engineering we mean the examination of mechanical elements by the structural analysis under, which can be done e.g. a specific part (shaft) or subassembly (machine base of a lathe or a milling machine) of a machine, or even the machine itself (machine centre) (*Figure 1*). The main purpose of the calculations is to determine the linear displacement or angular of rotation, from which additional quantities may be derived, such as elongation, stress or reaction force.



Figure 1
Catalog image of the examined machine tool [2]

The CAE (Computer Aided Engineering) software, what we used during the simulations, is the ANSYS Workbench R19.1, which is generally an extremely complex engineering software package, that can be widely used in the industry due to its large number of simulation capabilities (*Figure 2*).

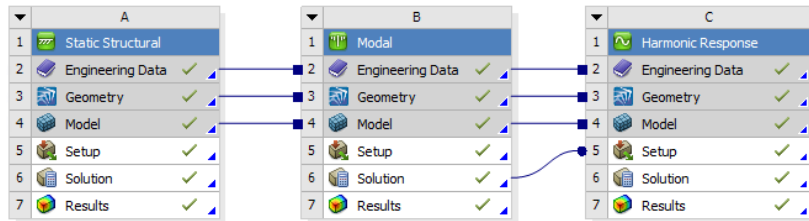


Figure 2

Types of simulations applied to the machine tool 3D model

Briefly the main types that can be examined using finite element software are:

- **Static analysis:** Method for the calculation of permanent deformation or stress due to time independent load. It does not take into account the elements causing possible damping and inertia, that is time-dependent loads.
- **Modal analysis:** Suitable for the determination of the vibration characteristics of the structure under simulation, as well as the individual natural frequencies and the representation of their oscillations. It can serve as a baseline for more detailed dynamic investigations (e.g. transient dynamic, harmonic or spectral analysis).
- **Harmonic response analysis:** Used to determine a steady-state response to a cyclically changing excitation over time. The test ignores transient phenomena occurring at the beginning of the load. It makes it possible to predict the long-term dynamic behaviour of the structure under investigation, to examine the phenomena of fatigue and resonance.

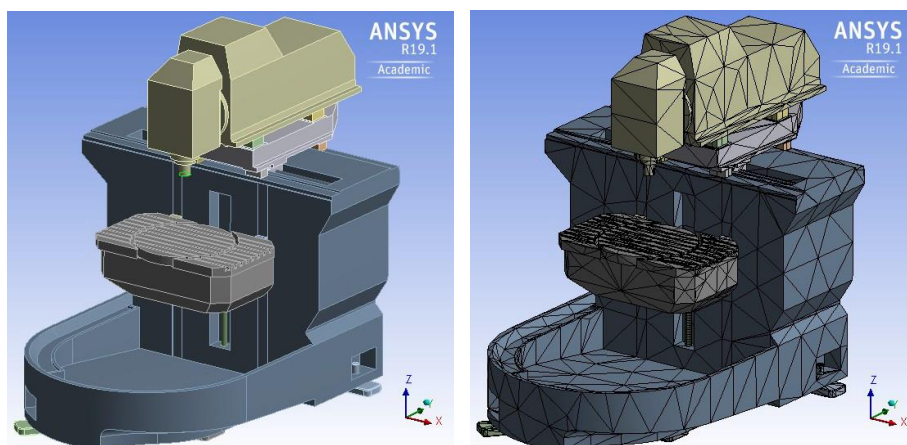


Figure 3

The studied 3D model after import and meshing

The (simplified) 3D model of the machine tool is essential for the test, what we made with a 3D design software, which called NX11, taking into account catalog data and a machine centre, which can be found in the department's workshop. *Figure 3* shows the 3D model of the machine, which is already in parasolid format, appears as an imported model in the ANSYS model space and in parallel with its post-meshed state.

2. MODAL ANALYSIS

Any physical system can vibrate or can do vibrating motion. In this case the natural frequencies of the possible free vibrations and the various vibrational forms (modes) are considered to be the properties of the system.

In an analytical case, after constructing the mechanical model of the system, solving the mathematical model (the differential equation describing the motion or the system of differential equations), the system's natural frequencies can be derived. Moreover, its associated eigenvalues, which is now executed by a finite element software based on the available information (e.g. 3D geometry, constraints, boundary conditions, mesh properties, element size, damping factors, material quality...).

During the analysis the built geometry of the model is completely broken into elements of finite size. Constructs stiffness, mass and damping matrices for the structure as a whole from matrices describing the characteristics of these elements.

Using the matrix method for dynamic systems leads to the following differential equation system [4] [6]:

$$[M]\{\ddot{x}\} + [D]\{\dot{x}\} + [K]\{x\} = \{f\}, \quad (1)$$

where $\{f\}$ is the forcing term, $[M]$, $[D]$, $[K]$ are the matrices of masses, dissipation and stiffness, while $\{\ddot{x}\}$, $\{\dot{x}\}$, $\{x\}$ are the coordinates of acceleration, velocity and displacement in that order.

Main steps of the simulation:

1. Import the 3D geometry of the machine centre into ANSYS.
2. Selecting the types of simulations, establishing the relations between the tests, as shown in *Figure 2*.
3. Check the relations and connections, what the ANSYS automatically created before, and if it is necessary correct that. After, define and assign material quality to each component.
4. Define meshing settings, methods and then meshing the model (*Figure 3*).
5. Specifying boundary conditions and constraints on the model.
6. Specify simulation settings: number of modes to look for, method selection, damping consideration, damping factors, and other settings.
7. Run the simulation and evaluate the results.

Following the above-mentioned steps, we have obtained the following results, which are the roots of (1) at the same time (*Table 1*):

Table 1
The natural frequencies computed numerically

mode	1	2	3	4	5	6	7	8
f [Hz]	108.16	132.98	159.49	229.01	325.65	379.22	538.34	663.45

After running the simulation, in addition to determining the values of the natural frequencies the software capable for displaying the degree of deformation of the individual natural frequencies in the simulation assembly as well. That is, the program displays the vibration images for each mode. After specifying the damping factors for each material type and, in the modal analysis settings with the damping option selected it is possible to determine the natural frequencies in the damped case. However, no significant change can be observed in the results obtained, since the effect of damping is primarily manifested in a decrease in the amplitude [5]. The software can display the oscillations shown in *Figure 4* below at some of the machine's natural frequency locations, that is for each mode:

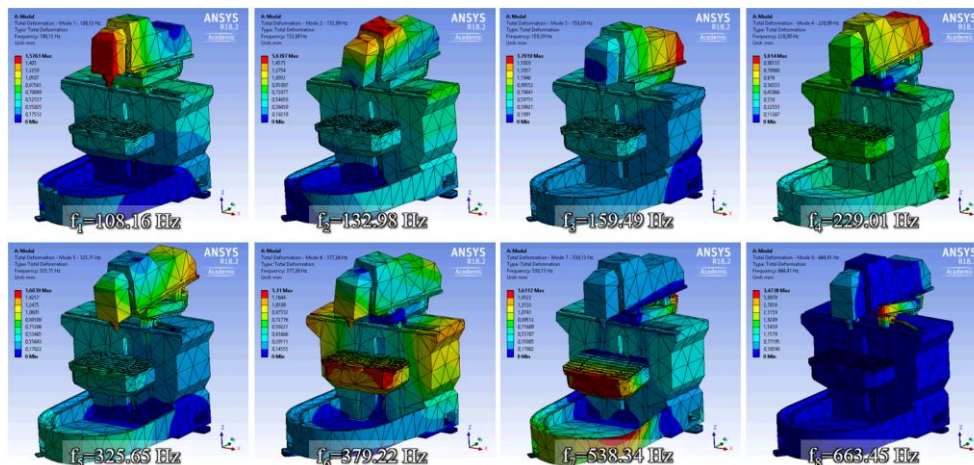


Figure 4
Results of modal analysis – vibration images

3. SUMMARY

In this article, we have presented a possible method for determining the dynamic stiffness (natural frequencies) of a machine centre. Testing with CAE (Computer Aided Engineering) software enables fast and accurate computation, if we have a right 3D model and the material quality of each element which information necessary to run the simulation. In terms of results, the previously analytically calculated natural frequency values approximate the software-calculated data. In addition, the vibration images show that the dynamic stiffness of the machine in the z-direction is the weakest.

ACKNOWLEDGEMENT

The described article/presentation/study was carried out as part of the EFOP-3.6.1-16-2016-00011 *Younger and Renewing University – Innovative Knowledge City – institutional development of the University of Miskolc aiming at intelligent specialisation* project implemented in the framework of the Szechenyi 2020 program. The realization of this project is supported by the European Union, co-financed by the European Social Fund.

REFERENCES

- [1] Kiss, R., Szilágyi, A. (2019). Analysis of the dynamic behaviour of the CNC machine centre by FEM. *DMS Journal*, Miskolc, Vol. 9, No. 1, pp. 24–28.
- [2] *DMU monoBLOCK Series catalogue*. <https://www.dmg.com>, downloaded: 2018. 01. 26.
- [3] Kiss R. (2019). *CNC megmunkáló központ dinamikai viselkedésének vizsgálata végelelem-módszerrel*. Diplomaterv, Miskolc.
- [4] Csernák G., Stépán G. (2012). *A műszaki rezgésstan alapjai*. Egyetemi jegyzet, Budapest, BME.
- [5] Dömötör F. (2008). *Rezgésdiagnosztika I*. Dunaújváros, Dunaújvárosi Főiskola.
- [6] Pascal, M. (2012). *Parallelization of Design and Simulation: Virtual Machine Tools in Real Product Development*. Doctoral Thesis, ETH Zürich.

ANALYSIS OF DMU40 MACHINE CENTRE BY VIBRATION MEASUREMENT

RÓBERT KISS – ATTILA SZILÁGYI

University of Miskolc, Department of Machine Tools
3515 Miskolc-Egyetemváros
robert.kiss9405@gmail.com, szilagyi.attila@uni-miskolc.hu

Abstract: This article is part of a longer research-analytical work, because it outlines the results and conclusions of the study according to the main topic of the research and the applied method. The central theme of the research is the dynamic stiffness of machine tools and the various methods for their determination. Following analytical analysis the machine tool natural frequencies were determined using a finite element software (ANSYS Workbench R19.1), which we now approach from a practical point of view, that is determined in the workshop by measurements. The results obtained are compared for each of the three methods.

Keywords: *DMU40, accelerometer sensor, measurement procedure, vibration measurement, natural frequency*

1. INTRODUCTION

The determination of the natural frequencies of different machines and equipment is important in several aspects, because this will allow the error to be detected in time and can assist in the repair or redesign of the equipment under investigation. It can also clarify the diagnosis made during the vibration test. Based on machine vibration, you can get a comprehensive picture of the machine state and consequently the current state of each machine part.

In the field of vibration diagnostics, three test methods are typically used: bearing vibration test, resonance test and motion-animation test.

The modal analysis analytically derived by the finite element method and executed by the software can be used in practice to describe the vibrations of flexible bodies and related properties [1] [2]. A flexible body can also be considered mechanically known if it is possible to predetermine the motion of the flexible body, even if it is excited at any point by a force function.

Calculations of the natural frequencies can be done by analytically (using the finite element method – modal analysis) [3], but this testing is very complicated and has a much higher chance of error and hence of error. We also used software to determine the individual natural frequencies, oscillations and resonance curves for the machine tool under examination.

Here the focus is on building the 3D model, because for various reasons it is not possible to create a machine tool model in such detail as in reality, various simplifications will result in inaccurate calculations [4] [5]. This is why experimental testing is needed to compare the results of previous calculations and measurements and to further refine certain elements of the 3D assembly as well as the vibration model itself.

2. MAIN FEATURES AND PROCEDURE OF MEASUREMENT

The purpose of the measurement is to investigate the dynamic stiffness of a 5-axis CNC machine centre at the department's workshop. Examination of the behaviour of a tool that is unbalanced during the measurement in the environment of natural frequencies which was previously defined by analytical and software as a function of speed.

Measuring instruments:

- acceleration sensor: Kistler 8632C50,
- teflon-insulated connection wiring,
- charging amplifier: Kistler 5134,
- measuring amplifier: HBM Spider 8,
- display device: laptop,
- evaluation software: HBM Catman 4.0

Measurement of vibration acceleration at unspecified tool at predetermined measuring point(s) near the spindle of the tested machine (CNC machine centre) by rotating the spindle at different revolutions, around the natural frequencies determined by previous calculations or software FEM analyses.

2.1. Preparation of the measurement, assembly of the measurement circuit

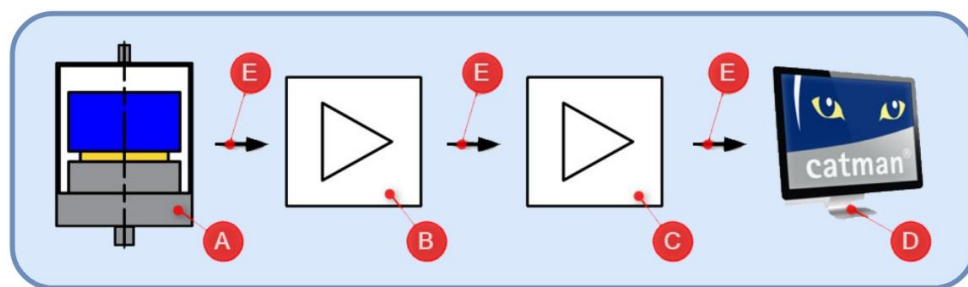


Figure 1
Outline of measurement set-up

Where the devices in *Figure 1* are: A) a vibration accelerometer; B) charge amplifier; C) measuring amplifier; D) an evaluation tool; E) wiring.

2.2. Determining the measuring point, fixing the sensor at the selected point

The machine cover makes it very difficult to place the accelerometer sensor. In the study, we focused primarily on the y-slide and within it the spindle environment. Since the excitation was not a pulse hammer, but the effect of unbalanced tool vibrations was investigated, it was advisable to place the measuring point as close to the spindle as possible.

2.3. Adding excitation to the system

After turning on the CNC machine centre, we set pre-determined speeds for the spindle speed. A diameter 40 mm cutting tool was installed in the spindle to hold four inserts, but to ensure unbalance, only one cutting insert was installed in the tool. After adjusting each speed, the sensor measured data (vibration acceleration values) were saved from Catman 4.0 in Excel format, so the measured data was further evaluated using Excel and Maple software.

2.4. Perform the measurement

Figure 2 depicts the measurement installation by displaying the accelerometer used for vibration testing.

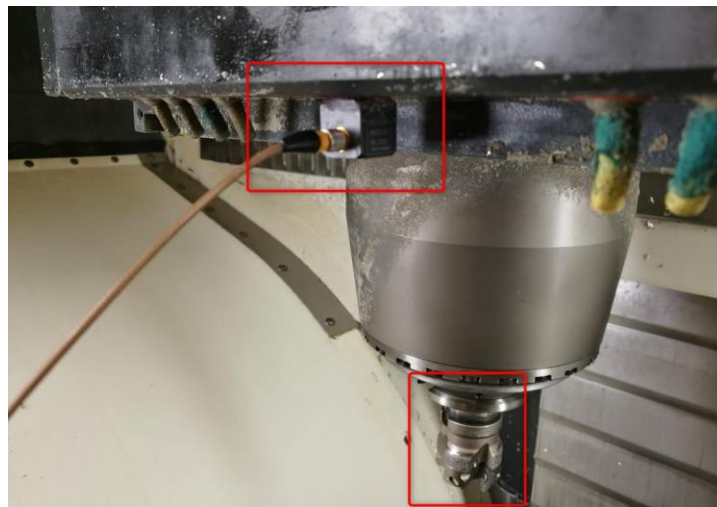


Figure 2

Vibration acceleration sensor at the measuring point and unbalanced tool

2.5. Evaluation of results

From the measurement results, that is the response of the machine tool, the characteristic frequency values of the machine at each speed can be read out using the frequency spectrum (*Figure 3, Figure 4, Figure 5*). Knowing these results, they become

comparable with previously obtained analytical results and with data calculated by the finite element software.

The final conclusion can then be drawn to determine the extent to which the calculated and measured results differ from each other and to adjust the vibration model and the 3D assembly drawing of the machine tool accordingly.

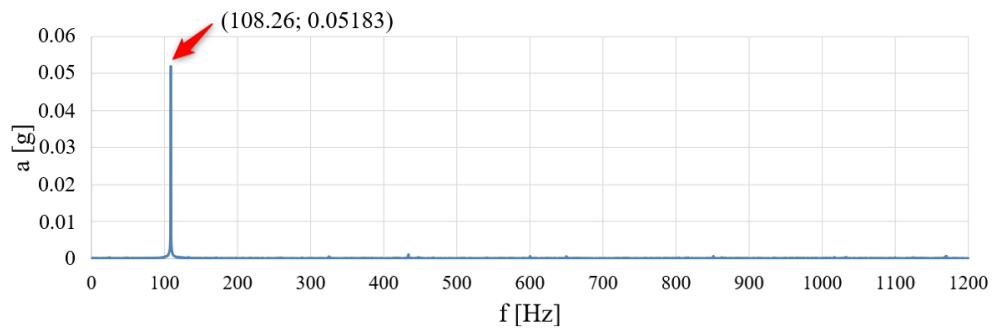


Figure 3
Frequency spectrum 1

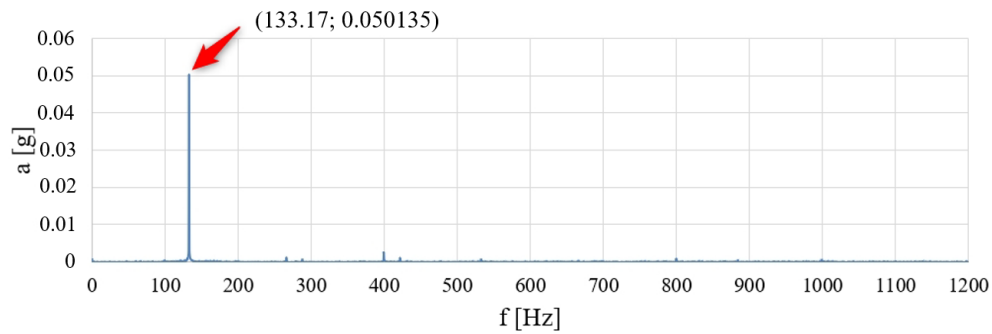


Figure 4
Frequency spectrum 2

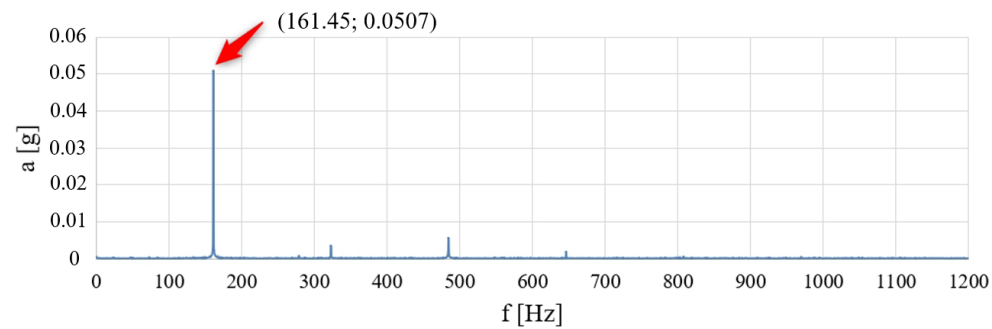


Figure 5
Frequency spectrum 3

The data obtained gives a visual picture, when the sample is transformed by Fourier-transformation and a frequency spectrum is plotted from them. The diagrams thus converted are illustrated in *Figure 3*, *Figure 4* and *Figure 5* above. Based on the above it can be concluded that the measured structure has its natural frequency at the following frequency locations:

1. 108,26 Hz
2. 133,17 Hz
3. 161,45 Hz

3. SUMMARY

In this paper we have presented another possible method for determining the dynamic stiffness (natural frequencies) of a machine centre. Testing with CAE (Computer Aided Engineering) software enables fast and accurate computation, if we have a right 3D model and the material quality of each element which information necessary to run the simulation. In terms of results, the previously analytically calculated natural frequency values approximate the software-calculated data. The results of the methods are summarized in *Table 1* below.

4. CONCLUSION

In order to achieve more accurate manufacturing and better surface quality, care should be taken to avoid operating the machine centre at and above its natural frequencies as defined during manufacturing.

Table 1
Comparing the natural frequencies computed analytically, numerically and experimentally

Natural frequency	Analytically	Ansys R19.1	Measurement
f ₁	107,39Hz	108,12Hz	108,26Hz
f ₂	134,22Hz	132,89Hz	133,17Hz
f ₃	160,04Hz	159,29Hz	161,45Hz
f ₄	221,20Hz	228,89Hz	–
f ₅	316,51 Hz	325,71 Hz	–
f ₆	378,71 Hz	377,26 Hz	–
f ₇	540,51 Hz	538,13 Hz	–
f ₈	659,27 Hz	664,41 Hz	–

ACKNOWLEDGEMENT

The described article/presentation/study was carried out as part of the EFOP-3.6.1-16-2016-00011 *Younger and Renewing University – Innovative Knowledge City – institutional development of the University of Miskolc aiming at intelligent specialisation*

project implemented in the framework of the Szechenyi 2020 program. The realization of this project is supported by the European Union, co-financed by the European Social Fund.

REFERENCES

- [1] Kiss, R., Szilágyi, A. (2019). Analysis of the dynamic behaviour of the CNC machine centre by FEM. *DMS Journal*, Miskolc, Vol. 9, No. 1, pp. 24–28.
- [2] Kiss R. (2019). *CNC megmunkáló központ dinamikai viselkedésének vizsgálata végelem-módszerrel*. Diplomaterv, Miskolc.
- [3] Csernák G., Stépán G. (2012). *A műszaki rezgés tan alapjai*. Egyetemi jegyzet, Budapest, BME.
- [4] Dömötör F. (2008). *Rezgésdiagnosztika I*. Dunaujváros, Dunaujvárosi Főiskola.
- [5] Pascal, M. (2012). *Parallelization of Design and Simulation: Virtual Machine Tools in Real Product Development*. Doctoral Thesis, ETH Zürich.

DEMAND FOR RECYCLING FILAMENT IN 3D PRINTING

BARBARA KMETZ – ÁGNES TAKÁCS

University of Miskolc, Department of Machine and Product Design
3515 Miskolc-Egyetemváros
takacs.agnes@uni-miskolc.hu; kmetzbarbara@gmail.com

Abstract: In the study the brief history of 3D printing is written, how the recent past and present is changing the open source movement. The FDM extrusion technology is reviewed in the text, also the areas where the technology can be used. There is a detailed description about the Creality Ender 5 printer and its printed objects. The study's next main part contains the conceptual design of a filament recycling machine. After the needed market and patent research the functions are established, concepts of the machine are determined. These were evaluated and an optimal sketch was chosen as a result

Keywords: *3D printing, recycling, Creality Ender 5, filament, Ceres (Valdez) principles*

1. INTRODUCTION

3D printing is becoming one of nowadays most popular additive manufacturing technologies. It spreads in wide scales during the past two decades, nowadays many types of 3D printing are existing. Its history cannot look back to a long time instead it began in the 1990s, so its evolution is well documented. With 3D printing three dimensional objects are made first with the help of three-dimensional designing programs, then the models are printed out with the chosen technology.

Specially manufactured materials should be used for 3D printing. These strings are called filaments. Filaments can contain metal, polymer, ceramic, composites, so called smart materials and even special materials like food (pizza). Some other materials can also be mentioned as a printing material such as textile, concrete and their numbers are expanding day by day. Though most of the filaments are polymers, which raises many environmental questions for us.

The application of 3D printing is amusingly vast. This technology is used in aerospace engineering, in the automotive industry, in the architecture industry, in the construction industry, in electronics, in medical areas and in many other fields of science. Today thousands of hobby 3D printers are brought around the world for personal use for those who want to create something unique. Hobby 3D printers are both reasonably priced and available for amateurs. The most common printing materials are polymers with different specifications. A great deal of filaments can be recycled therefore filament recycling machines are needed. The aim of the study was to establish the conceptual design of a filament recycling machine. [3]

2. THE TECHNOLOGY OF 3D PRINTING

The reason for the different kind of printing technologies is the same in case of a regular 2D printing. The following six points are the most defining in connection with what kind of technology we should use for making the objects. These factors are the following: the price of the printer, the quality of the printer, the printing speed, the limitations of the printer, which printer is practical for the print and what are the expectations of the user. The printer should be selected by carefully examining all the parameters, which are required for the printing and the object should be made according to these factors. [4] The steps of the printing processes are quite alike for all the technologies with some minor differences:

- Necessary a three-dimensional designing software,
- Creating the 3D model in the designing software,
- Saving the print in CAD (Computer Aided Design) format, like *.stl, *.step, *.iges,
- Downloading a 3D printing software (Cura, MakerBot Print, PrusaSlicer, Simplify3D), 95% of these softwares can be purchased for free,
- The 3D model should be imported into the program and it must be sliced according to the installed parameters,
- The program saves the appropriate code for the printer then the code is copied to a data storage or transferred directly to the printer,
- The printer reads the code and starts to print the object layer by layer,
- The printed object is finished.



Figure 1
The process of the printing

2.1. Fused Deposition Modelling (FDM) printing technology

Fused Deposition Modelling is one of the most popular printing technologies, because the machines are affordable (relatively cheap) and the required softwares are available easily for everybody, besides the printing materials are also well priced and can be accessed easily. The FDM printing was first introduced by the Stratasys Ltd. in 1980 after Scott Crump developed the process. In most cases thermoplastic polymers are the printing materials. With the help of FDM process functional, accurate prototypes, conceptual models and manufacturing components can be made. Before the printing starts, the user must slice the beforehand designed 3D models, so the printer could translate and execute the commands, after these motions the preheating

of the nozzle and bed must happen before the printing can start. The printer lays the levels on top of each other one-by-one until the model is completely ready. The machine extrudes the melted filament which is after placed on the heated bed. It is important to ensure the proper adhesion on the bed. Like with all technologies, it is important to note that the time of the printing depends on the size and complexity of the object. Postproduction can include the removal of the support material or sand grain grinding so this way the objects get a mirror surface. BMW and Nestlé are also using FDM technology at their factories. [5]

3. THE ENDER 5 PRINTER AND ITS PRINTED OBJECT

The Creality Ender-5 printer, besides being a reasonably priced printer, carries many advantages. It has countless useful functions. This printer is an FDM printer which means that it heats, melts and extrudes the used filament. After extruding the material, it creates layers on the heated bed on top of each other as it was already mentioned it earlier. This work continuous till each layer is done and the model is complete. The printing area is $220 \times 220 \times 300$ mm, so this is the maximum size which the printer is capable for. The printer is manufactured and distributed by a Chinese company. The Ender 5 was priced at 300 dollar in 2019 June, which approximately means 90 thousand forints in Hungarian currency. The Creality company makes a great deal about packaging, it is extremely important for them to transfer the printers to the buyers in perfect condition, buyer satisfaction is always a key component when it comes to choosing manufacturers. The company is labelled according to the users submitted evaluations. Both the ordering and the shipping part was easy and quick. The communication and the problem solving with the buyers is fast and polite. The printer arrived in a complete kit, in cardboard box. The parts were disassembled and placed in protecting sponge material. The printer must be assembled before use according to the instruction manual. The assembling took about 1–1.5 hours, it was not complicated to piece it together. After the assembly and filament filling, only the calibration was left. In this machine the calibration happens manually, the nozzle's height must be adjusted by eye. After the calibration test printing can be started either from the printer's memory (code installed in advance) or we can print anything (own models) we put on the SD card. It is recommended that we make test prints beforehand to install the right printing parameters. One of the printer's advantages is that in spite its price-value rate the printing quality is good, and the printing area is considerably large. However larger models take longer time to print. Long printing time comes with a risk of power break or any other power failure and the printing can stop. This problem is solved by a special function which resets the print from where it stopped before the power break so the printing can continue from the layer the print was suspended. This was the printing can be saved and continued after-wards. The proper printing level is not easy to find, so some practise is needed. There was only one problem with a failing part and that one was the filament extruding part. After a few weeks of printing the polymer extruding element broke and could not extrude the right amount of filament from the nozzle. It is recommended to replace

the polymer part with a metal one or with an even more advanced closed box extruder. Either extruding part can be purchased easily for a few thousand forints. Since this part was replaced there was not any other problems with the extrusion. Another weak point on the printer is the bed which is not supported the right way and it trembles sometimes when a high and slim part is printed. A more rigid framework would not let this shaking happen. This problem can also be solved with some support tools, which can be printed with the 3D printer. Despite these little bumps this printer is quite capable and smooth while working. The printer is also user friendly with an operating screen. All in all, the Ender 5 is a fine choice for a user who is starting to get in touch with 3D printing.

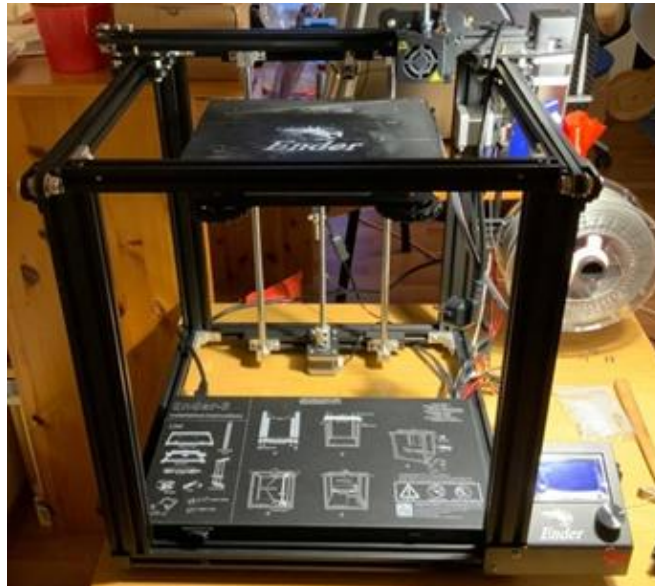


Figure 2
Creality Ender 5

The following pictures demonstrate some of the test prints. Every single printed model is unique in their own way, there are not two models that look exactly alike. Every piece has its own difficulties during the printing process. The little white octopus is a special model because its body is segmented, but it can be printed in one piece, the arm's parts are printed at the same time in the same printing process. This model does not need any further piecing together later on. The satin blue clamp, which as in the printing process during the time the photo was taken serves the role of securing the filament spool in place. The little black boxes play a part in cleaning the filament from dust or any other pollutions before it is extruded. From these objects we can see that hobby printer users have many opportunities when it comes to printing something useful. They can also print such parts which can enhance the printer's capability.

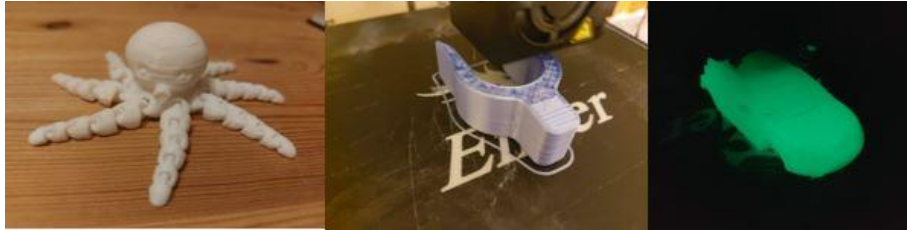


Figure 3

Printed articles for personal use and ornaments

There are special materials among the printing materials, for example there is a filament which changes colour when the temperature changes, it is called thermo filament. There is another material which glows in the dark, we can see a photo of the fluorescent filament where a car is being printed. The last two models to be mentioned are connected to engineering. One of the models is a twin-screw, the other one is a planetary gear which was a great help during the studies.



Figure 4

Printed and fitted machine parts

4. CONCEPTUAL DESIGN OF A FILAMENT RECYCLING MACHINE

Many of the amateur printers print at home and they learn all the mishaps by themselves, resulting that it is almost impossible to do everything right the first time. Luckily at University of Miskolc students have an extracurricular activity group called Fast Prototyper's Club which is for everyone who is interested in 3D modeling and printing. We can collaborate on different projects with other students and we can also share our experiences with each other. Despite having more and more experiences, we still make mistakes every day during printing and we must learn hundred more facts about 3D printing. One thing we definitely have to learn is to prepare less waste. Recycling filaments would be a great possibility for that. It is a fact that the manufacturing of a machine is also harmful for the environment, but the great amount of recycled filament would balance the environmental impacts of a filament recycling machine. [2]




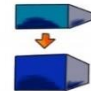
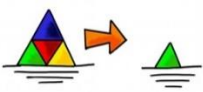
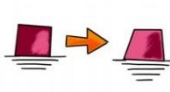









Figure 5
Waste filaments

4.1. Functional subassemblies of the recycling machine

Functional designing can happen through different paths. For a better demonstration, the functional subassemblies are represented with figures. It makes it easier to visualize the functioning mechanism if we see a visual indicator such as a drawing or figure, therefore I choose this method to explain my ideas. [1]

Table 1
Functional segments

Storing box		Spooling mechanism	
Feeding unit		Modular function (changeable extruder size)	
Chopping unit		Forwarding, moving unit	
Heating unit		Size monitoring unit	
Temperature controlling unit (temperature check)		Power source	
Cooling unit		Controlling unit (the machine's "brain")	
Extruder			

4.2. The optimal concept

The presented concept is full of functions, the complexity itself means compact performance, because the whole system is automatic from placing the filament in the machine to receiving the finished filament spools. The power source and the controlling unit is managed with a micro-controller platform. The polymer placed in the container box is moved from the feeder unit to the chopping unit. The machine chops the polymer into pieces for the easier heating. The material pieces are transferred to the heating unit where the polymer is melted down. The temperature controlling unit is responsible for keeping the material at the right temperature through the process. The melted polymer leaves through the extruder, where it goes under size verification and cooling. After cooling down the filament, the machine cools the spool down, rolls it up and stores it inside. The special function of this concept is that the extruder head is modular which means that it can be changed into a different size. The two preferred filament sizes are 1.75 mm and 2.85 mm. This solution is complex, but its production is fast and easy thanks to the automatic working.

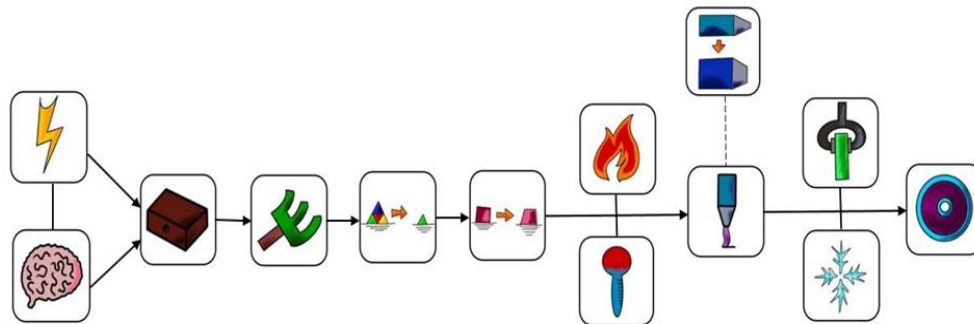


Figure 6
The optimal concept

5. SUMMARY

The study focuses on getting acquainted with the 3D printing technology. The technologies widespread-functionality and usability is mentioned in the paper. The Fused Deposition Modelling technique is introduced and there is a brief explanation about the 3D printing process as well. Following these topics, the own experiences of a Creality Ender 5 printer and a few printed models were introduced. After establishing the need for filament recycling machines, the last main part of the article deals with the conceptual design of such a machine. The functional units were also illustrated and explained in detail. In the near future the construction of this filament recycling machine will be worked out.

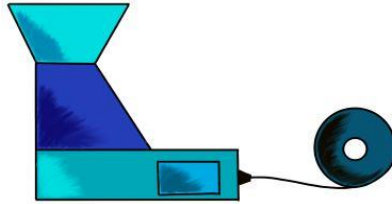


Figure 7
Sketch of the filament recycling machine

ACKNOWLEDGEMENT

This research was supported by the European Union and the State of Hungary, co-financed by the European Social Fund in the framework of TÁMOP-4.2.4.A/2-11/1-2012-0001 *National Excellence Program*.

REFERENCES

- [1] Otto, Kevin N., Wood, Kristin L. (2001). *Product Design. Techniques in Reverse Engineering and New Product Development*, Prentice Hall Upper Saddle River, New Jersey, USA.
- [2] Jayatilleka, S., Okogbaa, G. (2014). *Accelerated Life Testing, 2014 Workshop on Accelerated Stress Testing and Reliability Conference*, Saint Paul, Minnesota, United States, pp. 1–21.
- [3] <https://3dinsider.com/3d-printing-history/>
- [4] <https://www.sculpteo.com/en/3d-learning-hub/basics-of-3d-printing/the-history-of-3d-printing/>
- [5] <https://3dsourced.com/guides/history-of-3d-printing/>

DRAG COEFFICIENT CALCULATION OF MODIFIED MYRING-SAVONIUS WIND TURBINE WITH NUMERICAL SIMULATIONS

MAHMOUD SALEH – ENDRE KOVÁCS

University of Miskolc, Department of Physics and Electrical Engineering
3515 Miskolc-Egyetemváros
mhmodsah84@gmail.com; kendre01@gmail.com

Abstract: Nowadays the importance of renewable energy is growing, and the utilization of the low wind energy potential is getting crucial. There are turbines with low and high tip speed ratio. Turbines with low tip speed ratio such as the Savonius wind turbine can generate adequate amount of torque at low wind velocities. These types of turbines are also called drag machines. The geometry of the blade can greatly influence the efficiency of the device. With Computational Fluid Dynamics (CFD) method, several optimizations can be done before the production. In our paper the Savonius wind turbine blade geometry was designed based on the so-called Myring equation. The primary objective of this paper was to investigate the drag coefficient of the force acting on the surface of the blade. Also, the Karman vortex was investigated and the space ratio of that vortex in our simulation was compared to a typical one. The power coefficient of a new Savonius turbine was investigated at different values of top speed ratio (TSR). For the sake of simplicity, a 2D cross-sectional area was investigated in the simulation with ANSYS Fluent 19.2.

Keywords: *Savonius wind turbine, Myring Equation, CFX, CFD*

1. INTRODUCTION

Wind turbine is a device which converts the kinetic energy from the wind to another form of energy by a mechanical mechanism. They consist of blades which rotate around an axis due to the wind force. There are many classifications of the wind turbines. According to the nature of the force used to produce the torque, wind turbines can be classified as “lift-wind turbines” or “drag-wind turbines” [1]. The main reason behind developing Drag-Wind Turbines is that they work regardless of wind direction. Drag-Wind Turbines do not need a yaw mechanism. This makes them ideal for small-scale usage such as remote areas with very small electric load. Their blades do not need a mechanism to change their angle when they operate with any wind direction. The small size means they can be integrated easily within an urban setting and present no danger to the wildlife in rural areas. The most commonly used Drag-Wind Turbine is the Savonius wind turbine. The Savonius wind turbine was created by Savonius in 1922. It is most basic design in an S-shape with two blades. The Savonius turbine depends on the drag force to push the blade to produce a torque which will make the rotor work. Aerodynamically it is the simplest wind turbine to

design and build which decreases its cost completely compared to other blades of the other wind turbines. Its working principle is extremely simple. The turbine revolves because of the difference in the values of the drag force acting on the concave and convex surfaces of its blades as shown in *Figure 1*.

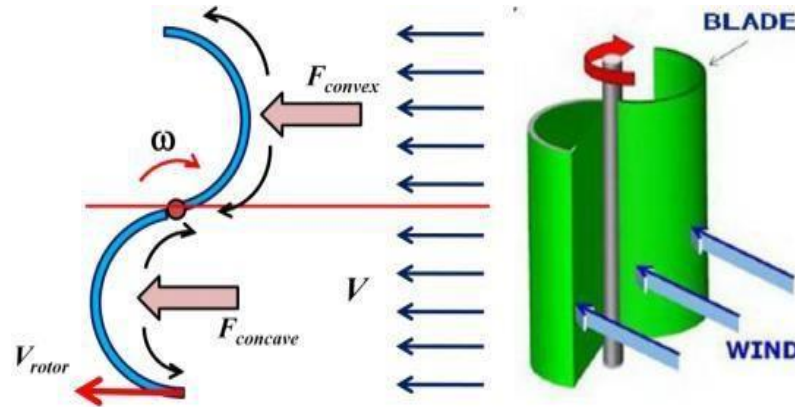


Figure 1
Working principle of a Savonius rotor

The air enters the concave surface and pushes the turbine. The flow that hits the convex surface does generate a drag which is lower than the force acting on the concave surface. It is the difference in the values of the drag forces that enables the turbine to work. The experimental study of E. Aymane [2] refers that Savonius wind turbines work well at low wind velocities (cut in speed at around 2.5 m s^{-1}). According to the same study, two blades operate better than three blades since more drag is dissipated in the three blades versions. The power coefficient of the two-blade design is higher than that of the three-blade design. The aim of this paper is to introduce a new design of the blade of the Savonius wind turbine and investigate the power and drag coefficients.

2. METHOD

Even though 2D-simulations fail to consider the 3D-simulation effects, previous studies have shown that two-dimensional simulations give acceptable results for Savonius Turbines [3]. Therefore, the three-dimensional effects are ignored, and two-dimensional transient simulations are carried out to reduce the time cost in this study. The simulations were done using Ansys Fluent 19.2.

2.1. Modified Savonius-Myring Blade

The net force which pushes the Savonius blade and produces the torque depends on two forces which are F_{convex} and $F_{concave}$ as shown in *Figure 1*. The net torque increases when $F_{concave}$ increases but it decreases when the F_{convex} increases. The

main goal of our study is to decrease the drag force acting on the convex surface of the Savonius blade and also increase the drag force acting on the concave surface so that we can enhance the efficiency of the turbine. Among many factors, the geometry of the blade is the critical factor in determining the value of those forces. In our study we chose to generate the surfaces based on the Myring Equation. It is widely used in the design of submarines working under the water and it is reported that it gives ideal results [4]. The formula of the Myring Equation in the Cartesian Coordinates is:

$$y = b \left[1 - \left(\frac{x}{a} \right)^2 \right]^{\frac{1}{n}}, \quad (1)$$

here a , b and n can be any positive number. That equation generates a wide range of geometries. When $n = 2$ it determines an ellipse and for special cases when $a = b$ it determines a circle. The parabola can be defined when the factor $a = 1$. In [3], the author defined $b = a = 0.25 \text{ m}$ and changed the value of the factor n in order to predict its influence on the efficiency. In our simulation, we held $n = 2$ and changed the factors a and b . This determined a half-ellipse shape. We connected two of them to generate the S-blade shape.

2.2. Fluid domain and Boundary conditions

For any blade with diameter D , and based on the study of W. Tian [3], the tunnel was given the dimensions $12D$ wide and $18D$ length. We chose these dimensions to make sure that the upstream flow is completely developed. The blade is placed at an equal distance between the top and the bottom boundaries, at distance $6D$ from the inlet boundary (*Figure 2*).

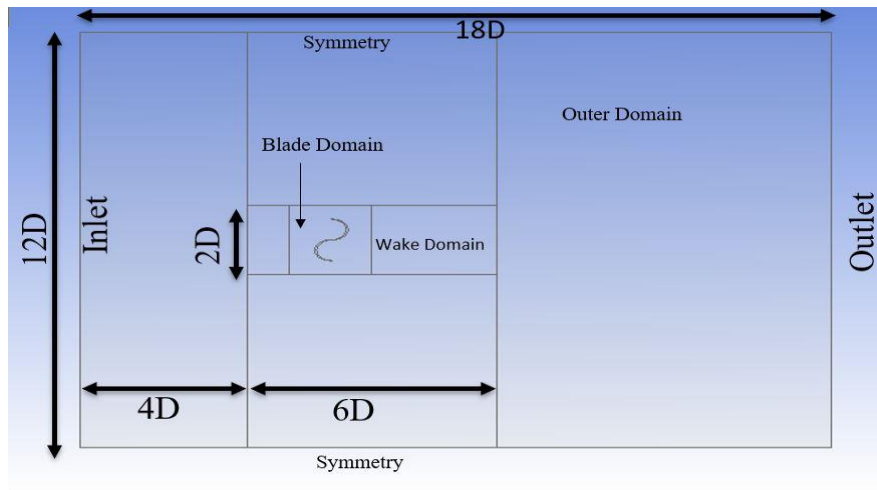


Figure 2
Fluid Domain and the boundary conditions

The whole domain was divided into three subdomains in order to control the mesh quality. The wake domain was given the dimensions $2D \times 6D$ while the blade domain was given the dimensions $2D \times 2D$. A uniform velocity profile was used at the inlet. The value of the inlet-velocity was set to different values for each blade, which were $\{3, 5, 6, 10\} \text{ m s}^{-1}$. The pressure outlet was used at the outlet of the tunnel. No slip-wall was applied at the surface of the blade. To improve the stability of the numerical simulations, symmetry boundary conditions were applied at both the top and the bottom edges of the domain. The symmetry boundary condition is useful because it allows the solver to consider the wall as part of a larger domain.

2.3. Mesh Generation

The mesh was generated by the Mesh tool in Ansys 19.2. As mentioned before, the whole domain was divided into three subdomains in order to control the mesh quality and the aspect ratio. As we will see later, the diameters of the blades are existing in the domain $\{1, 1.2, 1.4\}m$. Taking into consideration the smallest blade diameter, the blade domain surrounding directly the blade has the finest mesh which was 10 mm, while the wake domain contains cells with 50 mm. It was generated to be able to capture the tail of the vortex in case an eddy formed. Far away from the blade in the outer domain, the resolution was the lowest. Multizone was the dominant method and the type of mesh was set as quadrilateral. *Figure 3* shows the gradient in the mesh size around the blade and outer domain. It can be seen also from *Figure 4* that the aspect ratio around the blade and in most of the domain is around 1 which is the ideal value of the aspect ratio. Even in some regions which have the highest value, the aspect ratio does not reach 6. It is known that aspect ratio with a value of 10 is still accepted. The inflation was generated around those surfaces in order to increase the accuracy of the calculations. For this purpose, the value of the y^+ was calculated to ensure that the height of the first layer of the inflation will be less than the thickness of the boundary layer.

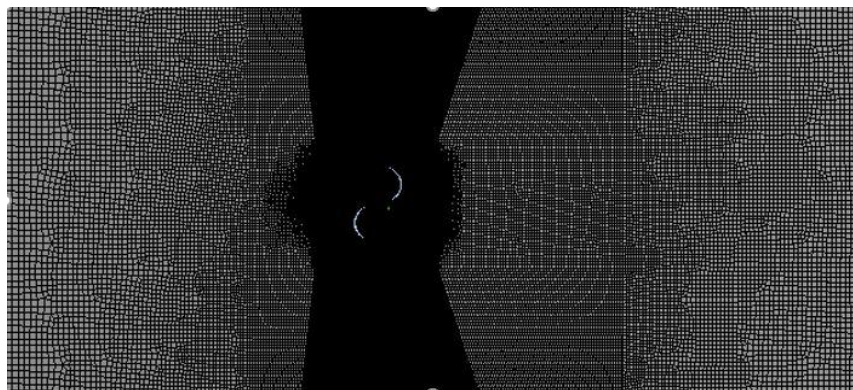


Figure 3
Generated Mesh

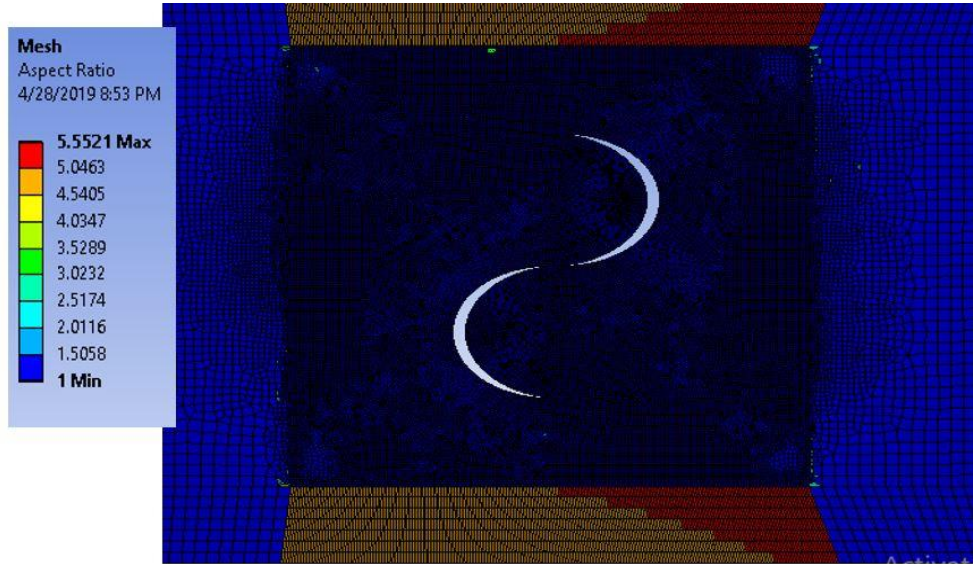


Figure 4
The aspect ratio

2.4. The Turbulence Model and Setup

Numerical (CFD) models intended to predict flow in a computational domain with the combination of Navier–Stokes equations and turbulence prediction techniques [5]. The transition SST turbulence model was applied. The transition SST model is based on the coupling of the SST $k - \omega$ transport equations with two other transport equations, one for the intermittency and one for the transition onset criteria, in terms of momentum-thickness Reynolds number. An ANSYS proprietary empirical correlation (Langtry and Menter) has been developed to cover standard bypass transition as well as flows in low free-stream turbulence environments. For transient formulation, second order implicit option was used. The value 500 was used as the number of time steps. To increase the accuracy of the calculations, the time step was set as 0.1 second. Solution was initialized with hybrid initialization. A Second Order Upwind spatial discretization algorithm was used for pressure and momentum.

2.5. Validation

To validate the method mentioned above we conducted 2D simulations with the following values of the Myring-Equation (1): $a = b = 0.25 \text{ m}$, $n = 2$. This determines a half-circle with a C-shape. We connected two C-shapes to produce an S-shape with 1.2 mm thickness. These values were taken from reference [6]. We tested our model at two different velocities which were $\{7, 14\} \text{ m s}^{-1}$. According to our simulations, the mean value of the static torque coefficient was roughly 0.25 in the both cases. In reference [7], the values were 0.25 and 0.22 at velocities 7 m s^{-1}

and 14 m s^{-1} , respectively. The values in that reference can be checked in *Table 1* and *Figure 7* when $\theta = 0$ (our turbine fixed in the tunnel in a way that made $\theta = 0$ as shown in *Figure 2*). Taking into consideration that our simulation had been conducted on a 2D model while the experiment was conducted on a 3D-real model, the result of the simulation is a good approximation. We have to pay attention that the negative value of the static torque coefficient in our simulation does not matter since it refers only to direction of the angular velocity.

3. RESULTS AND DISCUSSION

3.1. Drag coefficient crisis and Von Karman vortex effects

In this simulation, we studied the drag coefficient by holding $b = 0.25 \text{ m}$, $a = 0.450 \text{ m}$ and $n = 2$. It determines a half-ellipse shape, the so-called C-shape. We connected two C-shapes to produce an S-shape. The simulation was conducted on both shapes. The velocity 3 m s^{-1} was applied at the inlet of both fluid domains. The value of the drag coefficient was defined as function of time as shown in *Figure 5*.

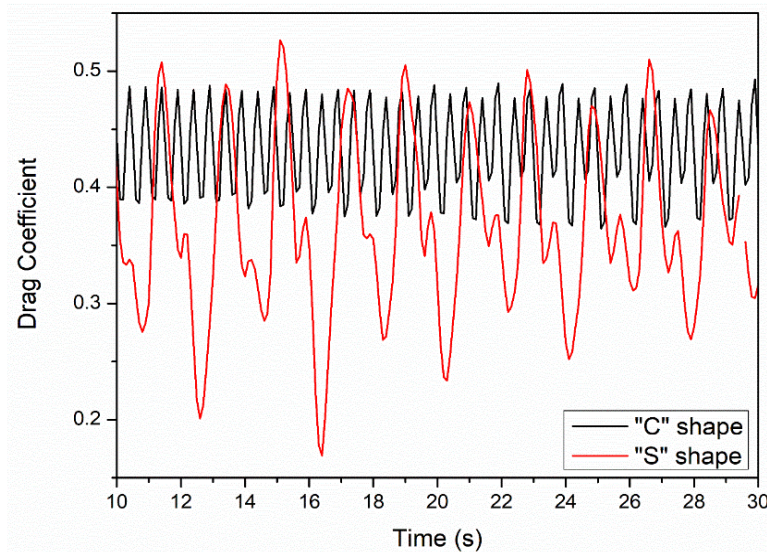


Figure 5

The drag coefficient as a function of time

In both cases, it was found that the function was changing with time. For the C-blade shape, the value of the drag coefficient changed roughly between 0.39 and 0.49 during the time interval. For the S-blade shape, the value changed in wider domain. The highest value was approximately 0.51 while the lowest value was around 0.25. For the S-blade shape, the velocity contour shows that the value of the velocity is zero along the whole surface of the blade which is called stagnation point as shown in

Figure 6. This can be explained by the fact that the kinetic energy of the fluid was converted into pressure energy. Comparing Figure 7 with that in the study of A. Kulkarni (Figure 1) [8], we notice that the vortex formulated behind our blade is Karman vortex street phenomenon.

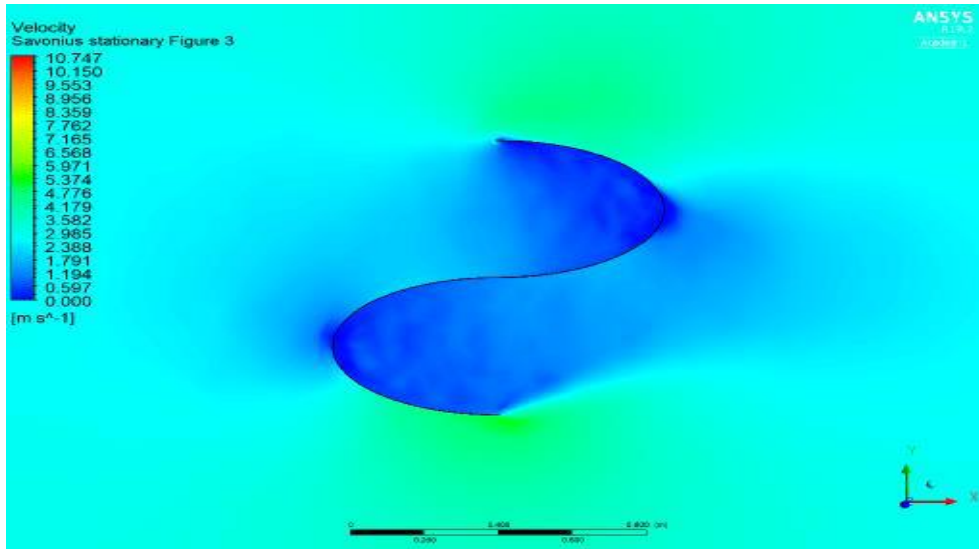


Figure 6
Velocity distribution

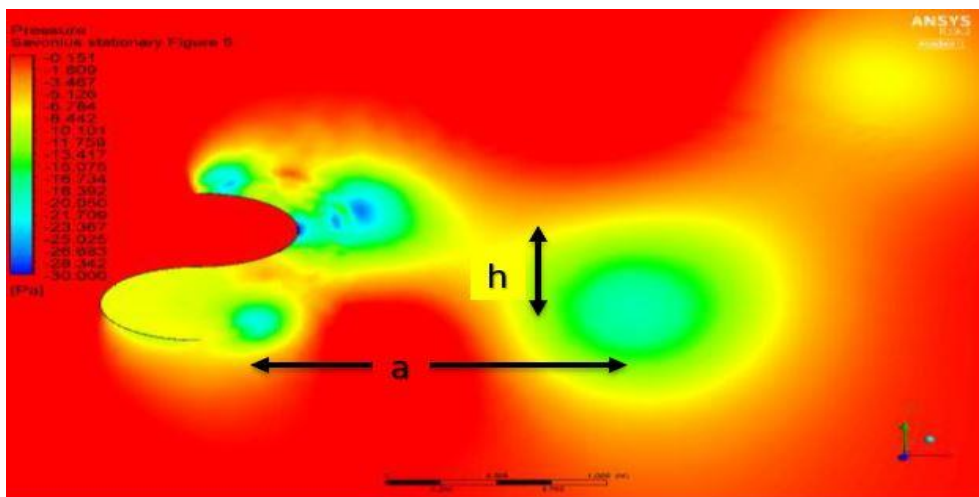


Figure 7
Karman vortex Street (Pressure Contour)

3.2. Drag Force and Drag coefficient

Holding $n = 2$ and $a = 0.375 \text{ m}$ while b changes in the domain $\{0.25, 0.3, 0.35\} \text{ m}$, the Myring equation determines a half-ellipse shape the so-called C-shape. Two C-shapes were connected to produce S-blade shape with diameter $D = 4b$. It means that $D \in \{1, 1.2, 1.4\} \text{ m}$. The simulations were conducted to show the effect that the b factor has on both the drag coefficient and the drag force. Each an S-blade was tested at four different velocities which were $\{3, 5, 6, 10\} \text{ m s}^{-1}$. Let us denote the first blade with $b = 0.25 \text{ m}$ as S_1 , the second blade with $b = 0.3 \text{ m}$ as S_2 and the third blade with $b = 0.35 \text{ m}$ as S_3 . Also, the drag force follows the renown empirical formula:

$$F = \frac{1}{2} \rho C_d V^2, \quad (2)$$

where ρ is the mass density of the fluid, C_d is the drag coefficient and V is the flow velocity relative to the object. For blade S_1 , the simulations show that the drag coefficient is constant at any velocity we used. The value of the drag coefficient is $C_{d1} = 1.25$. The values of the drag force are $\{7, 20.1, 27, 78\} \text{ N}$ at velocities $\{3, 5, 6, 10\} \text{ m s}^{-1}$ respectively. For blade S_2 , the simulations show that the drag coefficient is also constant at any velocity we used. The value of the drag coefficient is $C_{d2} = 1.5$. The values of the drag force are $\{8.7, 25, 35, 100\} \text{ N}$ at velocities $\{3, 5, 6, 10\} \text{ m s}^{-1}$ respectively. For the third blade S_3 , the graph of the drag coefficient is stable at any velocity we used. The value of that drag coefficient is $C_{d3} = 2$. The drag force values are $\{11, 29, 40, 120\} \text{ N}$ at velocities $\{3, 5, 6, 10\} \text{ m s}^{-1}$ respectively. It can be seen from *Table 1* that the drag force follows the renown empirical *Equation (2)*.

Figure 8 shows the values of the drag force at each velocity for each blade.

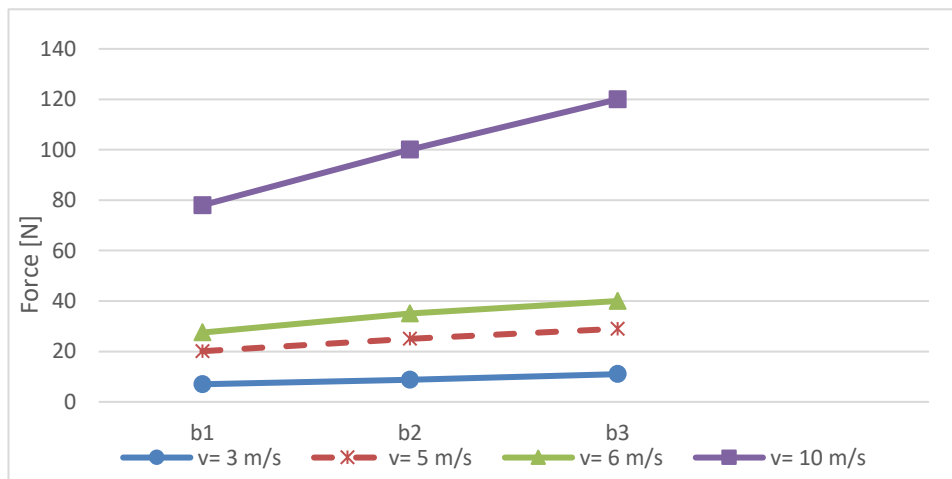


Figure 8

The drag force acting on the three blades at different velocities

In that figure, b1, b2 and b3 refer to blades S_1, S_2, S_3 respectively where the diameter of any blade is $D = 4b$. It can be clearly seen that the higher the velocity, the higher the drag force is, as it is expected. It can be also noticed that the relationship between the drag force and the diameter of the blade is linear at velocities $\{3, 5, 6, 10\} m s^{-1}$. As a result, the drag force acting on the blade with diameter between 1 m and 1.4 m and working at previous velocities can be interpolated. Also, the drag coefficient increases when the diameter of the blade increases as shown in Figure 9. However, the relationship is not linear in this case.

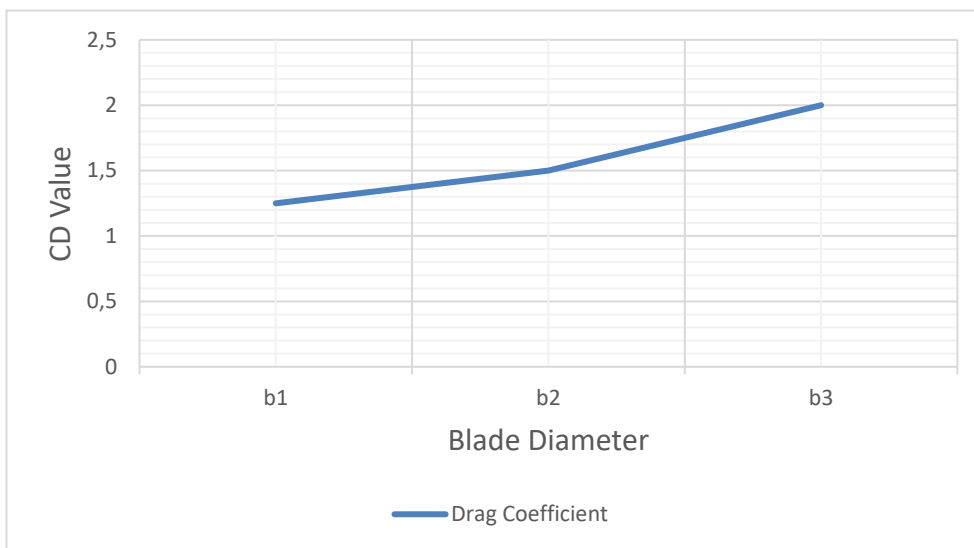


Figure 9

The drag coefficient as a function of blade diameter

Table 1

The drag force values

FORCE [N]	$V = 3 m s^{-1}$	$V = 5 m s^{-1}$	$V = 6 m s^{-1}$	$V = 10 m s^{-1}$
F_1	7	20.1	27.5	78
F_2	8.75	25	35	100
F_3	11	29	40	120

3.3. The Power Coefficient

We investigated the power coefficient of the two-blade turbine (S1 blade). A sliding mesh model was used to simulate the rotation of the rotor. The turbine was tested at different Tip Speed Ratio (TSR). Each simulation lasted for many revolutions to allow for convergence. The number of revolutions depended on the angular velocity of the turbine. Four simulations were carried out with the following values of TSR

{ **0.4, 0.6, 0.8, 1** } corresponding to inlet velocities { **3, 5, 6, 10** } respectively. The Tip Speed Ratio TSR has the following formula:

$$TSR = \frac{D\omega}{2V}, \quad (3)$$

where D is the diameter of the rotor ($4b = 1.2$ m in our case), ω is the angular velocity of the turbine and V is the inlet velocity. The power coefficient can be expressed as follows:

$$C_p = \lambda C_m, \quad (4)$$

where C_m is the torque coefficient given by the following formula [9]:

$$C_m = \frac{4T}{\rho A_s D V^2}, \quad (5)$$

where T is torque, ρ is air density, A_s is the swept area, D is the turbine diameter and V is the air velocity.

Since the torque coefficient was fluctuating (*Figure 10*), its averaged value was considered at the last revolution to allow for convergence. In Reference [3], the authors carried out simulations to investigate the power coefficient and the highest value was 0.2573 at TSR = 0.8. In our design, we can go beyond this value. At TSR = 0.8, the power coefficient was 0.28 for our turbine *Figure 11*.

Table 2
Torque coefficient with respect to TSR

λ	0.4	0.6	0.8	1
C_m	0.05	0.09	0.35	0.06

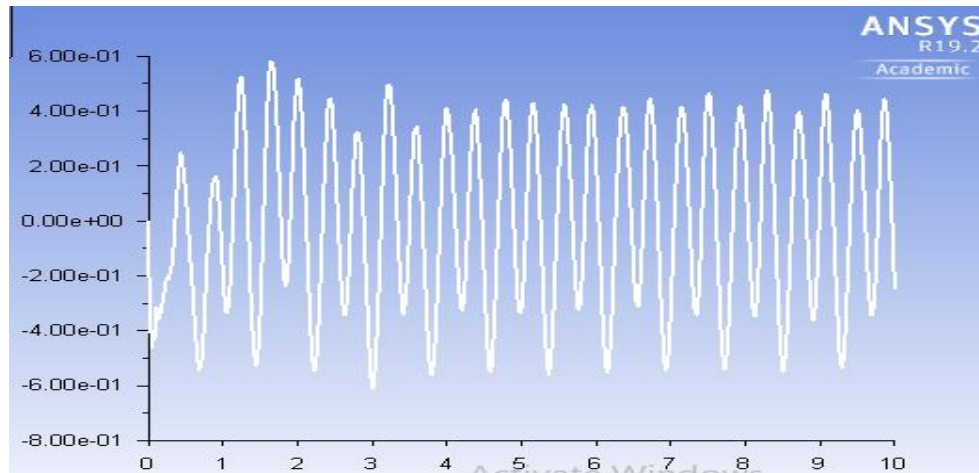


Figure 10

The torque coefficient as a function of time at TSR = 0.8

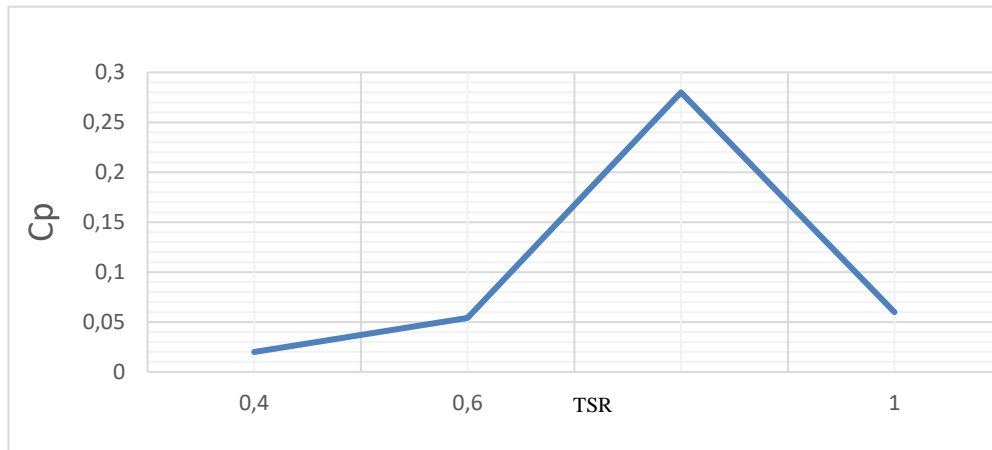


Figure 11
Power Coefficient with respect to TSR in case of the first blade S1

4. SUMMARY

The numerical simulations had been carried out to investigate Savonius wind turbine. The following results were obtained:

- The drag force and drag coefficient increase with respect to the diameter of the rotor.
- The value of the drag coefficient showed stability for the all the three cases.
- Since the relationship between the drag force and the diameter is linear, the drag force for such a design can be expected for any diameter in the domain {1, 1.4} m.
- The simulations conducted on turbine S_1 to investigate the power coefficient showed a high value of that coefficient at $TSR = 0.8$. It was $C_p = 0.28$. This value is better than any value of the power coefficient that the authors obtained in reference [3].
- Although our turbine has showed a high efficiency at $TSR = 0.8$, it has a very low power coefficient at another TSR. So, it is suggested to be used at certain conditions to ensure that the value of TSR is close to 0.8.
- The high value of the power coefficient for the first turbine is a promising result. This encourages us to investigate this turbine more deeply. Also, the second and third turbine must be investigated.
- We have to pay attention that the values obtained from the simulations are usually higher than those obtained from laboratory. So, it is recommended to investigate our design experimentally.

REFERENCES

- [1] Manwell, J. F., McGowan, J. G., Rogers, A. L. (2010). *Wind Energy Explained: Theory, Design and Application*. Vol. 2, USA, John Wiley & Sons, Ltd, 2nd edition.
- [2] Aymane, E., Darhmaoui, H., Sheikh, N. (2017). *Savonius Vertical Wind Turbine: Design, Simulation and Physical Testing*. School of Science and Engineering, Alakhawany University.
- [3] Tian, W., Song, B., VanZwieten, J. H., Pyakurel, P. (2015). Computational Fluid Dynamics Prediction of a Modified Savonius Wind Turbine with Novel Blade Shapes. *Energies*, Vol. 8, pp. 7915–7929.
- [4] Saleh, M., Szodrai, F. (2019). Numerical Model Analysis of Myring-Savonius Wind Turbines. *International Journal of Engineering and Management Sciences*, Vol. 4, pp. 67–71.
- [5] Szodrai, F. (2020). Quantitative Analysis of Drag Reduction Methods for Blunt Shaped Automobiles. *Applied Sciences*, Vol. 10, pp. 1–19.
- [6] Baracu, T., Benescu, S. G. (2011). Computational Analysis of the Flow Around a Cylinder and the Drag force. In: *The 2nd Conference of the Young Researchers from TUCEB*, At Technical University of Civil Engineering of Bucharest, Bucharest, Romania, 17–18 November 2011.
- [7] Blackwell, B. F., Sheldahl, R. E., Feltz, L. V. (1977). Wind Tunnel Performance Data for Two- and Three-Bucket Savonius Rotors. New Mexico, Sandia Laboratories.
- [8] Kulkarni, A., Harne, M. S., Bachal, A. (2014). Study of Vortex Shedding Behind Trapezoidal Bluff Body by Flow Visualization Method. *International Journal of Engineering Research & Technology (IJERT)*, Vol. 3, No. 9, September 2014, pp. 1057–1062.
- [9] Feng, F., Li, S., Li, Y., Xu, D. (2012). Torque Characteristics Simulation on Small Scale Combined Type Vertical Axis Wind Turbine. *Physics Procedia*, Vol. 24, pp. 781–786.

DYNAMICAL SIMULATION OF A CNC TURNING CENTER (SURVEY PAPER)

AL-ZGOUL MOHAMMAD – ATTILA SZILÁGYI

University of Miskolc, Department of Machine Tools
3515 Miskolc-Egyetemváros
mohammadzgoul90@gmail.com

Abstract: This paper shows the most common rotor systems which can be used to analyse a CNC turning center. Starting with the simplest rotor system representation (single-degree-of-freedom) up to analysing multi-degree-of-freedom and infinite-degree-of-freedom rotor systems using the TMM (Transfer Matrix Method) when it comes to cases like multi desk rotors and Jeffcott-rotors.

Keywords: rotor systems, turning center, Transfer Matrix Method

1. INTRODUCTION

These days, dynamical simulation of machine-tools is essential and very important. The reason for this is to maximise these machines' accuracy and productivity [1]. The main goals behind performing dynamical analysis in most cases are to monitor, analyze and reduce mechanical vibrations in machine-tools [2]. In general, and most commonly, the model which is simulated by CAD 3D modelling and modal analysis is verified by a mathematical model [3]. The dynamical analysis and simulation of a CNC turning center have special focus on describing the dynamical behaviour of the spindle and the impact of each part connected to the spindle itself [4]. Special rotor-models have been set up during recent years in order to conduct more detailed dynamical investigations which result in a much clearer overview of the nonlinear behaviour of this especially important part of a turning-center. In the following sections, the most frequently applied dynamical models of the main spindle of a turning-center are overviewed.

2. ROTOR MODELS

Rotor models have a noticeable history of development, mainly due to the interaction between the theory and the practice [5]. The wide array of rotor models provides the researcher or engineer the flexibility to pick out the most suitable model for analysis or research and development.

2.1. Single-DOF rotor model

The simplest representation of a rotor system can be modelled as a single-degree-of-freedom system (*Figure 1*). The whole rotor is treated as a single mass. This mass

takes one of the following forms: a point mass, a rigid disc or a long rigid shaft. The two supports are assumed to be flexible and that is why each support (bearing) is assumed to have a stiffness of a specific value which leads to having an overall effective stiffness for the summation of the stiffnesses of the supports. The main disadvantage of this model is that it only deals with the translatory transverse motion of the rotor along one axis and it does not deal with the rotational motion and the translatory motion of the rotor [6].

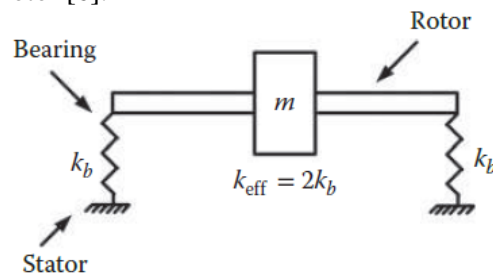


Figure 1
A SDOF rotor system

2.2. Jeffcott rotor model

The single-DOF rotor model can only show the oscillation in one transverse direction. This is one of this model's primary limitations. It is more accurate to have a model that can describe the orbital motion of the rotor in two transverse directions. This model is the typical Jeffcott rotor. It consists of a flexible, massless, simply supported shaft with a thin disc installed in the middle of it (*Figure 2*). There is an eccentricity of e between the disc center of rotation, C , and its center of gravity, G . The shaft spins at a speed of ω . The whirl frequency is represented by ν . For this case, the synchronous whirl is assumed (i.e. $\nu = \omega$). The sense of rotation of the shaft spin and the whirling are the same forming what is known as a forward synchronous motion [7].

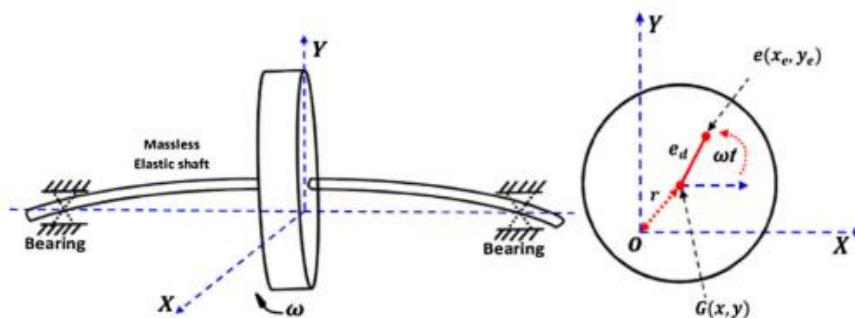


Figure 2
Jeffcott rotor system [8]

2.3. A two-disc torsional rotor system with a stepped shaft

The previous models consider only the transverse vibrations of rotor-systems. Meanwhile, the torsional vibration of rotor-systems is another very important kind of vibration that must also be taken into consideration. The following system best represents the case of torsional vibrations. This system consists of a stepped shaft with two large discs at the ends. It is assumed here that the shaft has a negligible polar mass moment of inertia compared to the large discs. In this approach, the actual shaft will be replaced by a uniform diameter equivalent shaft. The equivalent shaft diameter should meet the smallest diameter of the real shaft and must have the same torsional stiffness as the real shaft. *Figure 3* illustrates the case [9] [10].

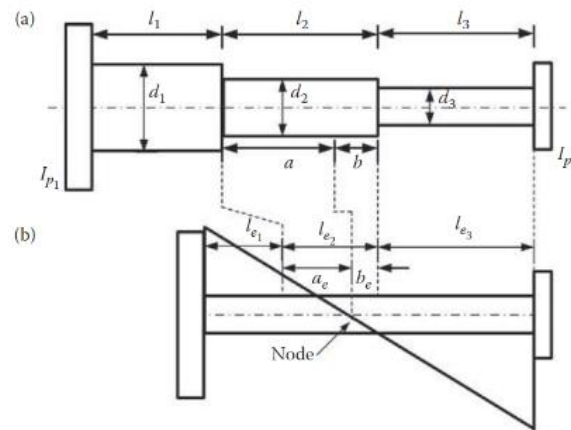


Figure 3

Two discs with (a) a stepped shaft and (b) an equivalent uniform shaft [11]

3. TRANSFER MATRIX METHODS

The previous rotor models are considered simple models. In real-life practice, more complicated models are to be analysed (multi-disc-rotor-system). Due to the large number of degrees of freedom, analysing such models, depending on the previous models, is a very complicated task. Here, the TMM is an adequate method of analysing such systems; it deals with a rotor system in a systematic way regardless the complexity of the system. In other words, the number of discs and their distribution over the shaft of a system do not complicate the case. In this method, the number of equations to be solved simultaneously, which forms the size of the system, generally depends on the dimensions of the state variable vector and does not depend on the number of stations. Practically, the TMM is suitable for long slender systems as in the case of rotating shafts [12].

A typical multidisc rotor system is shown in *Figure 4* and *Figure 5*. It is supported on frictionless supports and the z -axis is taken as the longitudinal axis whose discs

have an angular displacement about, ϕ_z . The discs are considered as thin and rigid and locate at a point and the shaft is treated as flexible and massless. N is the number of discs and 0 to $(n + 1)$ represents the station number. Then the system has the total number of stations as $(n + 2)$.

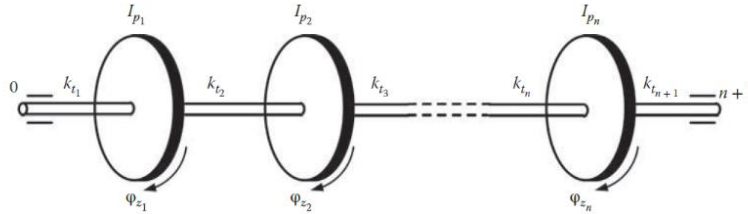


Figure 4
A multidisc rotor system [13]

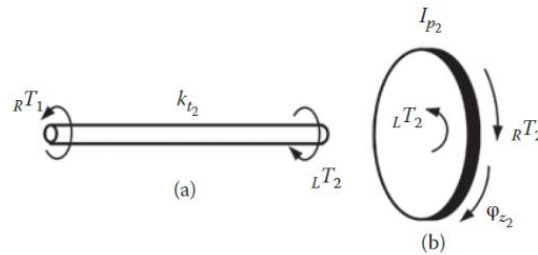


Figure 5
(a) A free body diagram of shaft section 2, (b) A free body diagram of disc 2

The so-called “point matrix” deals with the state variables at both ends of a thin disc. This is done to determine a state vector on the right-hand side relative to the state vector on the left-hand side. What the point matrix does is relates a state vector left of a disc to a state vector right of the disc. The so-called field matrix deals with the relationship between state variables at two ends of a shaft segment. Therefore, the role of the field matrix is to relate a state vector that is at the left end of a shaft segment to the right end of the shaft segment. Finally, the overall system transfer matrix relates the state vector at the far left to the state vector at the far right of the shaft. The overall transfer matrix elements are a function of the torsional natural frequency of the rotor system and they are a function of the excitation frequency for the case when the external torque is present [14] [15]. Below is an example on a matrix-system of a turning center spindle system. The total number of stations of the system is 3.

$${}_L\{S\}_1 = [F]_1[P]_1\{S\}_0 = [U]_1\{S\}_0 \quad (1)$$

$${}_L\{S\}_2 = [F]_2{}_R\{S\}_1 = [U]_2\{S\}_1 \quad (2)$$

$$\begin{Bmatrix} 0 \\ \varphi \\ M \\ S \end{Bmatrix}_L = \begin{bmatrix} u_{11} & u_{12} & u_{13} & u_{14} \\ u_{21} & u_{22} & u_{23} & u_{24} \\ u_{31} & u_{32} & u_{33} & u_{34} \\ u_{41} & u_{42} & u_{43} & u_{44} \end{bmatrix} \begin{Bmatrix} -y \\ \varphi \\ 0 \\ 0 \end{Bmatrix}_0 \quad (3)$$

$$[U]_1 = \begin{bmatrix} 1 & 0 & 0 & 0 \\ 0 & 1 & 0 & 0 \\ 0 & -m\omega_{nf}^2 I_d & 1 & 0 \\ m\omega_{nf}^2 & 0 & 0 & 1 \end{bmatrix}_1 = \begin{bmatrix} 1 + \frac{1}{6}m\omega_{nf}^2\alpha l^2 & l - \frac{1}{5}I_d\omega_{nf}^2\alpha l & \frac{1}{5}\alpha l & \frac{1}{6}\alpha l^2 \\ \frac{1}{5}m\omega_{nf}^2\alpha l & 1 - I_d\omega_{nf}^2\alpha & \alpha & \frac{1}{5}\alpha l \\ m\omega_{nf}^2 l & -I_d\omega_{nf}^2 & 1 & l \\ m\omega_{nf}^2 & 0 & 0 & 1 \end{bmatrix} \quad (4)$$

4. CONCLUSION

Among the various methods and models of analysing rotor systems, each presents advantages and disadvantages. Analysing simple systems with the dynamic approach is in some occasions faster when a high degree of accuracy is not required. On the other hand, for more complicated systems (multi-degree-of-freedom systems), the TMM is a better option due to its ability to deal, in a relative manner, with a greater number of DOF's with less complicated calculations.

ACKNOWLEDGMENT

The described article/presentation/study was carried out as part of the EFOP-3.6.1-16-2016-00011 *Younger and Renewing University – Innovative Knowledge City – institutional development of the University of Miskolc aiming at intelligent specialisation* project implemented in the framework of the Szechenyi 2020 program. The realization of this project is supported by the European Union, co-financed by the European Social Fund.

REFERENCES

- [1] Holub, M., Blecha, P., Bradac, F., Marek, T., ZAK Z. (2016). Geometric errors compensation of CNC machine tool. *Modern Machinery (MM) Science Journal*, pp. 1602–1607.
- [2] Hadas, Z., Vetiska, J., Juriga, J., Brezina, T. (2012). Stability analysis of cutting process using of flexible model in ADAMS. *Proceedings of 15th International Conference Mechatronika*, 5–7 Dec 2012, pp. 1–6.
- [3] Brezina, T., Hadas, Z., Vetiska, J. (2011). Using of Co-simulation Adams-Simulink for Development of Mechatronic Systems. *14th International Conference Mechatronika*, 1–3 Jun 2011, pp. 59–64.
- [4] Fortunato, A., Ascari, A. (2013). The virtual design of machining centers for HSM: Towards new integrated tools. *Mechatronics*, Vol. 23, Issue 3, pp. 213–229.

-
- [5] Glasgow, D. A. Nelson, H. D. (1980). Stability analysis of rotor-bearing systems using component. *Transactions of the ASME Journal Mechanical Design*, Vol. 1, 102, pp. 352–359.
 - [6] Tiwari, R. (2018). Transverse Vibrations of Simple Rotor Systems. *Rotor Systems: Analysis and Identification*. CRC Press, Taylor & Francis Group, p. 22.
 - [7] Rao, J. (2011). Rotor Dynamics Methods. In: *History of Rotating Machinery Dynamics*, Altair Engineering, Chief Science Officer, pp. 188–190.
 - [8] Saeed, N. A., Kamel, M. (2017). Active magnetic bearing-based tuned controller to suppress lateral vibrations of a nonlinear Jeffcott rotor system. *Nonlinear Dyn*, 90, p. 500.
 - [9] Tiwari, R. (2018). A Two-Disc Torsional Rotor System with a Stepped Shaft. In: *Rotor Systems: Analysis and Identification*. CRC Press, Taylor & Francis Group, pp. 262–263.
 - [10] Tiwari, R. (2018). Transverse Vibrations of Simple Rotor Systems. *Rotor Systems: Analysis and Identification*, CRC Press, Taylor & Francis Group, pp. 22.
 - [11] Tiwari, R. (2018). *Rotor Systems: Analysis and Identification*. CRC Press, Taylor & Francis Group, pp. 22, 33, 35, 50, 256, 257, 258, 259, 262, 277, 282.
 - [12] Behzad, M. (1994). Introduction. In: *Transfer matrix analysis of rotor systems with coupled lateral and torsional vibrations*. A degree of doctor of philosophy dissertation, University of New South Wales, p. 2.
 - [13] Tiwari, R. (2018). Transverse Vibrations of Simple Rotor Systems. *Rotor Systems: Analysis and Identification*. CRC Press, Taylor & Francis Group, p. 227.
 - [14] Genta, G. (2005). Transfer matrices approach. In: *Dynamics of Rotating Systems*. Springer Science + Business Media, Inc., 233 Spring Street, New York, NY 10013, USA, pp. 141–151.
 - [15] Vance, J., Zeidan, F., Murphy, B. (2010) Computer simulations of rotordynamics. In: *Machinery vibration and rotordynamics*. John Wiley & Sons, Inc., Hoboken, New Jersey, pp. 131–134.

DYNAMICAL SIMULATION OF A CNC TURNING CENTER

AL-ZGOUL MOHAMMAD – ATTILA SZILÁGYI

University of Miskolc, Department of Machine Tools
3515 Miskolc-Egyetemváros
mohammadzgoul90@gmail.com

Abstract: This paper deals with the analysis of a CNC turning centre, more specifically the spindle system. The FEM analysis shows the natural frequencies of the spindle system and the same system was analysed by using the TMM and the influence coefficients method. These analyses pave the way to compare these three methods.

Keywords: *dynamical analysis, turning center, Transfer Matrix Method*

1. INTRODUCTION

Having accurate and productive machine-tools is an essential need. It is very important to be able to dynamically simulate these machines so that accuracy and productivity goals are achieved [1]. In machine-tools, the machines' vibration is a serious problem to be monitored and analysed in order for them to be reduced through mechanical solutions and control systems [2]. The logical approach of doing so is by means of 3D modelling through the help of CAD packages and by FEM modal analysis using special programs (ANSYS, MADYN, etc.). Afterwards, the results are to be verified via mathematical models [3]. For a CNC turning center, it is very important to analyze and simulate the main spindle assembly so the dynamical behavior of the machine-tool is understood from the point of view of mechanical vibrations [4].

2. CNC TURNING CENTRES

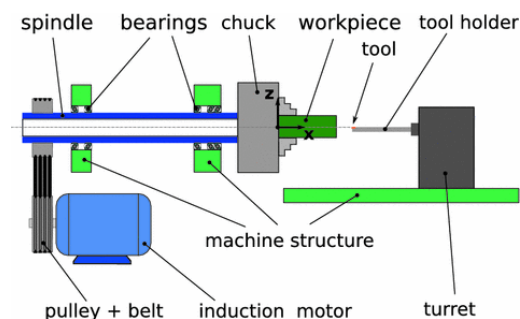


Figure 1
An outline of a metal lathe [6]

As any rotary machine, a CNC turning centre experiences mechanical vibrations for many reasons (*Figure 1*). For example, the inertia of any moving part in the machine or the unbalance of the rotating parts may cause vibrations since having them perfectly balanced is almost impossible. Another source of vibration in such a machine could be the characteristic natural vibration frequencies (eigenvalues) of the structure and supports of the machine itself [5].

3. THE CASE STUDY AND THE ANALYSIS MODEL

The study and analysis model used is a model of a Haas ST-20T CNC turning centre. Some simplifications should be done so the mathematical model can be constructed. Before starting the simplification procedure, *Figure 2* shows the non-simplified model which was extracted from the machine 3D model (*Figure 2*).

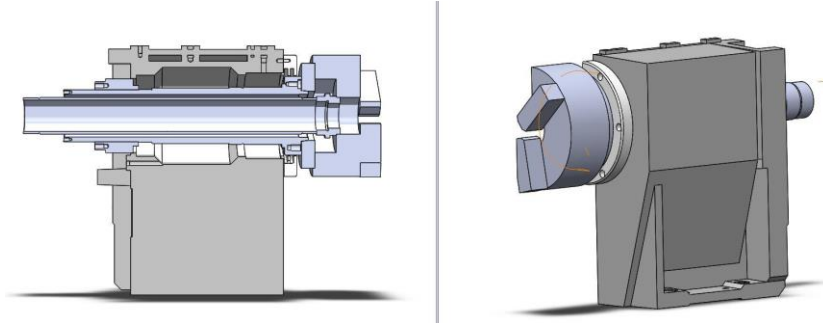


Figure 2
The CAD model of the spindle

4. RESULTS

The previously mentioned turning centre was analysed by three methods: the TMM, the influence coefficients method and the FEM. The results of these three methods will be presented in this chapter so the comparison between them can be performed.

4.1. The TMM

The goal of this analysis is to obtain the values of the natural frequencies of the spindle system. This can be achieved by using the TMM to extract and solve the frequency equation. The system consists of two shaft segments. The overall system transfer matrix relates the state vector at the far left to the state vector at the far right of the shaft. Below is the state vector of station 2 as an example of the matrix form.

$$\begin{matrix} \left\{ \begin{matrix} y \\ \varphi \\ M \\ S \end{matrix} \right\}_2 \\ \begin{matrix} l \\ \\ \\ \end{matrix} \end{matrix} = \begin{bmatrix} \left(l\bar{u}_{21} + \frac{1}{2}\alpha\bar{u}_{31} + \frac{1}{6}\alpha l^2\bar{u}_{41} \right) & 0 & 0 & \frac{1}{6}\alpha l^2 \\ \left(\bar{u}_{21} + \alpha\bar{u}_{31} + \frac{1}{2}\alpha l\bar{u}_{41} \right) & 0 & 0 & \frac{1}{2}\alpha l \\ \left(\bar{u}_{31} + l\bar{u}_{41} \right) & 0 & 0 & l \\ \bar{u}_{41} & 0 & 0 & 1 \end{bmatrix}_2 \begin{matrix} \left\{ \begin{matrix} -y_0 \\ 0 \\ 0 \\ R_a \end{matrix} \right\} \end{matrix} \quad (1)$$

Extracting the equations from the matrix form then substituting the factors (\bar{u} and α) values and applying the boundary conditions we can get the frequency equation:

$$mI_d l_1^3 (3l_1 + 4l_2) \omega_{nf}^4 - 6EI(2ml_1^3 + 6I_d l_1 + 2I_d l_2 + 2ml_1^2 l_2) \omega_{nf}^2 + 36(EI)^2 = 0 \quad (2)$$

$$\omega_{nf1} = 85946.17 \frac{\text{rad}}{\text{s}} \text{ and } \omega_{nf2} = 3850.1 \frac{\text{rad}}{\text{s}}$$

4.2. The influence coefficients method

The influence coefficient method deals with rotor dynamics as categorized cases. For each case, the coefficients calculated result in more accurate analysis results. The current case is considered an overhung rotor system and therefore, the frequency values can be obtained via the following equation:

$$\Omega = \frac{J_a}{J_p} \omega + \frac{-1 + \omega^2 a m}{[\beta - (\alpha\beta - \gamma^2) m \omega^2] J_p \omega} \quad (3)$$

$$\omega_{nf1} = 1577 \frac{\text{rad}}{\text{s}}$$

4.3. FEM analysis

The FEM analysis were carried out ANSYS. The spindle geometry had slight modifications so it became 100% an axisymmetric geometry since having an axisymmetric geometry is the condition for the program to consider the gyroscopic effect (Figure 3). The constraints were defined in the positions of the bearings. The material properties were defined based on having a spindle system made of ASTM A36 steel. The maximum rotation speed was defined based on the manufacturer's data (4,000 rpm). Finally, the model was meshed and the analyses were carried out.

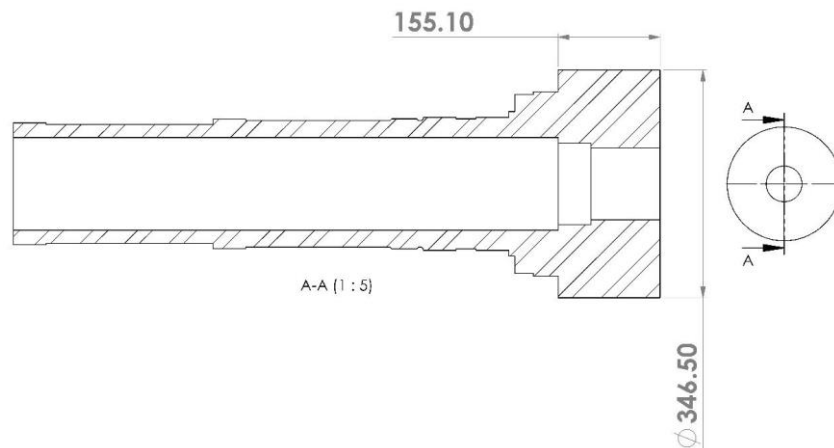


Figure 3
The spindle-chuck model (the analysis model)

For the meshed model, the number of nodes is 12,564 and the number of elements is 7,038 (Figure 4). For the sizing of elements, the adaptive sizing option was used with a minimum edge length of 0.041 mm. The bearings were defined as remote displacements with zero translations in the X, Y and Z directions and free rotations about these directions so they accurately comply with the bearings' role.

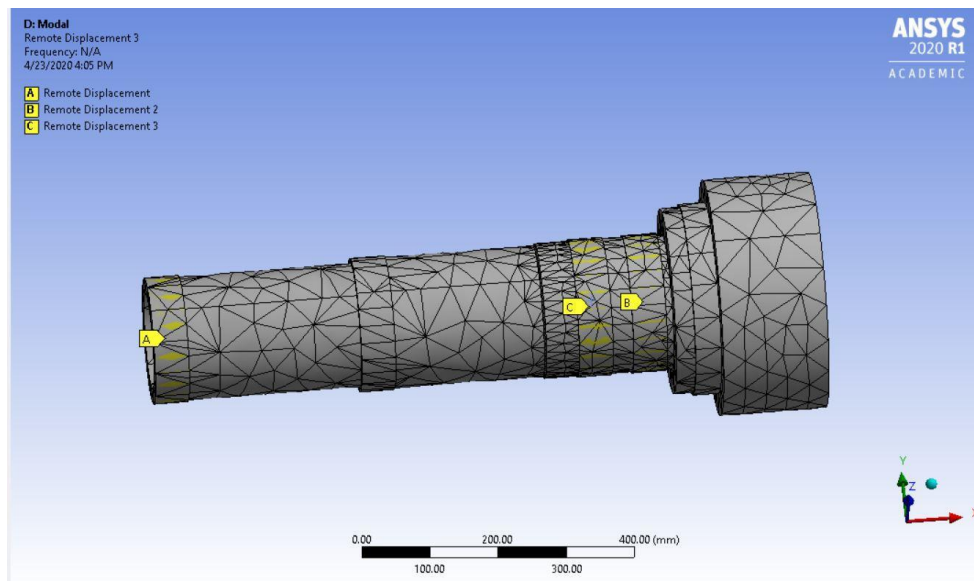


Figure 4
The meshed model with the bearing definition

After selecting the analysis type (modal), importing the geometry, defining the material, defining the geometry fixation conditions, meshing the geometry, activating the rotordynamics properties (Coriolis effect and Campbell diagram), defining the rotational velocity and running the analysis, the following frequency values were obtained (Table 1 and Figure 5).

The results of the FEM analysis are listed in the table below.

Table 1
The values of the frequencies

Mode	Frequency [Hz]
1	1.3086e-003
2	611.82
3	612.82
4	1262.6
5	1262.9

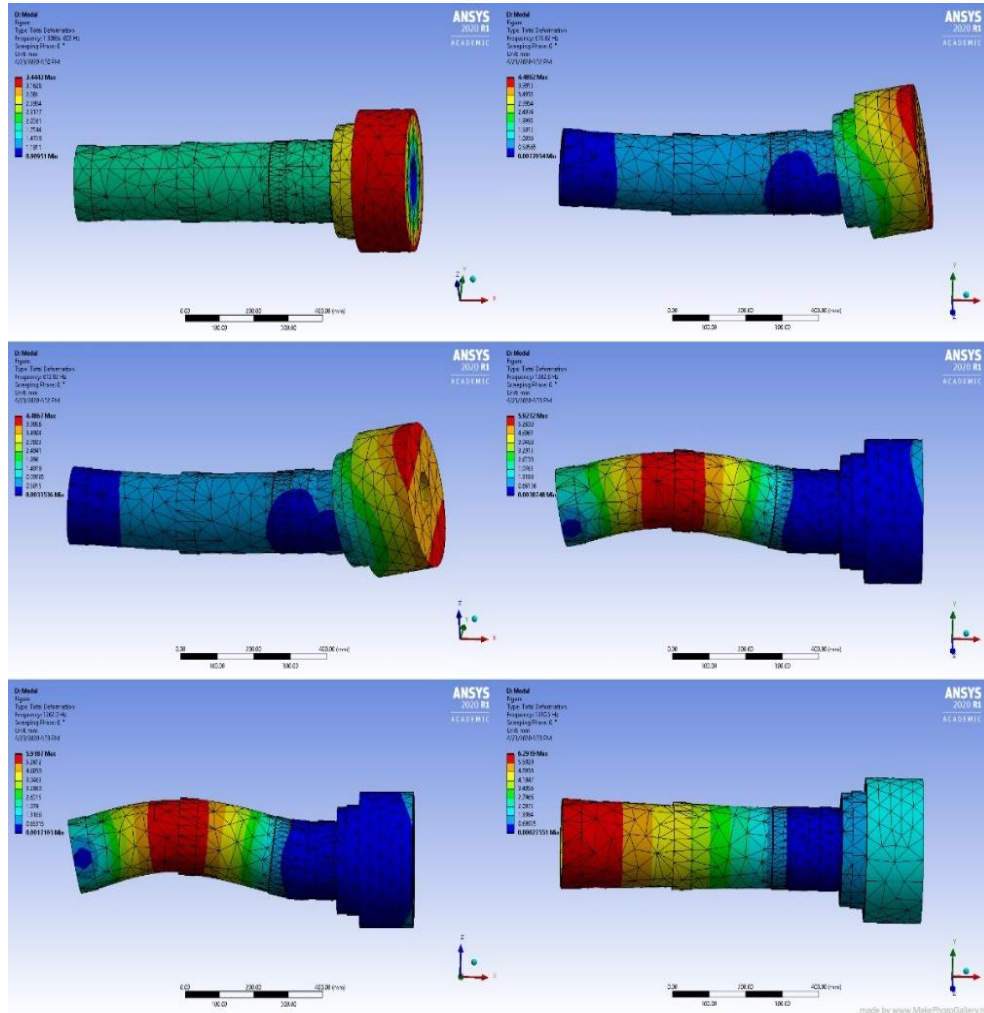


Figure 5
Modes of spindle system deformation

5. CONCLUSION

The TMM analyses were based on the assumptions of having a massless shaft and a lumped-mass whenever having a disk. These assumptions clearly affected the results. The shaft length-diameter ratio clearly affects the analysis using the TMM; the slendrer the shaft, the more accurate the results. The round-off error accumulates gradually through the process of the calculations due to the matrices' multiplication in the TMM. Finally, the results concluded that the influence coefficients method provided less error than the TMM.

ACKNOWLEDGEMENT

The described article/presentation/study was carried out as part of the EFOP-3.6.1-16-2016-00011 *Younger and Renewing University – Innovative Knowledge City – institutional development of the University of Miskolc aiming at intelligent specialisation* project implemented in the framework of the Szechenyi 2020 program. The realization of this project is supported by the European Union, co-financed by the European Social Fund.

REFERENCES

- [1] Holub, M., Blecha, P., Bradac, F., Marek, T., Zak, Z. (2016). Geometric errors compensation of CNC machine tool. *Modern Machinery (MM) Science Journal*, pp. 1602–1607.
- [2] Hadas, Z., Vetiska, J., Juriga, J., Brezina, T. (2012). Stability analysis of cutting process using of flexible model in ADAMS. *Proceedings of 15th International Conference Mechatronika*, 5–7 Dec. 2012, pp. 1–6.
- [3] Brezina, T., Hadas, Z., Vetiska, J. (2011). Using of Co-simulation Adams-Simulink for Development of Mechatronic Systems. *14th International Conference Mechatronika*, 1–3 June 2011, pp. 59–64.
- [4] Fortunato, A., Ascary, A. (2013). The virtual design of machining centers for HSM: Towards new integrated tools. *Mechatronics*, Vol. 23, Issue 3, pp. 213–229.
- [5] Vance, J., Zeidan, F., Murphy, B. (2010). The main sources of vibration in machinery. In: *Machinery vibration and rotordynamics*. Hoboken, New Jersey, John Wiley & Sons, Inc., pp. 17–18.
- [6] Okabe, E. P., Suyama, D. I. (2019). Modelling and Simulation of the Drivetrain of a Metal Lathe. *Mechanisms and Machine Science*, Vol. 1, 62, p. 475.

RESEACH INTO THE USES OF SANDBLASTING WASTE

ÁDÁM SÁNDOR PINTÉR – FERENC SARKA

University of Miskolc, Machine Tools and Mechatronics
3515 Miskolc-Egyetemváros
pinter.adam.1998@gmail.com

University of Miskolc, Institute of Machine and Product Design
3515 Miskolc-Egyetemváros
machsf@uni-miskolc.hu

Abstract: This article deals with an investigation into the recycling possibilities of sandblasting waste. As part of this, we are investigating the loss of mass of components or the materials in the waste. Furthermore, the potential for the use of these substances in different industries will help to reduce environmental pressures and meet the high demand for raw materials.

Keywords: *sandblasting, grain scattering, raw material, sand, recycling*

1. INTRODUCTION

The idea of writing this article is a joint project work, LIMBRA project, involving students from Hungary, Poland, the Czech Republic and Slovakia, and their teachers together with BPI Group Hungary and the University of Miskolc, Institute of Machine and Product Design. Within this framework we have been involved in the investigation of sandblasting technology and its generated waste. Hence this became the basic idea for this article theme. The company mentioned above cleans metal parts by sandblasting which at the end of the process produces a significant amount of waste, which is stored in landfill. Deposit of this waste is not the targeted way as the company is focused on environment. The question may therefore be arisen: whether the waste contains any recyclable raw materials? Of course, when examining the process, it is clear that it contains. As the starting material of the sandblasting in this case is glass beads or broken glass, they certainly appear in most of the waste and are likely to contain materials useful for other raw materials. It is worth thinking about how sandblasting waste can be the raw material of a new product or how it can appear on the market as a finished product.

2. TESTING OF THE MATERIAL USED

We started our work by examining the material used for sandblasting. The pre- and post-use status of the substance was also examined. First, we did microscopic examination scans of the samples we received. In *Figure 1 (a)* you can see the macroscopic

image of the material used (taken with a normal camera). One of the microscopic images can be seen in *Figure 1 (b)*.



Figure 1

(a) Pre-use condition, clearly visible that it is not sand but broken glass,
(b) microscopic recording

The microscope scans were taken using a Zeiss Discovery V12 type microscope. With the help of a program called Axio Vision for the microscope we were able to make measurements of the particle size of the resulting sample. The measured values are clearly visible in *Figure 1 (b)*, the material used had approximately 0.5 to 0.6 mm particles initially. Observing the shape of the particles you can see sharp, pointed surfaces. Particles of this shape can function as the edge of a cutting tool during sandblasting. The BPI Group Hungary has also given us a sample classified as waste. The consistency of this is almost flour-like. Classification of granular substances can be carried out on several scales (Atterberg, Krumbein, ISO14688-1) [1]. The microscopic recording is shown in *Figure 2*.

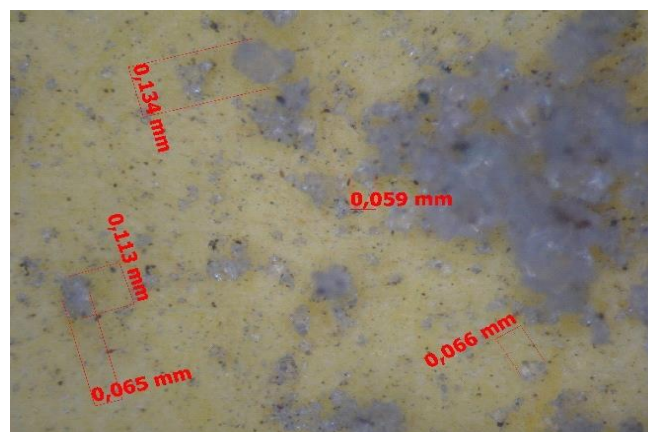


Figure 2

The broken glass after usage

3. TESTING OF RESULTING WASTE USING A SCANNING ELECTRON MICROSCOPE

We hypothetically assume that there are also components in the waste that are not indicated in composition data received from BPI, so the waste was tested using a scanning electron microscope. *Figure 3* shows the resulting waste sample at a magnification of 20 times. Let's look at what we can see in the microscope image: it is clear that there are two types of material that make up the waste, one is the glass used for cleaning, which appears in grey and the other is illuminated in white, these are metals in the waste. The majority is silicon, but also significant amount of potassium came from the glass raw material (potash-glass). As a result of the test we can conclude that a measurable amount of material is removed from the surface of aluminium components by the particle dispersion technology. Material removal changes the dimensions of the purified elements. The mass of the component is reduced.

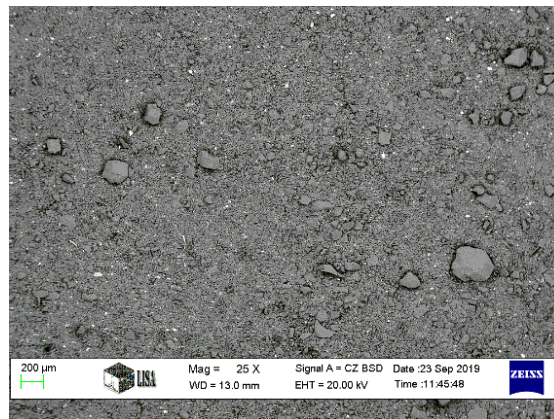


Figure 3
Image of scanning electron microscope 20× magnification

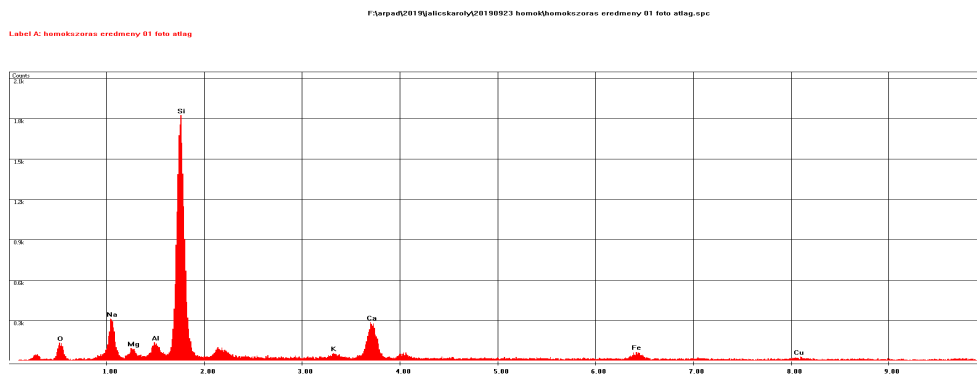


Figure 4
Composition of waste shown in Figure 3

4. SEPARATION OF WASTE INTO CONSTITUENT ELEMENTS, FINDING POSSIBLE SOLUTIONS

As part of the LIMBRA project Slovak-Czech team members carried out experiments to separate the waste with hydrochloric acid. We would like to present a description of the experiment we performed, the course of the tests and their results are summarized below. Exact description of the experimental method is:

- 20 grams of uncleaned glass waste was measured and placed in beaker. 50 ml of 1 : 1 hydrochloric acid solution was added to the waste then thoroughly mixed and then allowed to dissolve for 15 minutes.
- The solution was filtered, so the acid solution was separated from the solid glass. The filtration was carried out with filter paper type 388 (84 g/m²).
- The remaining glass was washed with water and then filtered.
- Drying was carried out at room temperature and allowed to dry for 48 hours.

The result is presented in *Figure 5*. You can see that the colour of the waste has changed (less dark) and it has become cleaner.

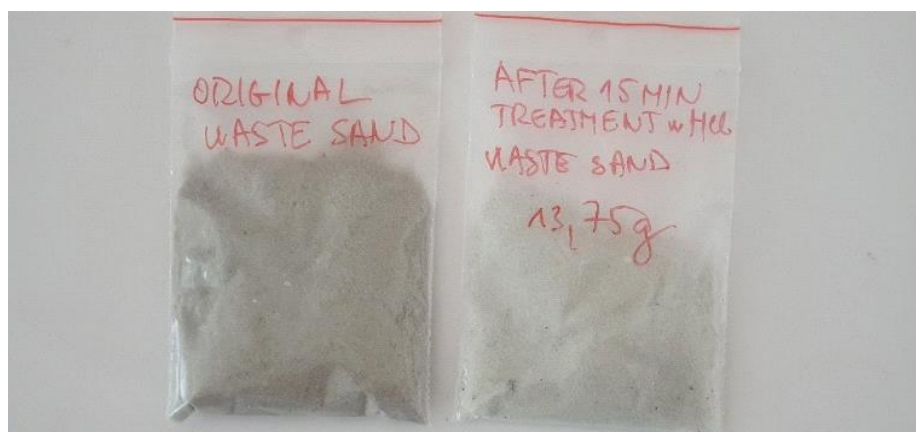


Figure 5

The result of the experiment after acid-treatment, filtering and drying

We can conclude that it is possible to clean up, so that not only the mixed material but also the purified material can be used for new applications.

5. WAYS TO USE THE WASTE

In the previous chapter we could prove that waste consist of variety of substances. We will look at the possibilities of using this waste. To make the subject clear we need to make assumptions as follows:

- Waste is not tested in its current mixed state but in a purified state;
- We assume that there are technologies to separate individual substances in waste;

- We take into account the main constituents and also as if they could be completely separated from other impurities.

Based on these assumptions the main ingredient in waste is the glass used for sandblasting, so its uses fall under primary attention. Of course such attention will also be paid to metals that appear in significant quantities in waste.

6. RECYCLING OF GLASS AS A SANDBLASTING MATERIAL

Here the primary goal is to produce particles of the same size as the original. Of course, this will be a procedure that can be quite costly since melting requires very high temperature, which entails a high energy requirement. In the process of producing glass different materials are fused and after cooling the fluid material we get the glass which can be melted again. That's a very important property. The temperature required for melting and glass cleaning depends on the exact composition but varies between 1,300 and 1,550 °C [2]. Since the heating of furnaces is traditionally achieved by burning fossil sediments it is necessary to look at the energy demand. This is important so that we can see how much energy is needed to produce glass but if we approach the same from the side where recycling does not need new glass significant energy can be saved. The melted glass is cooled and shaped to form depending on the technology: a large block is formed and then cut to the right size, broken or machined straight to the right size, i.e. the formation of a glass bead from the melt.

7. RECYCLING OF GLASS IN THE CONSTRUCTION INDUSTRY

Construction is specifically a sector where there is a high demand for raw materials, and it can make very good use of the properties of glass. There are many benefits to reusing glass in the construction industry. The main advantage of this is that we can reduce the need for raw materials during the construction of building materials or constructions. This is very important aspect when you consider that the earth's energy reserves are finite and therefore, we do not have an unlimited amount of raw materials. If you look at the simplest case glass waste can be used as a filler for various fillings and foundations. However much better solutions can be found in this industry so the next way to use it is to produce glass wool. Glass wool is made from a mixture of raw materials in the glass industry: glass tiles, limestone, sand, dolomite, sodium carbonate and boron oxide or boric acid [3]. Unusable damaged and mixed glass debris may be used for road construction when mixed with asphalt. The so-called glass asphalt made in this way complies with professional standards and has the same property and durability as conventional asphalt. In its manufacturing part of the natural additive is replaced by glass debris. However, its most important use can be observed in the production of concrete. This is of particular importance, since concrete production requires a lot of raw materials, so we can replace them, resulting in significant savings in raw materials. Natural additives can be replaced by glass waste. In cement production when milled glass is mixed with cement it increases the strength of large concrete bodies and dams. The second case is a technology called

“Geofil Bubbles”. “Geofil Bubbles” is a glass-based expanded gravel additive from recycled waste with a high glass content of industrial and communal waste (from the collection of packaging waste).



Figure 6
Geofil Bubbles

Glass waste with a high glass content mixed with contaminated paper and caps is milled to appropriate particle size, homogenised with gas-forming waste and then granulated. After heat treatment of the granules, a material with a high specific surface is applied as the last layer in order to control the ability to absorb water. After drying, a rotary oven with adjustable rotational speed and slope angle is heat treated and cooled abruptly. The density of the foam gravel thus produced shall vary between 200–1,200 kg/m³, water absorption capacity is between 0.1 and 45% by weight as needed.

8. GLASS AS AN ABRASIVE RAW MATERIAL

Particle with such sizes which are no longer possible to use for machining metals may be used for sandblasting of other surfaces. Use the Mohs hardness table: most of the grains used in sandblasting are in 7th hardness level, which is quartz, but in the factory a small amount of corundum material is also used for sandblasting. So, we can conclude that the tiny grain-sized glass could be suitable for glasses, window panes, etc. sandblaster, which can be used to engrave any pattern or possibly letters in the glass.

Let us take a closer look at the abrasive paper for the purpose of producing such a product from existing purified glass. As we look at the structure of the sandpaper itself, it can be said that the substrate of a good part of the abrasives on which the particles are fixed is paper or canvas, on the surface of which the abrasive particles of various materials and sizes are encapsulated in a special binder layer. Abrasives

can be divided into three groups according to their fineness. The fineness grade may be determined by the number of particles per 1 mm².

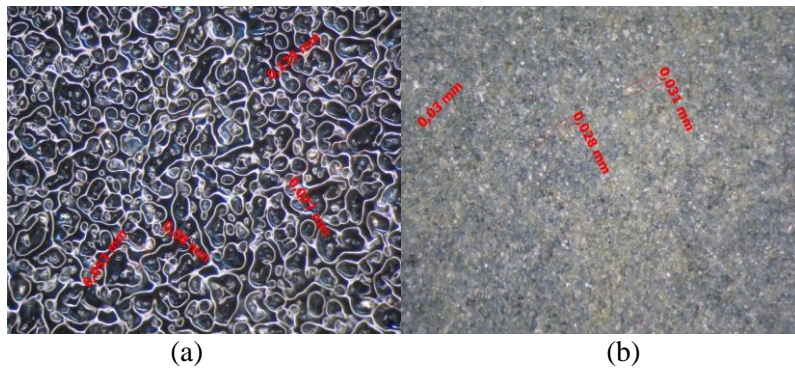


Figure 7
 (a) P400 sandpaper at 100× magnification,
 (b) P1200 sandpaper at 100× magnification

Here we can consider the results to be significant. This means that the particle size on P400 sandpaper is adequate, or that any finer sandpaper can be produced with further milling of the existing crystals. Since the desired particle size has already been achieved, the focus should now be placed on the granules. In general, 4 different materials are used as abrasives: Silicon carbide, Al-oxide, zirconium ores and ceramic corundum [4]. The most common substance of these is also silicon carbide. The classification of particle varieties by hardness, toughness and area of use can be examined in *Figure 8*. Since we have silica, which is not as hard as silicon carbide, it is clear that it would wear out faster during use. However, the hardness difference is not so large so we can say that our material could clearly be used as abrasive material as it has been used for a long time.

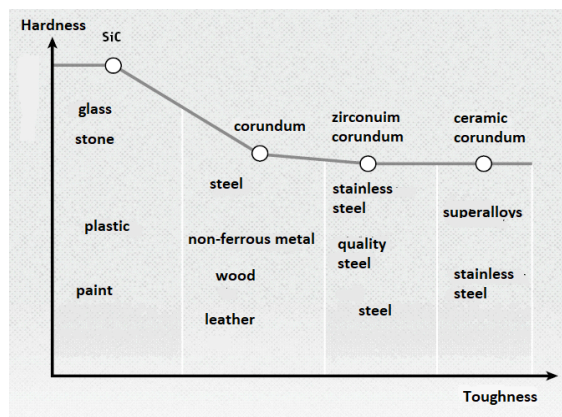


Figure 8
 Classification of grain varieties

9. SCRAP METAL USES

The most basic option is to sell metals on the market in their sorted form so we can melt these metals and serve as the raw material for any product in the future. Of course, this is the easiest way. Here we can mention any industry that works with metals the automotive industry is the simplest example, but to connect to BPI we can also produce new generator housings, self-starter housings or brake callipers from these metals. If we start from the particle sizes it can also be said that in the sinter technology, we could use these particles as raw materials or in metal printing, thus finding new industrial applications for scrap metal. However, there is a very important industry where particles of different metals could be widely utilized. It's the paint industry. Take some basic knowledge of the production of paints with special attention to the production of coloured paints. Paints consist of 3 main components: binder, pigments, solvents. The quality and quantity of pigment determine ink/dye properties such as colour, colour strength, colour durability and opacity. Pigments are predominantly micronin so we need to look at the size of our available particles [5]. *Figure 9* shows the size of two different metal particles.

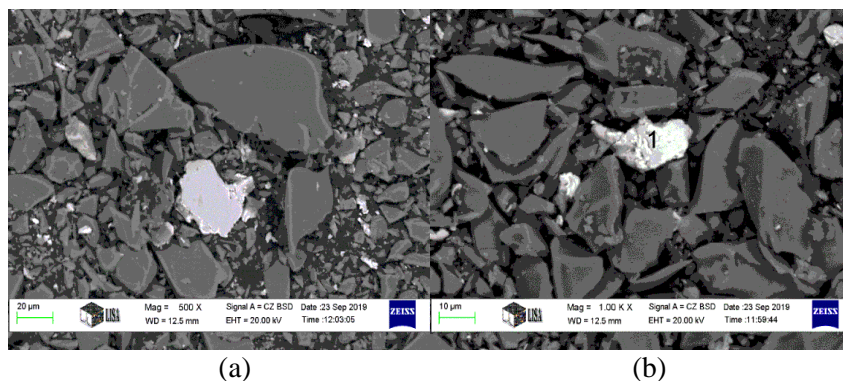


Figure 9
 (a) a Fe grain at 500× magnification,
 (b) a Zn grain at 1,000× magnification

According to the results the average size of the particles varies from 10 to 30 micrometres, so this is too large for paint. However, if you continue to reduce the size, they may be suitable for this purpose.

10. SUMMARY

Based on the above chapters we can conclude that the blasting technology removes a significant amount of material from the surface of the cleaned parts. Removed material is present in the waste. Furthermore, the most significant part of the waste is the sandblasting material, the glass. As you can see in this article it is an important question in today's raw material hungry world to ponder how these materials could be recycled. We were able to find many solutions for both glass and scrap metal.

Thus, in summary certain substances in sandblasting waste could be used very widely and these uses would make a major contribution to reducing waste emissions, thus reducing the environmental pressures. It could also be an important link to the European Union's new Green Deal plan.

ACKNOWLEDGMENTS

The described article/presentation/study was carried out as part of the EFOP-3.6.1-16-2016-00011 *Younger and Renewing University – Innovative Knowledge City – institutional development of the University of Miskolc aiming at intelligent specialisation* project implemented in the framework of the Szechenyi 2020 program. The realization of this project is supported by the European Union, co-financed by the European Social Fund.

REFERENCES

- [1] ISO 14688-1:2002. *Geotechnical investigation and testing – Identification and classification of soil – Part 1: Identification and description.*
- [2] ISO 6721-11:2012. *Plastics — Determination of dynamic mechanical properties — Part 11: Glass transition temperature.*
- [3] Almusaed, Amjad (2012). *Effective thermal insulation: the operative factor of a passive building model.* 978-953-51-0311-0, InTech, Rieka, Croatia.
- [4] Kanegsberg, Barbara, Kanegsberg, Ed. (2011). *Handbook for Critical Cleaning: Cleaning Agents and Systems.* 978-1-4398-2827-4, CRC Press, Boca Raton, Florida, United States of America.
- [5] Buxbaum, Gunter, Pfaff, Gerhard (2005). *Industrial Inorganic Pigments.* 978-3-527-30363-2, Wiley-VCH, Weinheim, Germany.

PRODUCT DEVELOPMENT FROM ECODESIGN POINT OF VIEW IN PRACTICE

LÁSZLÓ SOLTÉSZ – LÁSZLÓ KAMONDI – LÁSZLÓ BERÉNYI

University of Miskolc, Institute of Machine and Product Design,
Institute of Machine and Product Design, Institute of Management Science
3515 Miskolc-Egyetemváros
solteszlaszlo1977@gmail.com; machkl@uni-miskolc.hu; szvblaci@uni-miskolc.hu

Abstract: During the development of new product designers must care about thousand of things to finally deliver a successful product to market. There is high pressure from manufacturing to using easy and usable technologies, quality team asking design robustness, management wants to see the product in the right time and on perfect cost level both form project product cost viewpoints. Nowadays, a responsible company and product development team must care and put high focus for an environmentally friendly solution and for sustainable product development. These things have to work together as a system. This paper presents a product development project in a household equipment producer company and company efforts to reduce environmental footprint.

Keywords: *new product development (NPD), design for environment, footprint reduction, product development in practice, project success*

1. INTRODUCTION

The importance of environment protection is relevant to all industries in the 21st century. The company is aware of these environmental rules and knows the importance of strategy-based control and evaluation of environment protection in everyday life. In accordance with the ISO 9001 standard, they were also aiming to reduce the harmful effects on the environment during the product development process and design of new industrial or automotive products.

With the supervision of Health, Safety and Environment Team, the investigated company is aiming to increase its performance according to environment protection, including the reduction of the ecological footprint.

This paper explains via an example of how possible to manage multi-level requirements of new product development.

In the 21st century, ecodesign directives came in the foreground at product development area too. Sustainable product designs and production systems become inevitable requirements from a social point of view. Every high runner at customer product market has to for new requirements. These wishes from market and customers also provide high opportunities to marketing and communication teams of companies.

The buzzword 'Ecodesign' could open new doors for products into the heart of customers easily.

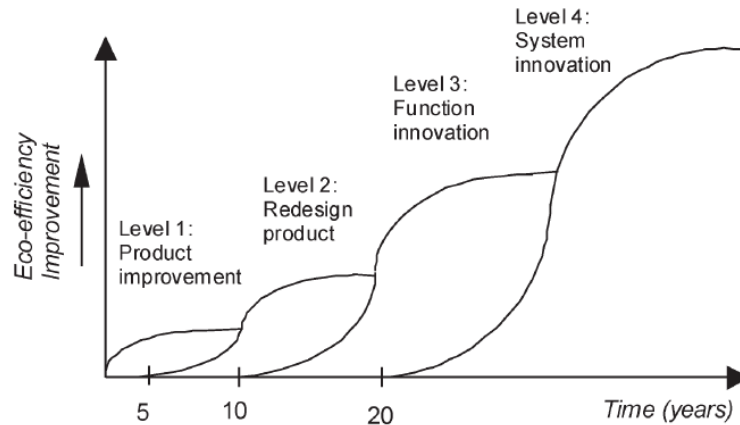


Figure 1
Four stage model of ecodesign innovation [1]

2. PRODUCT RELATED GREEN ACTIVITIES

Table 1 [6]

Ecodesign strategies	Ecodesign principles
1. Selection of low-impact materials	Clean materials Renewable content materials Recycled materials
2. Reduction of materials usage	Reduction in weight Reduction in volume
3. Optimisation of production techniques	Clean production techniques Fewer production steps Low/clean energy consumption Less production waste Few/clean production consumables
4. Optimisation of distribution system	Less/clean/reusable packaging Energy-efficient transport mode Energy-efficient logistics
5. Reduction of impact during use	Low energy consumption Clean energy source Few consumables needed Clean consumables No waste of energy/consumables
6. Optimisation of initial lifetime	High reliability and durability Easy maintenance and repair Modular/adaptable product structure Classic design Strong product-user relation

7. Optimisation of end life	Reuse of product Remanufacture/refurbishment Recycling of materials Safe incineration (with energy recovery) Safe disposal of product remains
8. New concept development	Shift to service provision Shared product use Integration of functions Functional optimisation

2.1. Green approach by company and people

Green product development, which addresses environmental issues through product design and innovation, is receiving significant attention from consumers, industries, and governments around the world [2].

Communication, innovation, and education of employees is an important aspect of environmental protection. Therefore, the employees of the company regularly take part in training. From the aspect of environmental protection, they are aiming for the minimum impact during the full life-cycle of our products, including the conceptual and constructional design, manufacturing, transportation and recycling of our products.

During the design phase, the usage of paper is restricted, and only a minimal amount is allowed under critical conditions. Various design computers, simulation software and hardware contribute to a fast and efficient design process in our company. Our developer team communicate using internal digital systems during the different cycles of the pilot valve design.

An everyday effort is to reduce the amount of communal waste. It is a daily task to separate, store, and transfer the waste generated in the plant, involving employees in any kind of activities. The storage of hazardous waste is a relevant example because companies of today are using several electric equipment and batteries during manufacturing and construction processes (during the constructing of the pivot valve too). In case of the machines that have independent power sources, there is a bin placed for collecting the used batteries in the near of the activity. This allows a safe way of storing hazardous waste and makes the transfer simpler from the production line.

The protection of products against dust and liquid is indispensable during shipping; therefore, the packaging phase is necessary. While doing so, the production line strives using more effective packaging and consuming less material. This means that the usage of thin wrapping material is the solution for this requirement.

Usage and properties of the wrapping material comply with European standards. Applied materials can easily be recycled and are degradable. Fully domestic and in-house production also reduces packaging of used semi-finished products, because it is not necessary to ship or pack these.

2.2. Details of product development

The design of the suspensions of vacuum cleaner motor is also delivered by Hungarian engineers. With optimal sizing, a significant proportion of engine vibration and noise levels have been reduced, thus contributing to the creation of a state-of-the-art product in terms of noise load. Selection of the raw material for the suspension was determined by detailed, multi-stage design and analysis of experimental results. Determining the technically impeccable design, technology and raw materials was a significant challenge, but at the same time, by preferring Hungarian suppliers, the highest proportion of the technological background available in Hungary was incorporated into the production and design process.

The complete verification of the product – including the new electronics, the accessory system and the high-efficiency engine – took place in the Hungarian test laboratory. Test equipment park was designed for the needs of the Energy Labelling and ECO design directives by Hungarian designers. In connection with the preparation for the Energy Labelling regulation, in recent years test laboratory in Hungary has grown into one of the largest centres for testing vacuum cleaners in Europe due to the significant expansion. Thanks to continuous improvements, there is no such thing today for the performance of vacuum cleaners. The European standard for longevity, for which we would not be able to carry out the necessary tests and inspections. The most important test equipment, which is the most important from the point of view of Energy Labelling – dust collection ability tester, suction power tester, dust emission tester equipment – was designed and constructed in accordance with the standards, but also in cooperation with Hungarian suppliers. I'm proud to say that the technical standard of these types of equipment reaches and even exceeds energy labelling grades of equipment manufactured by the suppliers and available in the market.

Motorised suction head developed by Electrolux is designed for high-efficiency carpet cleaning. There are different types of carpets in households with different heights (fibre lengths) that we want to clean with the same high efficiency. One of the main features for effective dust removal is the distance between the suction head and the mat. As we want to meet the needs of all our customers to the maximum, motorised power nozzle is equipped with a unique height adjustment mechanism, which can be adjusted comfortably with the pedal on top of the nozzle. The given height setting is confirmed by the LED lighting, which illustrates the four height levels in the low-extra high range. In the low (LO) position, hard floors or low fibre length carpets, while in the highest (X-HI) position, extra-sized carpet fibres can be cleaned above the level specified in energy class "A".

2.3. Maximum grade in all class

In addition to the basic features of the device, AAAA rating is made possible by the following features:

Achieving "A" energy efficiency is ensured using high-performance, yet very low energy, high-efficiency and high suction power level motors.



Figure 2

AAAA and ECO force label to show high suction power to customers [3]

Dust removal on carpet “A” is aided by a motorised suction head, which allows you to clean the deeper layers of the carpet without much strain, as the motor-driven rotary brush bristles can be removed from the carpet increase the dust content to $\geq 91\%$ according to tests performed in accordance with the relevant regulations.



Figure 3

AeroPro Extreme Power Pro nozzle for A grade dust pick-up on carpet [4]

Dust removal “A” on the hard floor is provided by specially designed AeroPro Parketto Pro suction head, which, thanks to its special design, allows a suction range beyond the width of the head, in addition to removing fine dust particles from the gaps in the floor; due to the arrangement of the brushes built into the nozzle and the distance between the nozzle and the floor, dust removal is $\geq 111\%$. 111% means that head can suck up all dust on test track under suction head what means 100%. Further extra dust is collected from outside of nozzle what cause extra amount of dust, in that case about 11%.



Figure 4

Parketto Pro hardfloor nozzle for A grade dust pick-up on hardfloor [5]

The combined use of high-quality sealing materials at the joints, the high-efficiency s-Bag dust bag and the Allergy Plus outlet filter achieves the “A” dust emission in the design of the device, as it was an important consideration in creating a healthy home. The amount of dust picked up by the appliance and returned to the air in the apartment should be kept to a minimum.



Figure 5
Hepa H13 washable filter for A grade dust emission [5]

3. ENVIRONMENT SAFETY OF PRODUCT DESIGN

Based on the results of market research, our customers are looking for products that are easy to use, have outstanding cleaning efficiency and can be used well on any surface in their home, with no obstacles in front of them. Protecting the environment and reducing the burden on the environment is one of the top priorities of our present and future. Customers are also becoming more environmentally conscious and, in addition to the above expectations, energy efficiency, and the use of recycled raw materials are important to them.

The Quattro was also the highest model in the Ultra One family, a true flagship, a well-thought-out and redefined version of the product family in the sense of the above. The product is described in detail in the so-called “EcoDesign” requirements, which came into force on 1 September 2014.

In addition to energy efficiency, another important aspect in design of the device’s plastic components was the reduction in the weight of the vacuum cleaner, which, in addition to making the device easier for consumers to use, significantly reduced the mass of materials used.

The design of the vacuum cleaner, as well as the use of recycled raw materials and a motor with minimal energy consumption in its production, not only set an excellent example of environmental awareness but also met the need for the fullest level of compliance with market and regulatory requirements.

All in all, as a result of the technical improvements and innovations described above, the Quattro of the Ultra One product family protects not only the environment but also our personal environment.

4. SUMMARY

Strict ecodesign rules and regulations by government does not cause any competence back draw for companies, if regulation is mandatory and valid for all parties in market. [7] Quattro vacuum cleaner development was extremely successful in that time when European Union introduced this regulation. Later due to pressure from some parties on market this regulation was cancelled and today it's not mandatory in EU, because some technology get potential market disadvantage – that technology was cyclonic dust separation systems.

This product development process analysis shows that possible to make market winner, best in class product development if targets are crystal clear in project. Other success factor was here the knowledge base what was in head of designer engineers and also in lessons learned database. Combination of these knowledge, experience and available good base of product for further improvement make Electrolux Small Appliances sector to 1st in the world who could provide AAAA rated cleaner to market.

ACKNOWLEDGEMENT

The described article was carried out as part of KDP-2020 Cooperative Doctoral Program project implemented with the support provided from the National Research, Development and Innovation Fund of Hungary and Ministry for Innovation and Technology of Hungary.

REFERENCES

- [1] Bhamra, T. A. (2004). Ecodesign: the search for new strategies in product development. Proceedings of the Institution of Mechanical Engineers, Part B, *Journal of Engineering Manufacture*, 218 (5), 557–569. doi: 10.1177/095440540421800509.
- [2] Chen, Chialin (2001). Design for the Environment, Environment: A Quality-Based Model for Green Product Development. *Management Science*, <http://dx.doi.org/10.1287/mnsc.47.2.250.9841>.
- [3] Electrolux (2014). *Electrolux presents the first AAAA vacuum cleaner in the market*. <https://www.electroluxgroup.com/en/electrolux-presents-the-first-aaaa-vacuum-cleaner-in-the-market-19544/>.
- [4] Márkabolt.hu (2018). *Electrolux ZUOQUATTRO porszívó*. https://www.markabolt.hu/electrolux/electrolux_porszivo/electrolux_porszivok/Electrolux.

-
- [5] Electrolux.hu (2020). *Electrolux EFH13W HEPA H13 szűrőbetét*. <https://www.electrolux.hu/vacuums-home-comfort/vacuum-cleaners/accessories/filter/efh13w/>.
 - [6] Van Hemel, C. (1998). *Ecodesign empirically explored – design for environment in Dutch small and medium sized enterprises*. PhD thesis, Bedfordshire, Deft University.
 - [7] Vajna, S. (ed.) (2020). *Integrated Design Engineering – Interdisciplinary and Holistic Product Development*. Heidelberg, Springer Nature, ISBN 978-3-030-19356-0.

PROJECT MANAGEMENT SUCCESS FACTORS: IN SEARCH OF PRODUCT DEVELOPMENT PROJECT SPECIALITIES

LÁSZLÓ SOLTÉSZ – LÁSZLÓ KAMONDI – LÁSZLÓ BERÉNYI

University of Miskolc, Institute of Machine and Product Design,
Institute of Machine and Product Design, Institute of Management Science
3515 Miskolc-Egyetemváros
solteszlaszlo1977@gmail.com; machkl@uni-miskolc.hu; szvblaci@uni-miskolc.hu

Abstract: Project success is a multifactorial issue, including difficult to quantify, soft factors as well. Project management style, collaboration within the team, and the level of standardisation may have an essential influence on the deliverables, moreover, on corporate performance. A prescription answer is not achievable considering the individual characteristics of projects but finding best practices and critical factors help to improve the performance. This paper presents the results of a survey among product development project experts (n = 112) evaluating the relevance of some success factors and their practical experience in the field. The results show that keeping the project plan and managing long-term issues like lessons learned database or module database are the most critical factors of success. The analysis did not find patterns of the responses that confirms the need for unique management actions.

Keywords: *project success, product development process, expert survey, IPA analysis*

1. INTRODUCTION

Companies, to keep competitiveness, must continuously find new and newest ways for creative and cost-efficient solutions. [1] One of the main goals of a company is to bring products to the market, whose performance and behaviour in providing this performance is desired by customers and users, and which, due to these characteristics, help the company to achieve continuously high profitability and financial stability, high acceptance by all social groups and possibly also market leadership. [2] Evolution of product development methods and processes are aligning into the clear cue, or we can say the direction of improvement is going into some main direction:

- Reduction of time of products development project, parallel this reduce cost what is spent to development. In the case of shorter development time cause quicker payback of development costs for the corporation. A further advantage to be on the market earlier than competitors can increase profitability dramatically in the case of ‘hungry’ market.
- Cost planning of product development projects is a key factor already from the start. [3] Due to the reduction of cost and development time payback period of investment of new product also reduce significantly.

- Increase of fulfilment of market needs and customer demands. One of the most critical objective of product development and the entire company to be on the market with products what exactly can cover customer demands as much as possible. This is the substance of professional product development.
- Improvement of product and process quality for entire supply chain and production. A high level of quality is just a ‘must’ but not an advantage. During the execution of the project, there is no way to make any concession of quality, the only way to change timing or cost if any fine-tuning is necessary even lightening of quality level can be an easier way to deliver product development project [3].

Although each project is a temporary endeavour undertaken to create a unique product, service, or result [4], due to market and corporate specifics, it is worth to analyse the lessons and develop the project management practices. It is not possible to determine with engineering accuracy the tasks and tools required for the success of the project, but the development of skills in the field can significantly contribute to managing the emerging risks and opportunities. The goal of the paper is to examine project management success according to product development processes.

2. PROJECT SUCCESS FACTORS

Project success is designated by the quality of results, budget, and timeframe [5] [6]. There are several factors which affect one or more of these factors. According to the stakeholder theory, project success can be evaluated on the satisfaction of the stakeholders [7] [8]. However, it is a great challenge to find the proper weights of the stakeholders’ expectations. Baccarini [9] highlights beyond the project management success, the product success covering the organisational expectations as a success factor. There is a change of focus point over time. The emphasis is moved from project management success (in the 1960s–1980s) to project/product success (in the 1980s–2000s) then to project/product, portfolio, and program success and narratives of success and failure in the 21st century [10].

The success of the project can be described and controlled by quantifiable indicators but achieving them are largely depending on leadership and management style [11]. A thorough investigation of collaboration between the project team, or the level of trust may bring to a closer understanding of project success [12] [13].

Moreover, knowledge integration capability [14] must also be considered. It is to note managing project knowledge appears asymmetrically. Of course, each project profits from previous lessons and welcomes the available information but generating explicit knowledge for the future requires additional efforts, and it is not acknowledged when created.

Best practices and pieces of evidence allow us to rethink and refine the influencing factors of project success, but there is no prescription answer. Targeted research activities that can contribute to expanding the knowledge base and re-check the previously established models are essential to improving project success. This paper investigates the opportunities according to product development projects.

3. METHODS AND LIMITATIONS

An online survey was conducted among product development experts in 2020. Assuming that project management is determinative in achieving project success, the survey included a list focusing on the project management responsibly. The experts were asked to evaluate the importance of the items on a 5-point scale (1: not important at all, 5: essential). Other questions of the survey asked to evaluate the performance of these issues. The comparison of the importance and performance allows exploring the most critical factors. Survey items are summarised in *Table 1*, including the sample sizes. The evaluation of importance is based on 112 responses in each case, but performance is not evaluated if the topic is not managed by the corporation.

Table 1
Factors of analysis

Factor	Note	sample size (performance)
Availability of written standards	Access and understanding to rules and expectations	112
Review of written standards regularly	Regular update in line with changes	112
Defined project goals	Clear and written goals known by who is concerned	112
Keeping the project plan	Frequency of changes in the plans	112
Feedback	The utilisation of former experiences	112
Project meetings	Average evaluation of the usefulness	112
Teamwork	Collaboration between the project team members	112
Managing lessons-learned	Availability and utilisation of a lessons-learned dataset	76
Managing module-database	Availability and utilisation of a module dataset	64
Involvement of production	Collaboration between the project and the representatives of production	112
Active attention of the project manager	The activity of project manager according to team and tasks.	112

The results of the survey are presented by the mean values of the evaluations including the standard deviations, and an IPA (importance-performance analysis) matrix based on the work of Marilla and James [15]. The correlation between the factors is

measured with the Spearman correlation coefficient [16]. Data analysis is supported by IBM SPSS 25.

The research presented in this paper cannot be considered as a complete or representative survey in the field of project management of product development, but the results are based on the responses of practising professionals of various corporations. Their opinion may be relevant in exploring critical problems.

4. RESULTS

4.1. Evaluation of project management success factors

The well-defined project goals (mean value 4.87 on the 5-point scale) and cooperation of the project team (4.84) are ranked the most relevant success factors. Review of the standards (3.87), managing the lessons learned from the project (3.84) and managing module databases (3.78) are at the bottom of the list (Figure 1).

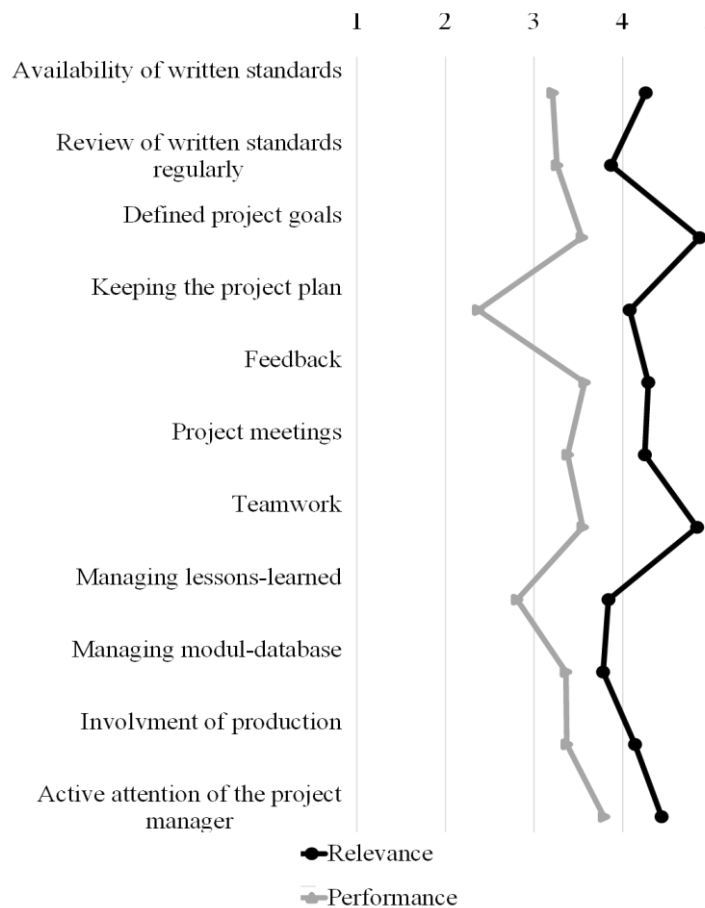


Figure 1
Survey results measured on a 5-point scale

The performance evaluation of the items shows two outlier values. Modification of the specifications is a common feature of the project (mean value is 2.37, lower value means more frequent need for changes). On the other hand, managing lessons learned (2.81) is rated lower than the medium value. Based on the distances between the evaluation of relevance and performance, the issues of well-defined goals, keeping the project plans and teamwork show the highest differences. In general, the distances by evaluation factors presented in *Figure 1* suggest that factors with the highest importance are in line with higher differences between relevance and performance. An exception is according to keeping the project plan.

That suggests that project management success is mainly focused on the short term (i.e., the interest of the current project overwrites other issues) in the view of the experts; corporate-level impacts are less important.

4.2. IPA analysis

The importance-performance analysis allows to point out the critical factors visually. Since the aspect of importance is rated to the high field in each case (all mean values are higher than the medium), *Figure 2* is zoomed. The performances in 9 of 11 factors investigated are between the values 3 and 4, which refers to a good performance. However, excellent ratings (performance indicator around 5) are missing.

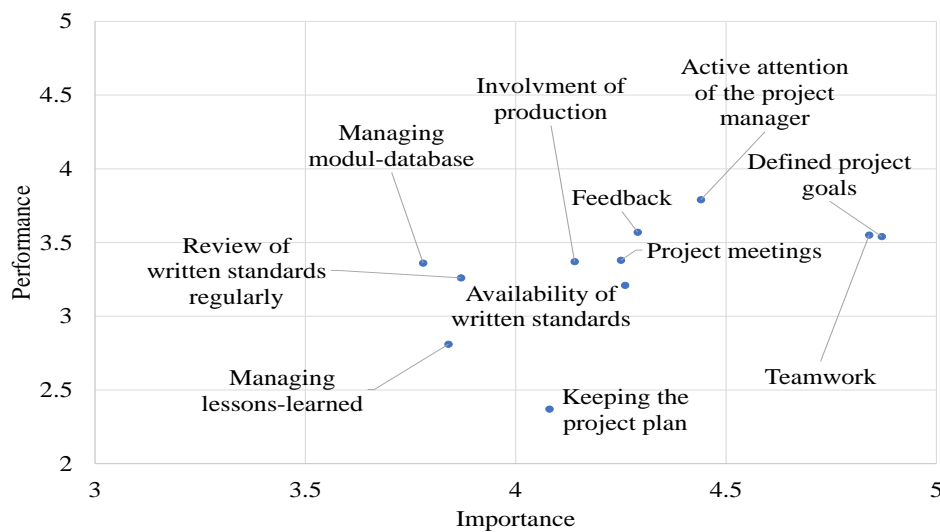


Figure 2
Importance-performance evaluation of project success factors

Based on the relative positions of the factors, managing lessons learned and keeping the project plan can be considered as the most critical ones. The strengths of project management are the active focus of the project manager both on the team and the progress. Information flow also has a good relative position within the project (feedback and the evaluation of project meetings), but the performance values clearly

Table 4*Spearman-correlations between relevance and performance by survey items*

	(1)	(2)	(3)	(4)	(5)	(6)	(7)	(8)	(9)	(10)	(11)
Availability of written standards (1)	-0.039	0.054	0.088	0.178	-0.035	0.115	.238*	0.032	0.03	0.136	-0.009
Review of written standards regularly (2)	-0.002	0.122	0.172	0.183	0.091	0.113	0.084	0.049	0.046	0.166	0.015
Defined project goals (3)	-0.098	0.091	0.169	.265**	0.127	.212*	0.159	0.138	-0.094	0.072	.193*
Keeping the project plan (4)	0.124	-0.027	-0.083	0.066	0.008	-0.037	-0.002	0.144	0.053	-	0.018
Feedback (5)	-0.155	0.061	0.099	0.152	0.117	0.004	0.018	0.053	-0.049	-	-0.106
Project meetings (6)	-0.091	0.125	0.117	0.145	-0.027	.210*	.188*	-0.025	-0.048	0.074	-0.008
Teamwork (7)	-0.091	-0.022	-0.042	0.04	-0.058	0.155	0.166	-0.003	-0.003	0.021	0.052
Managing lessons-learned (8)	0.151	0.205	.352**	0.154	0.1	0.038	-0.04	0.2	0.131	-	-0.04
Managing module-database (9)	-0.045	0.021	0.058	0.083	-0.034	0.041	-0.082	0.087	-0.084	0.076	0.085
Involvement of production (10)	-0.086	0.043	-0.016	.218*	0.08	0.015	.228*	0.185	0.14	.241*	0.13
Active attention of the project manager (11)	0.165	.368**	0.142	.300**	.290**	0.052	0.157	.211*	0.181	.241*	0.125

According to the evaluation of importance, there are few significant and high-value correlations. This suggests that the factors are parallelly crucial for project success. Theoretically, exploring patterns of the evaluations is feasible by cluster analysis, but the analysis did not find relevant grouping opportunity. This result confirms that all factors are important; however, this also can be a result of the fact that the experts ranked all importance items high. The diagonal values of the correlation analysis between the importance and performance factors show significant results in two cases (project meetings and the involvement of production). Performance evaluation shows significant and high correlations. Cluster analysis was conducted to explore patterns based on the responses, after dimension reduction of the data by principal component analysis. Still, grouping must have been rejected in this case as well.

5. CONCLUSION

Although the purpose of a project is to contribute to improving corporate performance by framing the changes systematically, projects also can be considered as individual units. The latter approach means the effectiveness and efficiency of project management will be evaluated and accounted for on a project-by-project basis. Project managers and team members are rewarded or punished by the project performance that may hinder a broader approach to success. In the case of product development projects, this more comprehensive approach would be particularly important because these determine further project initiations.

Understanding project management characteristics include several soft factors. These are difficult to measure with an engineering approach, but experience supports the consideration of them. The survey results confirm that the long-term approach is less important based on the evaluations of the experts in the field. The selected success factors of the survey are all rated quite relevant, and the performance evaluation show shortcoming compared to the importance. Literature [4] [17] emphasises the utilisation of former project experience is essential for saving time, cost and reducing

the risks of a project. The survey does not confirm the excellence of practical applications. Managing module-databases and especially lessons-learned, are among the most critical factors in the survey.

Beyond this, the specification in project plans are often changing, but these changes are considered quite usual (relevance of keeping the project plans is rated relatively low compared to other factors). It is to note, that in the meanwhile the need for well-defined and well-understood project goals are considered among the most important factors.

Endeavours to find patterns of the opinions are failed. This suggests that the opinions and the problems which the experts meet are diversified. In terms of development opportunities of the tools of product development project, an extensive generalisation is available.

ACKNOWLEDGEMENT

The described article was carried out as part of KDP-2020 Cooperative Doctoral Program project implemented with the support provided from the National Research, Development and Innovation Fund of Hungary and Ministry for Innovation and Technology of Hungary.

REFERENCES

- [1] Soltész, L. (2019). Product development project of high performance electrical power pilot valve in practice. *GÉP Journal*, Vol. 70, No. 4, pp. 21–25., ISSN 0016-8572.
- [2] Vajna, S. (ed.) (2020). *Integrated Design Engineering – Interdisciplinary and Holistic Product Development*. Heidelberg, Springer Nature, ISBN 978-3-030-19356-0.
- [3] Soltész, L., Berényi, L., Kamondi, L. (2020). Analysis and assessment of the product development process. *GÉP Journal*, Vol. 71, No. 3–4, pp. 61–71., ISSN 0016-8572.
- [4] *Project Management Body of Knowledge* (2017). 6th Edition, Project Management Institute, Newtown Square, ISBN 978-1-62825-184-5.
- [5] Görög M. (2019). *Projektvezetés a szervezetekben*. Budapest, Panem Kiadó, ISBN 978-9-63545-537-9.
- [6] Aranyossy, M., Blaskovics, B., Horváth Á. A. (2018). How universal are IT project success and failure factors? Evidence from Hungary. *Information Systems Management*, Vol. 35, No. 1, pp. 15–28., ISSN 1058-0530.
- [7] Eskerod, P., Huemann, M., Savage, G. (2015). Project stakeholder management: past and present. *Project Management Journal*, Vol. 46, No. 6, pp. 6–14., ISSN 8756-9728.

-
- [8] Ligetvári É., Berényi L. (2013). A project érintettjeinek kezelése. *Magyar Minőség*, Vol. 22, No. 7, pp. 11–19., ISSN 1789-5510.
- [9] Baccarini, D. (1999). The Logical Framework Method for Defining Project Success. *Project Management Journal*, Vol. 30, No. 4, pp. 25–32., ISSN 8756-9728.
- [10] Ika, L. A. (2009). Project Success as a Topic in Project Management Journals. *Project Management Journal*, Vol. 40, No. 4, pp. 6–19., ISSN 8756-9728.
- [11] Horváth V. (2019): Projektmenedzsment kompetencia – Definíciók, modellek, standardok és a gyakorlati alkalmazás lehetőségei. *Vezetéstudomány*, Vol. 50, No. 11, pp. 2–17., ISSN 0133- 0179.
- [12] Henderson, L. S., Stackman, R. W., Lindekilde, R. (2016). The centrality of communication norm alignment, role clarity, and trust in global project teams. *International Journal of Project Management*, Vol. 34, No. 8, pp. 1717–1730., ISSN 0263-7863.
- [13] Bond-Barnard, T. J., Fletcher, L., Steyn, H. (2018). Linking trust and collaboration in project teams to project management success. *International Journal of Managing Projects in Business*, Vol. 11, No. 2, pp. 432–457., ISSN 1573-8378.
- [14] Todorović, M. L., Petrović, D. Č., Mihić, M. M., Obradović, V. L., Bushuyev, S. D. (2015). Project success analysis framework: a knowledge-based approach in project management. *International Journal of Project Management*, Vol. 33, No. 4, pp. 772–783., ISSN 0263-7863.
- [15] Lin, S. P., Chan, Y. H., Tsai, M. C. (2009). A transformation function corresponding to IPA and gap analysis. *Total Quality Management & Business Excellence*, Vol. 20, No. 8, pp. 829–846., ISSN 1478-3363.
- [16] Georg, D., Mallery, P. (2019). *IBM SPSS Statistics 26 Step by Step: A Simple Guide and Reference IBM SPSS Statistics 26 Step by Step: A Simple Guide and Reference*. London, Routledge, ISBN 978-036717-435-4.
- [17] *The Standard for Portfolio Management*. 4th Edition, Newtown Square, Project Management Institute, ISBN 978-162825-197-5.

BRIEF OVERVIEW OF GENERATIVE DESIGN SUPPORT SOFTWARE

KRISTÓF SZABÓ – GYÖRGY HEGEDŰS

University of Miskolc, Department of Machine and Product Design
3515 Miskolc–Egyetemváros
szabo.kristof@uni-miskolc.hu

Abstract: The new generative design process that has emerged in recent years has become available in more and more software. With the classic rapid prototyping procedures, it was not possible to test the designed products during long-term operation. However, the advent of metal powder printing and additive technology already allows for the long-term testing of designed prototypes, and even, if the deviation from the required properties of the product is negligible, the production of the final products. As a result, with the generative design process, design engineers also can create products that seemed unthinkable so far.

Keywords: *shape optimization, topology optimization, generative design*

1. INTRODUCTION

The shape of a product is primarily determined by the functions to be implemented by that, which may be slightly influenced by the manufacturing process properties of the product (e.g. machined or cast parts). During the development of a given product, it is advisable to perform various engineering tests and then improve the product by its analysis. This can happen by the reduction of the weight of the product, the of the load capacity of the product, or the change of the final geometry. This iterative design-development process can also be considered as the search for an optimal solution; however, this process is time consuming and requires a more experience. If the traditional manufacturing technology operations are considered (e.g. prismatic milling) when developing a product, solutions may have which are limited by manufacturing technology. Most *CAD/CAM* modules in computer-aided design systems, or most custom *CAD* and *CAM* software, support modelling procedures or manufacturing processes that conform to the traditional design approach. The built-in algorithms that provide shape optimization in the software have been designed to meet the limitations of the traditional design approach. However, using additive manufacturing technology, products that were previously thought to be unmanufacturable can also be produced (e.g., inaccessible surfaces, “native” elements). It should be noted that additive manufacturing is a collective term, including the long-known rapid prototyping processes, which mostly work with polymeric raw materials, however, due to the development of technology, the processes working from metallic raw materials e.g. by developing and disseminating the properties of

Selective Laser Melting (SLM), *Laser Metal Deposition (LMD)* and the base metal powders, the product thus produced is not a prototype but an end product [1]. If additive manufacturing technology is considered during the design process, producing the geometry of the part to be optimized with traditional modelling methods is an extremely time-consuming operation. Generative design software and modules were created in order to solve these kinds of issues.

2. SHAPE OPTIMIZATION AND TOPOLOGY OPTIMIZATION

Optimization during mechanical design means the best solution selected under the given operating conditions, which is selected from the set of solutions produced. Mathematically, optimization means the determination of the maximum or minimum of an objective function. In general, the optimization searches for the best value of an objective function in each acceptable range, where both the acceptable range and the objective function can be of different types. Often the objective function defined at the design phase is multi-objective and multivariate, so optimization can be defined as the calculation of several target values.

During shape optimization, the shape of the margin surface of the generated body model is changed so that the best possible value of the objective function is obtained by observing the optimization conditions. The *CAD* model data also includes design variables, design parameters, material properties, and boundary conditions for finite element tests. During shape optimization, the design variables are selected from the parameters describing the geometry, this parametric data set (e.g. dimensions, shape features, part history) is automatically generated in the applied parametric integrated design systems. Since a model of a part can be produced in several ways (e.g. choice of shape features, sequence of operations, dimensions of sketches), it is important to note that this can affect the optimization task, so the geometry must be carefully prepared already during modelling.

In case of topology optimization, the goal is to determine the optimal design of the part within a given volume under predefined boundary conditions and loads. During topology optimization, the elements of the initial volume are deleted from the design space, considering the design variables and the objective function. A detailed elaborate initial geometry is available for shape optimization, while it is not necessary for topological optimization. There may be names for some software that refer to shape optimization, but the result produced is the result of a topology optimization. The difference between shape and topological optimization is made clear by the applied procedure. Topological optimization procedures require computationally intensive numerical and finite element algorithms, and their proliferation has become possible in recent decades. In practice, several methods have been developed, which can be divided into two major groups:

(1) gradient type methods:

- material distribution method: *SIMP (Solid Isotropic Microstructure/Material with Penalties)* [2],
- homogenizing methods *OMP (Optimal Microstructure with Penalization)* [3],

- discrete, global methods [4],
 - topological derivative and level set method (*LSM – Level Set Method*) [5],
 - method using *Sudden Death Method*, e.g. *ESO (Evolutionary Structural Optimization)* [6];
- (2) non-gradient-type, heuristic methods [7].

One of the most efficient and computationally simple methods is the *SIMP* method, most software developers use this method in their systems for topological optimization.

3. THE MECHANICAL GENERATIVE DESIGN PROCESS

Generative design can be applied not only in mechanical but also in other fields, like in architectural, furniture, artistic works. The design process can be generalized; however, the approach focuses on mechanical design processes. Due to the spread of additive and hybrid manufacturing technology, there has been an increasing emphasis in recent years on the emergence of generative design methods in mechanical design systems. Generative design is a new type of design process, the main features of which are artificial intelligence-based software and machine learning, which allows the shape and composition of a part to be determined by physics-based simulation and other analysis methods, taking into account expected requirements and optimizing objectives (e.g. minimum cost and/or weight). This new design process differs from traditional methods in that the generative algorithm evaluates and changes the product model for the next analysis iteration without user intervention and results in far more solution variants for a given function. The traditional design process requires additional – user-driven – iterations until we get to the manufacturing process, which increases the product implementation time.

In the generative design process, the software uses nature-based evolutionary approaches using machine learning. The user only needs to define the design variables (e.g. materials, design space, weight, manufacturing technology, production cost). Knowing this, the software produces all possible combinations by knowing the variables and parameters. Compared to traditional design processes, the number of versions produced can be orders of magnitude larger. Since each of the generated solution variants meets the prescribed manufacturability conditions, the individual that represents the final solution can be selected from the set.

Another feature of generative design is that it can be applied at an early stage of the design process without an existing conceptual design being available. As a result, the generative algorithm creates completely new solutions by considering the manufacturability aspects, thus significantly reducing the time of the part testing process. In the traditional design process, shape or topology optimization targets an already manufactured version, which removes material that is unnecessarily operational, in a way that ignores manufacturability and manufacturing costs. As a result, further modelling, conventional simulation, and testing may be required. In generative design, simulation is integrated into the design process. In the generative design process, the characteristics of the manufacturing technology can be specified as a design

variable (e.g. additive manufacturing, 2.5–5D milling, and casting), so the software only produces solutions that meet the specified variables. Considering additive and hybrid elaboration, generative design can be used to combine multi-component products (function combination) into a product that was not previously possible due to traditional manufacturing technology, which can lead to further cost savings for later use, e.g. for the supply chain or for maintenance and installation.

4. EXAMPLES OF SOFTWARE SUPPORTING GENERATIVE DESIGN

Software supported generative design appeared in the first half of the 2010s. During these years, *AutoDesk* has developed optimized structures for *Airbus*, where *Jesse Coors-Blankenship* was the chief engineer in the development department. Using the experience gained here, he founded a company called *Frustum*, where he developed a kernel to support generative design called *TrueSOLID™*, a product that is available in several design software. The other big developer is *AutoDesk*, where a product to support generative design was created from a project called *Dreamcatcher* running in its research department, which is also available. Recognizing the need for generative design, products from newer software developers have become available. These are characterized by extensive optimization capabilities (e.g., size, weight, strength, material quality, cost, schedule, manufacturability) as well as cloud-based service. Computational performance in iterative processes of the generative design process is much more costly than traditional tasks, so cloud-based computing provides cost-effective access to many generated variants. *Table 1* summarizes and briefly presents the best-known products that support generative design.

Table 1
Generative design software [8]

<i>Developer</i>	<i>Product</i>	<i>Properties</i>
<i>Frustum</i>	<i>Generate</i>	A cloud-based application that combines a voxel-based design algorithm with finite element analysis. It was a stand-alone product until November 2018, after which it was acquired by <i>PTC</i> .
<i>nTopology</i>	<i>Element</i>	A generative, function-based application that provides instant feedback during design as it optimizes the shape of the object as well as the manufacturing process.
<i>ParaMatters</i>	<i>CogniCAD</i>	A cloud-based design platform that focuses primarily on additive manufacturing processes.

Procedures supporting topological optimization and generative design are also available in simulation software supporting engineering development (e.g. *FEM*, *CFD*) (*Table 2*).

Table 2
CAE software supporting generative design [8]

<i>Developer</i>	<i>Product</i>	<i>Properties</i>
<i>Altair</i>	<i>OptiStruct</i>	It allows to run in parallel to perform large-scale optimization tasks quickly.
<i>ANSYS</i>	<i>ANSYS Mechanical</i>	<i>ANSYS</i> topology optimization algorithm can be started from the desktop, so it can be integrated into the simulation workflow.
<i>Dassault Systèmes</i>	<i>Tosca Structure, Tosca Fluid</i>	The <i>Tosca</i> structure optimization package integrates with the <i>CAE</i> environment in cooperation with the <i>ABAQUS</i> , <i>ANSYS</i> and <i>MSC Nastran</i> finite element solvers.
<i>ESI Group</i>	<i>PAM-STAMP, ProCAST, SYSTUS</i>	Offers built-in generative design techniques as well as special shape optimization in the <i>SYSTUS</i> simulation package
<i>MSC Software</i>	<i>MSC Nastran Optimization</i>	It offers a variety of processes, from shape and topology optimization to process management solutions.

Modules supporting generative design are also available in parametric design systems (*Table 3*). These are basically the products of the developers described above, which are available in an integrated way in the systems.

Table 3
Integrated system including generative design module [8]

<i>Developer</i>	<i>Products</i>	<i>Properties</i>
<i>Autodesk</i>	<i>Fusion 360, Inventor</i>	Provides access to optimization settings and calculations, as well as cloud computing resources for premium subscriptions.
<i>Dassault Systèmes</i>	<i>TOSCA suite</i>	Provides access to the <i>TOSCA</i> optimization package for <i>CATIA</i> and <i>SOLIDWORKS CAD</i> software.
<i>Robert McNeel & Associates</i>	<i>Rhino</i>	Grasshopper relies on a visual programming language and environment to automate design. Users logically connect parts by pulling operations as planned.
<i>PTC</i>	<i>Creo Simulate</i>	<i>Vanderplaats</i> uses <i>R&D GENESIS</i> for optimization. It converts the results to free-form (<i>B-rep</i>) objects, thus avoiding polygon models used elsewhere. From <i>Creo 7.0</i> , it uses <i>Frustum</i> technology.
<i>Siemens</i>	<i>NX, Solid Edge</i>	Integrates the <i>Frustum Generate</i> kernel for generative design. Users can modify the generated results with convergent modelling.
<i>Altair</i>	<i>solidThinking Inspire</i>	Topological optimization is integrated into the <i>CAD</i> modelling process.

The advantage of modules available in integrated systems is that models generated by generative design can be used directly in the given system, so there is no need to exchange product data between different software, which can cause conversion errors.

5. CASE STUDY OF GENERATIVE DESIGN

On the 12th of June in 2013, *General Electric* published a call for tenders on the *grabcad* community interface, which required the optimization of an aircraft engine mount, assuming additive manufacturing technology [9]. Considering the requirements in the tender and using the generative design method based on the available model, we produce a couple of possible solutions with *AutoDesk Fusion 360* and *Solid Edge 2020* software, the results of which are described in this chapter.

The material of the component to be tested is *Ti-6Al-4V*, the assumed yield strength $Re = 131 \text{ ksi}$, the operating temperature $T_o = 75 \text{ F}$, the minimum wall thickness $t = 0.05 \text{ in}$ (the values given in the tender were used when specifying the units). The component analysis is examined for four load cases:

- (1) a load of 8000 lbs on the pin surface in the opposite direction to the y axis,
- (2) a load of 8500 lbs on the pin surface in a direction parallel to the z axis,
- (3) a load of 9500 lbs in the yz plane, enclosing an angle of 42° in case of the load F_1 ,
- (4) a torque of 5000 lb-in through a midpoint of the axis of symmetry of the pin surface and arousing about an axis parallel to the z axis (*Figure 1*).

In case of topological optimization, the objective function (minimum weight) was performed with a given safety factor ($n_s = 2$), the original weight of the part was $m = 2.038 \text{ kg}$.

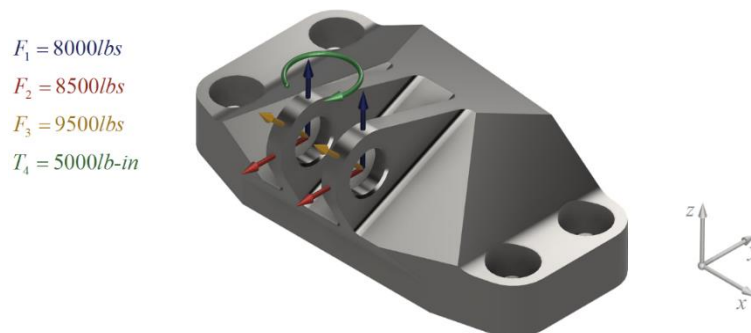


Figure 1
Load cases to be tested for the clamping element.

In addition to additive manufacturing technology, *Autodesk Fusion 360* software also supports the ability to set criteria for manufacturing products made with milling ($2.5D$ – $5D$) machining, 2-axis machining, and casting technology. This means additional solutions in the number of versions generated. In the case study, $5D$ milling

and additive manufacturing were considered for machining technologies, and the tabular results generated in the software are illustrated in *Figure 2*.

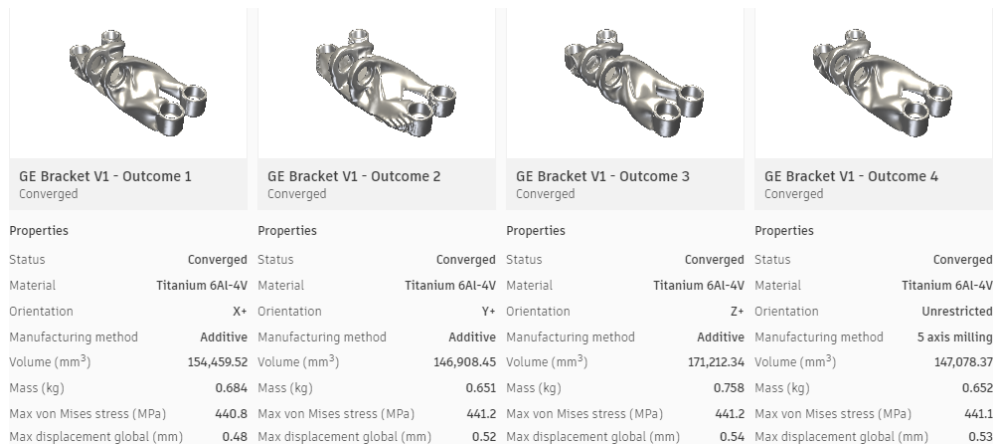


Figure 2
Results of generative design using AutoDesk Fusion 360 software

The generated solution variants can be compared to each other, users can analyse the selected results, which basically allows the load distribution on the part (*Figure 3*).

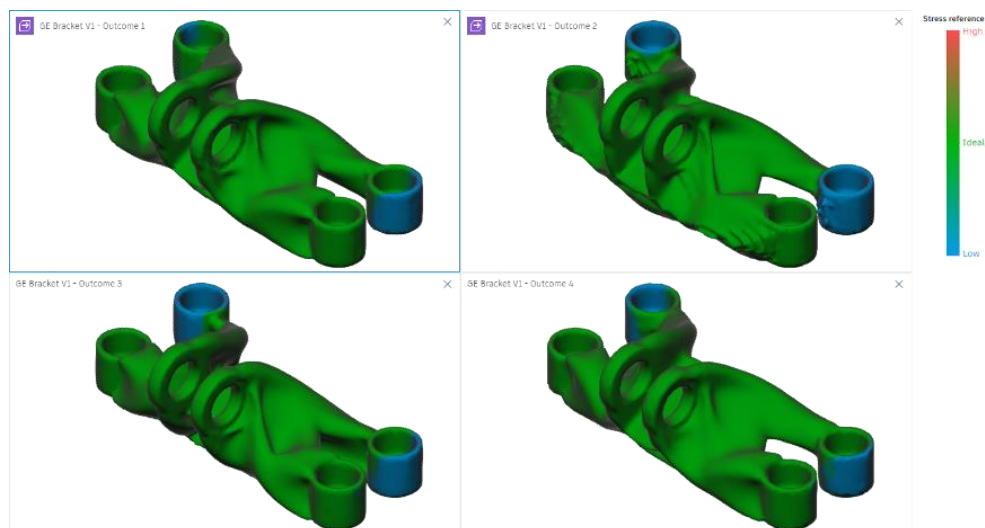
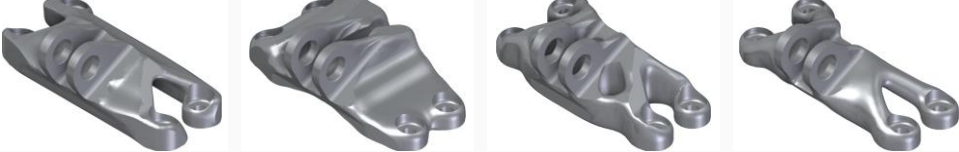


Figure 3
Results of load distribution of generated versions in AutoDesk Fusion 360 software

The load distributions observed in the figure above are in the ideal range, the magnitude of arising stresses in some of the fixing holes is low, in practice the display of

the load distribution in this case provides only useful information, numerical values can be determined by finite element analysis. The Premium version of *Solid Edge 2020* provides the ability to perform generative design processes, however, services are more limited, and operations require more user intervention, which results in more time. For manufacturing processes, additive as well as conventional (e.g. casting, turning) machining can be selected; however, it is not possible to specify more than one machining mode in one test.



Extraction	x	Extraction	y	Extraction	z	Extraction	No
Manufacturing	Additive	Manufacturing	Additive	Manufacturing	Additive	Manufacturing	Additive
Volume (mm ³)	241,533	Volume (mm ³)	304,937	Volume (mm ³)	198,612	Volume (mm ³)	126,785
Weight (kg)	1,088	Weight (kg)	1,374	Weight (kg)	0,894	Weight (kg)	0,571

Figure 4

Results of generative design using Solid Edge 2020 Premium software

If test of multiple manufacturing methods is required, the user must create additional generative tests (*Figure 4*). If the generated versions are available, it will also be possible to compare them. The results of the load distribution in case of the different variants are illustrated in *Figure 5*.

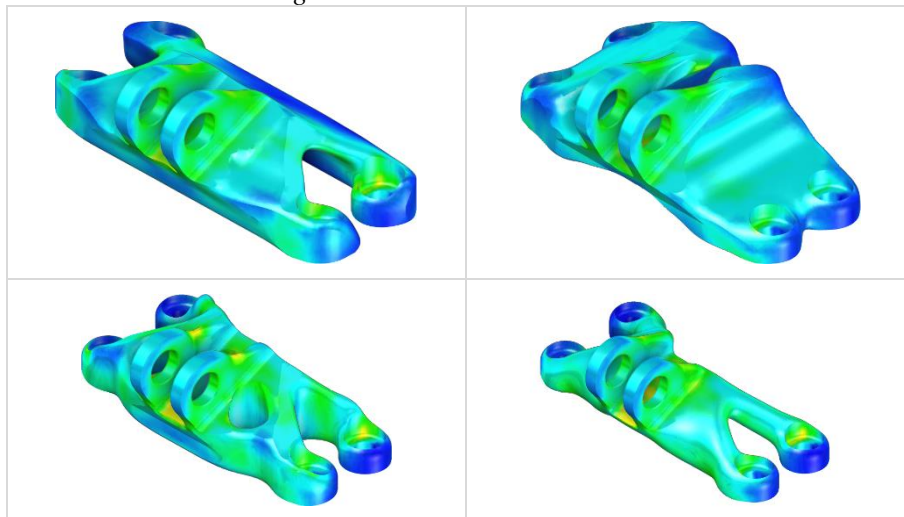


Figure 5

Results of load distribution of generated versions using Solid Edge 2020 Premium software

It is not possible to examine the numerical values of the load distribution, like *AutoDesk Fusion 360* software. The results obtained are only for information, which allows the identification of load-critical regions; however, the load distribution is not ideal, as previously illustrated in *Figure 5*. The disadvantage is that the software does not allow the tabular display of the results and the simultaneous visual comparison of the generated versions, and the user does not even have information on the numerical values of the characteristic geometric data (e.g. volume), maximum of *von Mises* stress and global displacement is not available for the user. Comparing the results of the two softwares, it is seen that we get different solutions even with similar configuration parameters.

6. SUMMARY

In this paper, we have briefly reviewed the various software applications that support the generative design process. The solutions of two large companies (*AutoDesk, Frustum*) developing a generative module, which is widespread in mechanical design systems, were examined through a case study. Comparing the two generative design modules, the cloud-based technology used in *AutoDesk Fusion 360* software shortens the time of the generative design process and the number of generable solutions can be significantly increased by adjustable machining parameters within a given test (one test – many solutions). The main feature of the *Frustum Generate* generative module integrated into *Solid Edge 2020 Premium* software is that it can be run on a given machine, so the computing capacity required for the generated models is limited by the user's computer. Another characteristic disadvantage is that only one manufacturing mode can be specified at a time in the tests, which reduces the number of solutions that can be generated within a test. If you want to create multiple solution variants, you need to run multiple studies (many solutions – many studies), which increases the time of the design process.

ACKNOWLEDGEMENT

The described article/presentation/study was carried out as part of the EFOP–3.6.1–16–00011 *Younger and Renewing University – Innovative Knowledge City – institutional development of the University of Miskolc aiming at intelligent specialisation* project implemented in the framework of the Szechenyi 2020 program. The realization of this project is supported by the European Union, co-financed by the European Social Fund.

REFERENCES

- [1] Gibson, I., Rosen, D., Stucker, B. (2010). *Additive manufacturing technologies*. New York, Springer, ISBN 978-1-4419-1119-3, <https://doi.org/10.1007/978-1-4419-1120-9>.

-
- [2] Zuo, K., Chen, L., Zhang, Y., Yang, J. (2007). Study of key algorithms in topology optimization. *Int. J. Adv. Manuf. Technol.*, 32, pp. 787–796, <https://doi.org/10.1007/s00170-005-0387-0>.
- [3] Rozvany, G. (2001). Aims, scope, methods, history and unified terminology of computer-aided topology optimization in structural mechanics. *Struct. Multidisc. Optim.*, 21, pp. 90–108., <https://doi.org/10.1007/s001580050174>.
- [4] Bendsøe, M. (1995). *Optimization of Structural Topology, Shape, And Material*. Berlin, Springer, ISBN 978-3-662-03117-9, <https://doi.org/10.1007/978-3-662-03115-5>.
- [5] Novotny, A., Sokolowski, J. (2013). *Topological Derivative in Shape Optimization*. Berlin, Springer, ISBN 978-3-642-35244-7, <https://doi.org/10.1007/978-3-642-35245-4>.
- [6] Huang, X., Xie, Y. (2010). *Evolutionary Topology Optimization of Continuum Structures*. Wiley, Chichester, ISBN 978-0-470-74653-0.
- [7] Tajs-Zielińska, K., Bochenek, B. (2018). A heuristic approach to optimization of structural topology including self-weight. *AIP Conference Proceedings 1922*, 020001, <https://doi.org/10.1063/1.5019028>.
- [8] *An Introduction to Generative Design – A Digital Guide from the Editors of Cadalyst*. Cadalyst, Longitude Media, (2018) https://cadalyst.tradepub.com/free/w_cada04/prgm.cgi.
- [9] <https://grabcad.com/challenges/ge-jet-engine-bracket-challenge>

THE METHODS OF NUMERICAL MECHANICS FOR THE IMPROVEMENT OF MACHINE-TOOLS

ATTILA SZILÁGYI – DÁNIEL KISS

University of Miskolc, Department of Machine Tools
3515 Miskolc-Egyetemváros
szilagyi.attila@uni-miskolc.hu, daniel.kiss@uni-miskolc.hu

Abstract: This paper gives a brief summary on the mechanical and thermal applicability of the finite element method (FEM) from the field of designing procedure of machine tools. The solutions of certain problems, as examples, are also demonstrated. First the summary of such phenomena is performed, where the application of numerical methods is inevitable. Through the brief summary of the general problem of elasticity, the justification of the numerical methods is demonstrated. Finally, examples are set to demonstrate the applicability of the numerical methods and the achieved results, which demonstrate the efficiency of the FEM applied for the development of machine tools. Among several numerical methods the FEM is focused on in this paper.

Keywords: *Machine-tools, numerical, mechanical, thermal, FEM*

1. INTRODUCTION

During the operation of any type of manufacturing device or machine-tools, several incidents should be taken into consideration from the fields of kinematics, dynamics, structural or thermal analysis which may influence the accuracy of the manufacturing process considerably. The influence of these factors already in the preliminary design-phase of the device, or during the operation of an existing machine needs to be considered. The preliminary judgement of such incidents can be conducted only in theoretical ways, by the means of the numerical methods of mechanics. The theoretical conclusions can be validated and completed by an experimental investigation of a similar device.

The mathematical description of such phenomena generally requires of setting up very complicated nonlinear ordinary or partial differential equations or equation-system. Due to the complicated boundary conditions coming from the geometry, the establishment of the exact, closed-form solutions of such governing equations may be blocked by impassable barriers and excludes the application of pure and exact analytical procedures. In order to overcome these theoretical difficulties, the application and the improvement of numerical methods have needed to be implemented. Due to capability of providing an excellent approximation, the finite element method (FEM) is assumed to be the most frequently applied numerical method.

Our paper, through the analysis of some simple cases, demonstrates the applicability and diversity of the FEM on the field of the design procedure of manufacturing devices and machine-tools. First of all, the need for the modelling procedure is mentioned in the followings, then the phenomena which require being modelled on the field of the machine-tools is summarized in the following chapter.

2. PHENOMENA ONE MAY ENCOUNTER WITH DURING THE OPERATION OF MACHINE-TOOLS

The phenomena may arise during the operation of a machine tool or a manufacturing device, and which may interact with each other yielding a significant negative influence on the accuracy of the manufacturing process, can be sorted into three fundamental groups of Physics: kinematics, mechanics and thermodynamics.

Among the phenomena from the field of kinematics, the errors from the geometrical uncertainties, the deviations from the ideal geometrical entities can be mentioned, such as the straightness error, the perpendicularity deviation, spherical deviation, or the eccentricity etc. Since the detection of such defects can be performed only at an existing device, hence the preliminary judgement of these properties can be done only during the design process of the device by the tolerance-calculations. We note, that the modern engineering iCAD softwares enable to conduct such calculations which, however, are not considered to belong to the group of the “classic” simulations, hence the phenomena from the field of kinematics are not focused on in this paper. The inertial forces and loads due to a motion analysis can also be considered as phenomena from the field of kinematics, however these problems would rather be investigated in connection with some dynamical points of view as a link to the structural or fracture mechanics of different structures.

Among the mechanical phenomena those ones can be mentioned which are in connection with the loadings induced by the operation of a machine, such as the contact stresses and stress concentration. Another group of phenomena from the field of mechanics are related with the deformation of the structure, such as the deformation of the rolling elements, guidelines and guideways, or the main spindle, and which may yield the plastic deformation of certain concentrated zones of the device. The fluid-dynamical (coolants and lubricants) and tribological (slideways, the stick-slip, aerostatic guides), as well as the problems of the lubrication-theory (hydrostatic and hydrodynamic guideways) can also be mentioned among the mechanical phenomena. The phenomena from the field of dynamics [6–7] can also be included by a large set within the mechanical ones, such as the inertial forces and moments which may induce the different types of vibrations (free, forced, self-excited and parametrically forced vibrations) that – in extreme cases – may contribute to the appearance of the phenomena from the field of fatigue and fracture mechanics. Among the vibrations, the strongly nonlinear transversal vibrations of the belts [3], the linear torsional vibrations of the main and sub spindles [2], and the strongly stochastic vibrations coming from the manufacturing process can be mentioned. The wide variety of the contact stress phenomena is worth mentioning separately, since the load-flow

spreading all along the machine-structure is composed of the contact stresses induced by the connecting machine elements, hence, the consideration of these forces, while the Saint-Venant-principle is also taken into account, is vital for creating a well approximating mechanical model for the numerical simulations. As still regarding the contact loadings, all the above-mentioned phenomena are induced or at least influenced by their contact forces.

Among the phenomena from the field of Thermodynamics, the influences from the heat sources of the machine can be mentioned, as well as the different types of the heatpropagation can also be focused on, let alone the temperature field and the heatdeformations and stresses yielded by the heatpropagation. The different types of the heat-transport processes belong also into this group, which may rise during the analysis of the coolants and lubricants. As regards the investigation of the thermodynamical phenomena, depending on being transient or stationary, may require a lot more complicated model and computational capacity, than that of the pure mechanical ones [4].

Some other types of phenomena can also be mentioned. These types cannot be classified as above, but may induce mechanical or thermodynamical phenomena during the operation of a machine. The electromagnetic phenomena coming from a linear-motor system can be sorted into this group. Beyond the electromagnetic influences, the so-called parasite-force, which is a concomitant phenomenon of a plane linear motor drive can be mentioned, that may influence the operation of a sliding guide by directing the guideways to extremely high friction forces. The nonlinear electrical phenomena of a control-system of a CNC-drive system can also be mentioned, that may take a drawing-back effect on the accuracy of the positioning. A specific optical phenomenon may rise during the operation of a special, ultraprecise manufacturing device operated by LASER. In this case the LASER beam with relatively long coherence length is applied for hologram printing. Since the LASER beams are flying in outer space this time, then the index of refraction of the air is vital to be stationary and constant, which can be achieved a properly designed cooling system.

It is well known, that the phenomena mentioned above might show up as the interaction of single ones, in other words the phenomena can be coupled by influencing each others' effects, which, in extreme cases, may yield the amplification of the single ones. As an example, a less stiff rotating shaft can be mentioned, which rotates an unbalanced heavy mass yielding large deformations and displacements that may induce the nonlinear unstable, parametrically excited vibration of the shaft. Another instance for the interaction of single phenomena may come from the fields of thermodynamics and the structural analysis, where the interaction of the mechanical and thermal deformations may have a negative influence on the accuracy of the manufacturing process. As a remark, we note, that the phenomena mentioned above – except the optical one – may show up at the same time within a modern motorspindle system, hence the theoretical analysis of such a device – mainly during the design phase – may have a serious challenge for the design engineers.

The experimental investigation of the phenomena mentioned above is detailed by the reference [1].

3. THE NEED FOR THE NUMERICAL COMPUTATIONS

Due to the complicated kinematical and dynamical boundary conditions, the analytical investigation of the above-mentioned phenomena, even if the physical law is assumed to be linear, may be blocked by impassable barriers. As an example, see figure below which depicts the fundamental problem of the strength analysis based on the theory of elasticity (*Figure 1*).

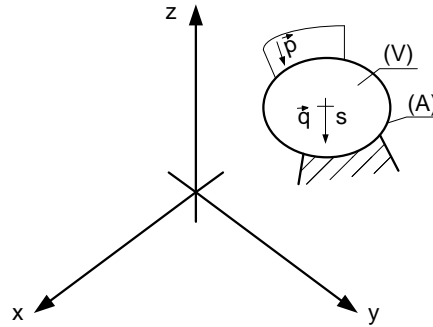


Figure 1
The fundamental problem of the strength analysis

The solution procedure of such problem is focusing on the establishment of the stress, deformation and the displacement fields of the elastic body subjected to a certain loading. The analytical investigation of this problem can be set up as follows [5].

Let $\vec{u}(\vec{r}) = u\vec{e}_x + v\vec{e}_y + w\vec{e}_z$ be denoted to the unknown displacement field, while the $\underline{\underline{A}} = \underline{\underline{A}}(\vec{r})$, and $\underline{\underline{T}} = \underline{\underline{T}}(\vec{r})$ tensor-quantities stand for the unknown deformation and stress fields as the functions of the x, y, z coordinates. As regards the symmetry of the tensors, $3+6+6=15$ pieces of field-quantities need to be established by the following equations. First of all, the

$$\underline{\underline{A}} = \frac{1}{2}(u \circ \nabla + \nabla \circ u) \quad (1)$$

geometrical equation, then the

$$\underline{\underline{T}} \cdot \nabla + \vec{q} = \vec{0} \quad (2)$$

equilibrium equation and, finally the

$$\underline{\underline{T}} = \underline{\underline{D}} \cdot \underline{\underline{A}} \quad (3)$$

law-of-material equation can be set up. The simplest case for (3) is the Hook'-law. Besides the *Equations (1)–(3)*, the $\vec{u} = \vec{u}_0$ ($\vec{r} \in A_u$) kinematical and the $\underline{T} \cdot \vec{n} = \vec{p}$ ($\vec{r} \in A_p$) dynamical boundary conditions are also available, where $A_u \cup A_p = A$.

At complicated geometrical entities and shapes, such as the welded or cast machine beds, stepped main spindles, subspindle-drives with rolling element bearings etc., the pure analytical investigations, even if they are based on linear partial differential equation-system, cannot be conducted by yielding exact, closed-form solutions. Still there is a strong demand from the side of the engineers for solving these rather complicated problems, even with the application of certain approximation methods, the special numerical methods of mechanics, by which an approximating solution of arbitrary accuracy can be obtained and the (1)–(3) problem can be investigated at arbitrary boundary conditions. There are several numbers of such softwares are available for the mechanical engineers. Generally, these softwares are the integrated parts of a wider engineering software package, such as the CAD-packages. The most frequently applied numerical mechanical method on the field of the mechanical engineering is the finite element method (FEM). The typical features and the applicability of an FEM-software through the analysis of some examples from the field of machine-tools are detailed in the following chapters.

4. THE NEED FOR THE NUMERICAL COMPUTATIONS

Unlike some other numerical procedures, such as the method of differences, the collocation method, the FEM will not yield the direct numerical solution of the original partial differential equation-system, but, bypassing this step, yields such solutions which are based on some variational principles. The detailed theoretical backgrounds can be found in [5]. The FEM, in any case, assumes an appropriately created geometrical model, which, due to the modern integrated engineering softwares, generally is called the digital prototype of the machine (*Figure 2*).



Figure 2

The digital prototype of the machine structure used for the FEM

The figure depicts a dome-shape machine structure of grey cast-iron. This structure is the central part of a large milling-drilling machining centre, which is being developed within the frames of a tender called the GINOP-2.2.1-15-2017-00093 project titled *The Development of Ultraprecise and Freedom Type Machining Centers*. Since this central part contributes to the novelty of the machine, several mechanical and thermal properties of this part needed to be investigated, then, in accordance with the preliminary concepts, the design and the geometrical shape of the structure had to be finalized. During the design and improving process, several number of structural and dynamical properties, which sometimes are interacting with each other, had to be investigated, and had to be taken into consideration in order to achieve an optimized geometrical structure.

Since an ultraprecise drilling-milling machining centre is investigated, the static stiffness of the central part of the entire machine is assumed to be the most important feature, which is the response to the static loading. The static stiffness of the machine structure is vital during a milling manufacturing process, since the mean value of the time-varying feeding-force component, which is superimposed by the periodic time-varying component, is not zero, hence the accuracy of the manufacturing process might strongly be influenced by the unsatisfactory stiffness. Similarly, also the dynamic stiffness of the construction is of utmost significance, since it is the interpretation of the response of the system to a time-varying – generally to a harmonic – forcing term, and can be expressed as the displacement amplitude considered along a particular direction. In extreme cases it might refer even to the resonance. It is always a 3D-environment modal analysis with a linear material law is conducted prior to the simulation of the dynamic stiffness of a structure, since it enables us to establish the arbitrary number of natural frequencies and the concomitant mode-shapes of the investigated structure in order to compute the necessary response features. The main objective of our investigation in this case was to design and create an optimized geometrical shape having as high first natural frequency as possible, since, this way, the higher order natural frequencies would be increased and shifted from the manufacturing frequency range yielding a reduced possibility for the resonance during manufacturing. The figure below depicts the mode shape belong to the first natural (*Figure 3*).

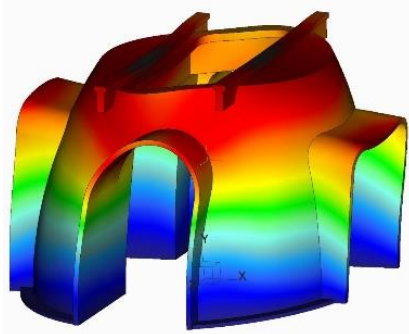


Figure 3
The 1st mode shape of the structure

Several other dynamical simulations with different damping coefficients have been conducted by the 3D model seen on *Figure 3*, such as the modal analysis mentioned above, then the subsequent analysis for establishing the quantities of the dynamical stiffness, then the one for establishing the response functions to the harmonic and impact forcing terms and, finally, the one for setting up the optimized geometry. As regards the static structural investigations, the quantities of the static stiffness have been computed, as well as the contact stresses, while prestressed loading also was assumed. Among others the surfaces of guides subjected to pressure have also been checked as well as several numbers of global sensitivity analysis were also conducted in order to create the final optimized geometrical shape of the structure. It is clearly seen, that due to the extremely complicated kinematical boundary conditions, these investigations cannot be conducted without applying the means of the numerical computational methods. The chart below depicts the state of resonance by displaying the time-history of the displacement response function at a special point of the construction (*Figure 4*). The influence of the damping of different raw materials were investigated by such charts.

Besides the dynamical simulations, several other structural (static) computations have also been conducted. As it has been mentioned above, the part seen on *Figure 2*, is the central structure of the entire machine and presents several novelties. Consequently, the investigation of all the quantities referring to the static stiffness has been performed, since the estimated total weight of the structure is roughly 60 tons, and at installation all these properties have to be taken into account. The figure below displays the entire structure (*Figure 4*).

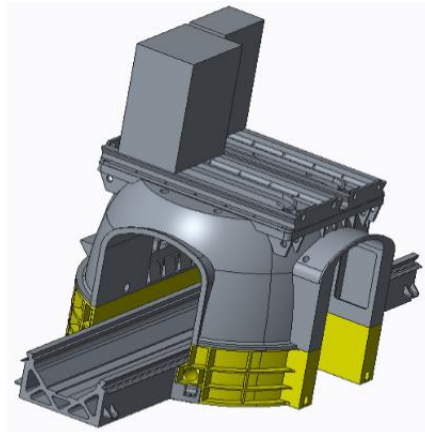


Figure 4

The assembly model of the entire structure of the machine

The wedge-like parts on the top of the central part of the structure symbolize the units for roughing and finishing machining operations and which are still in design phase, but their influence on the static stiffness cannot be ignored. One of our simu-

lations targeted the behaviour of the structure during the different stages of the installation and assembling process, when at a certain stage the entire structure is supported only by the pins on bottom of the structure, and when the filling material layer between the floor and the structure is not yet prepared. Among these simulations, one referred to the investigation of the deformation field of the structure, when the model is subjected to the gravitational force. The completed mechanical model, including the material properties, the kinematical and dynamical boundary conditions, and the FEM-meshing, is depicted by *Figure 5*.

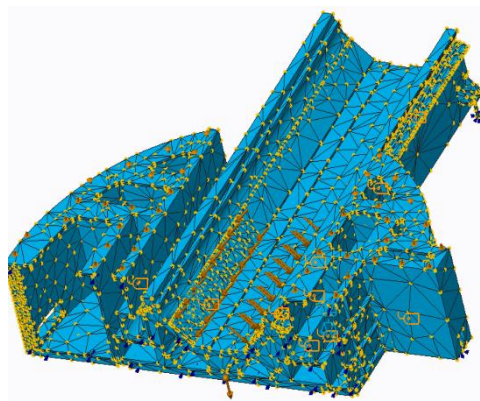


Figure 5

The structural model using the symmetrical features

It is clearly seen, that only one half of the entire structure is included by the investigations. This enabled by the symmetry of the geometry and the boundary conditions, hence the number of the finite elements, thus the computational time and capacity is reduced significantly, while the accuracy of the computations can be increased. The refinement of the model above is achieved by adding the influence of the prestressed bolt-connections between the parts of the construction and, after the computations, the following displacement field is yielded (*Figure 6*).

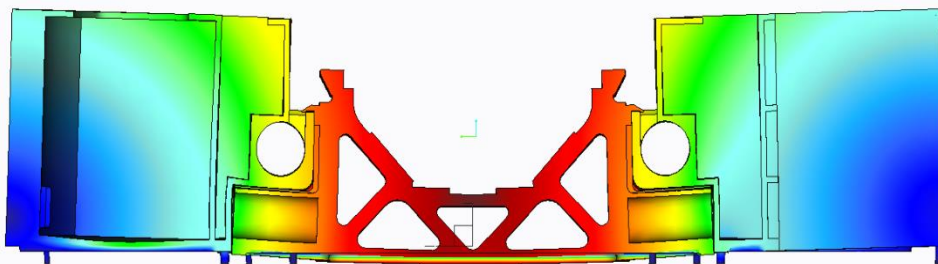


Figure 6

The displacement field at a cross-section in deformed state

The simulation mentioned above has given an evidence and supported the preconceptions of the design engineer i.e., some additional supporting pins are necessary to be placed on the bottom surface of the X-bed in order to compensate the mechanical stresses due to the large deflection of the construction hence, the risk of the fracture failure during the installation is reduced significantly.

As regards the static stiffness of the ram of the unit for the roughing machining operations, the need for similar structural simulations mentioned above have risen. The stroke of the ram is 800 mm hence, due to the loadings from the manufacturing process, it is subjected to bending loading which depends on the actual extension of the ram. The coloured chart below depicts the deformed displacement field at a certain extension of the ram (*Figure 7*). The ram includes and grabs the manufacturing tool and is displayed in red on the chart below.

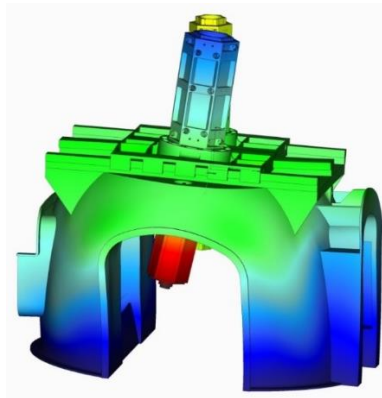


Figure 7

The deflection of the ram at rough milling

Each simulation conducted for investigating the bending loading of the ram at each extension, is included by one global sensitivity analysis, by which a chart is yielded displaying the deflection of the end of the ram (i.e., the assumed tool center point referred as TCP in the followings) versus the actual extension of the ram (*Figure 8*).

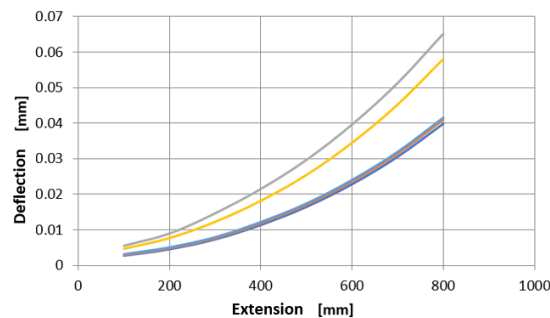


Figure 8

Deflection of the TCP vs. the extension of the ram

The curves of the chart above refer to such varieties of the ram, which have different cross-sections and guides i.e., rams with hexagonal or octagonal cross-sections and with rolling or sliding guides placed at various places and numbers have been investigated. The figure below depicts a housed ram with guides placed along the stroke and the number of the guiding elements at each cross-section (*Figure 9*).

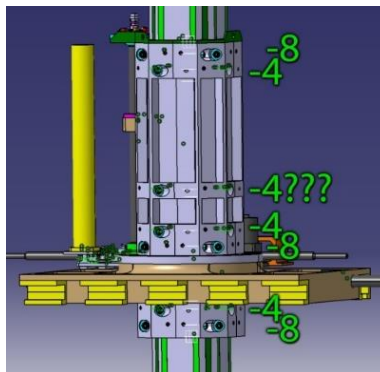


Figure 9

The housed ram with indicating the guided cross-sections

For the sake of the simplicity and an instant preliminary comparison, the applied loadings are assumed to be static during the investigations. For further detailed simulations, dynamic loading cases were also applied for judging the dynamic stiffness properties.

Another investigation has been conducted on the structural properties of the X-bed and the X-lathe operating along the X-axis (*Figure 10 – left*). The result of the computations referring to the displacement field is displayed in *Figure 10 – on the right*. This latter simulation was to uncover the structural features (displacement and stress fields) of the X-lathe, which is subjected to the loadings from the roughing manufacturing operations and the gravitational force. These computations served as a basis for the optimization simulation of the static stiffness of the X-lathe.

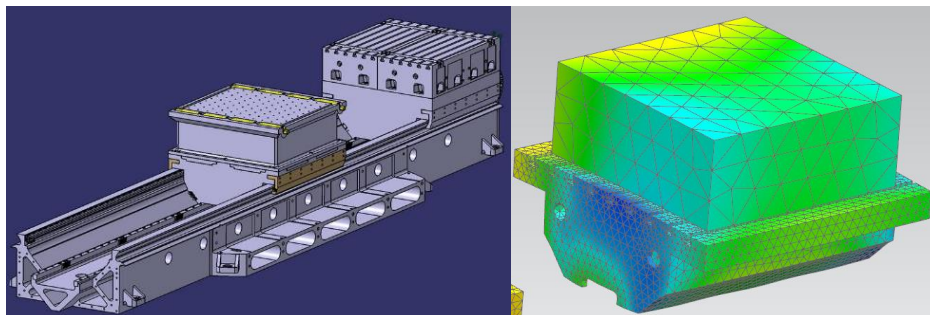


Figure 10

The 3D geometrical model – on the left, the structural analysis – on the right

As a result of these numerical calculations, the geometrical shape of the structure was finalized, which enabled the manufacturing of the cast (*Figure 11*).



Figure 11

The cast of the structure with optimized geometry

5. SUMMARY

This paper summarizes the most important phenomena from the field of mechanical engineering, which rises frequently during the operation of a manufacturing device or a machine-tool. We pointed out that the overwhelming majority of these phenomena cannot be investigated by the means of the theoretical analysis properly, the establishment of the exact and closed-form solutions can be conducted only in minor cases. In these case the numerical methods of the mechanics or thermodynamics are preferred to the analytical ones. Among the numerical methods, the finite element method (FEM) is assumed to be the most frequently applied on the field of engineering. The efficiency of the FEM was demonstrated through the analysis of certain examples and we can claim that the method is a very comfortable procedure for enabling the investigation of the phenomena related with the operation of machine tools. This is particularly true for so called comparing studies, by which the directions of the design and development can be set up and the dead-end constructions can be avoided. The quality of the meshing however requires special attention, particularly when the problems related with contact analysis, where the accuracy and the optimal computational time is vital

ACKNOWLEDGEMENT

The described article/presentation/study was carried out as part of the EFOP-3.6.1-16-2016-00011 *Younger and Renewing University – Innovative Knowledge City – institutional development of the University of Miskolc aiming at intelligent specialisation* project implemented in the framework of the Szechenyi 2020 program. The realization of this project is supported by the European Union, co-financed by the European Social Fund.

REFERENCES

- [1] Baráti A. (1988). *Szerszám gép vizsgálatok*. Budapest, Műszaki Könyvkiadó.
- [2] Faragó K. (1985). *Színhajtású szerszám gép főorsók nemlineáris rezgései*. Candidate dissertation, Miskolc.
- [3] Kollányi T. (2003). *Szjágak transzverzális lengései*. PhD dissertation, Miskolc.
- [4] Mekid, S. (2009). *Introduction to precision machine design and error assessment*. Boca Raton–London–New York, CRC Press Taylor&Francis Group.
- [5] Páczelt I. (1999). *Végeselem módszer a mérnöki gyakorlatban*. I. kötet, Miskolci Egyetemi Kiadó pp. 36–37.
- [6] Patkó Gy. (1998). *Dinamikai eredmények és alkalmazások a géptervezésben*. Habilitation booklet, Miskolc.
- [7] Patkó Gy. (1984). *Közelítő módszer nemlineáris rezgések vizsgálatára*. Candidate dissertation, Miskolc.

COMPARISON BETWEEN A CONVENTIONAL AND AN ANTIVIBRATING BORING BAR IN THE INTERNAL TURNING OF LONG OVERHANGS

THOMAS WALLYSON – ZSOMBOR FÜLÖP – ATTILA SZILÁGYI

University of Miskolc, Department of Machine Tools and Informatics
3515 Miskolc-Egyetemváros
szmwally@uni-miskolc.hu

Abstract: The main objective of this work is to evaluate the use of an antivibrating in an internal turning tool in the machining of hardened steel, comparing it with a conventional solid bar, in order to verify if it is able to cut deep holes without damaging workpiece surface quality and tool life.

Keywords: *impact damper, hardened steel, surface quality, tool life*

1. REVIEW OF LITERATURE

Internal turning of deep holes is a critical operation due to the fact that it demands the use of tools with long overhangs (distance between the tool tip and the tool fixation in the machine turret), what usually leads to tool vibration and, consequently, to high values of workpiece surface roughness [1].

Some passive dampers are:

- Damper Vibration Absorber (DVA) – consists of an additional mass-spring system connected to the bar, which needs to be set up in order to be tuned with the natural frequency of the structure [4]. According to the literature, this kind of damper works efficiently up to a tool bar L/D ratio of 15 [1].
- Tool bar with viscous elastic material – they are easy to apply in any kind of structure [3]. An example of this tool bar is the one called Silent Tool by the manufacturer. It consists of an interchangeable head and a body made of a heavy metal, supported by elements of rubber and oil [4].
- Friction Damper – it consists of several disks placed inside a cavity of the tool bar. Each disk rubs to other disk and also to the cavity wall in such way to dissipate vibration energy [5].
- Impact damper – the most usual of these dampers is the “particle impact damper”, which consists of hundreds of small particles (metallic, ceramic of little sizes) placed inside either the tool bar cavity or the workpiece wall using a reservoir stuck to it. These particles impact against the tool bar cavity while it vibrates and dissipate vibration energy [6]. A scheme of this kind of damper for internal turning tool bar is shown in *Figure 1* [7]. The behaviour of this

kind of damper is non-linear, what implies in some difficulties to control damping parameters like static stiffness (the bar loses some rigidity due to the cavity made in it), the restitution coefficient between the bar and the particles and the gap between the particles and the cavity wall [8]. On the other hand, it can provide high levels of damping along a large range of frequencies [9].

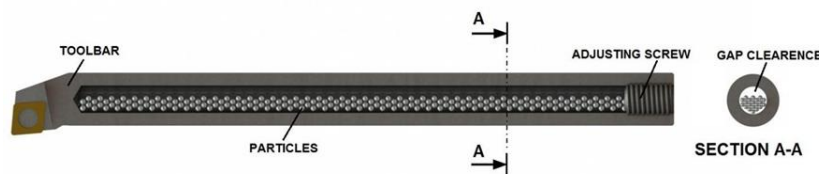


Figure 1

Scheme of a particle impact damping used in an internal turning tool [3]

2. MATERIALS AND METHODS

All the internal turning experiments of this work were performed using a CNC lathe with 20 CV of power in the main motor and maximum spindle rotation of 4.500 rpm. Two types of internal turning tool holders (also called tool bars) were used in this work. The first was the one cited in the previous paragraph, which we call “solid bar”. The second kind of bar was also the same kind of holder, but with its axial hole filled with spheres, which we called “impact damped (ID) bar”. Three different diameters of spheres were used inside the ID bar – 5, 6.5 and 8 mm. Tool vibration was measured using a piezoelectric accelerometer stuck close to the tool tip placed in such a way to measure vibration in the radial direction related to the workpiece.

3. RESULTS

The first part of the experiments had the purpose of evaluating the influence of the type of tool bar (solid and impact damped bar) in the maximum tool overhang possible. This evaluation was performed through the measurement of workpiece surface roughness and tool vibration in the internal turning of hardened steel.

Figure 2 shows the values of surface roughness for different tool overhangs and type of bars. The first thing to be pointed out in this figure is that for all type of bars, surface roughness remained almost constant as tool overhang increased up to an overhang value where a sudden increase of roughness occurred. The values of roughness above this point are too high to be used for turning of hardened steel (operation which intends to replace grinding). This sudden increase of roughness occurred with just few millimetres of increase (1 or 2 mm) in the tool overhang. This result indicates that the tool bar is very sensitive to small variations of rigidity when the tool overhang is in a value close to the limit. Therefore, this tool overhang value was considered the limit value for stable cutting and will be used to compare the performance of the different bars.

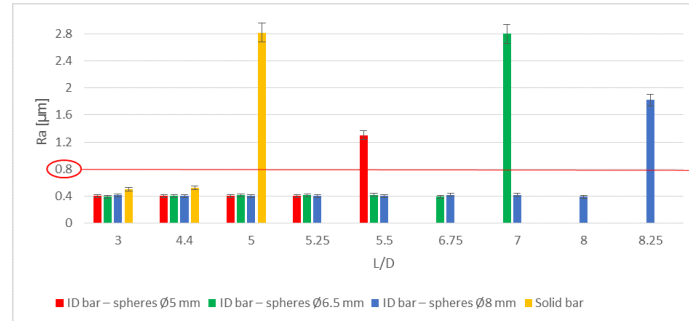


Figure 2
Roughness (R_a) obtained with all types of bars tested

To better understand the tool vibration effect on surface roughness, *Figure 3* was built. It shows the RMS of the tool acceleration signal (signal obtained by the accelerometer stuck on the tool) against the length to diameter (L/D) ratio for all types of bars used in the experiments. The main points to be highlighted based on the results shown in this figure are:

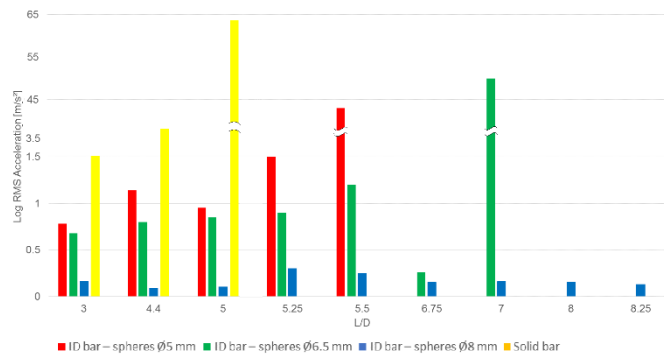


Figure 3
Tool vibration (RMS of the acceleration signals) for all types of bar tested

- Tool vibration remained almost constant with the increase of the tool overhang up to the point it suddenly increased in a certain value of tool overhang (called limit value for stable cutting). Small changes in the tool overhang close to the limit region generated this sudden variation, indicating that the tool bar is very sensitive to the rigidity change in this range of overhang;
- The use of internal turning tool bars with impact damper caused an increase of the limit value for stable cutting and, consequently, made possible the turning of deep holes;
- As the diameter of the spheres increased, the limit value for stable cutting also increased, indicating that the damping effect is higher when the mass of the spheres is higher and the gap between the spheres and the cavity wall is lower,

which cause, the increase of the impact momentum transfer. It is important to remember that the increase of the sphere diameter from 5 to 8 mm (respectively the smallest and the highest diameter used in this work) caused an increase of more than four times in the sphere mass.

4. CONCLUSION

Based on the results obtained in this work, it can be concluded for internal turning operations of hardened steels, in conditions similar to those used here, that:

- As tool overhang increases, the workpiece surface roughness and tool vibration keep almost constant up to the point where they increase suddenly (limit of stability). This point occurs, for impact damped tool bar with a tool overhang much longer than for solid bar;
- Tool vibration obtained with the impact damped bar is much smaller than the vibration obtained with solid bar even when the cut is stable. Even with this difference, surface roughness obtained with both kind of bars are similar, proving that, up to a certain level of tool vibration, it does not influence surface roughness;
- The use of the tool impact damper with spheres like the one tested in this work makes feasible the machining of longer holes than when a solid bar is used, without damaging surface roughness and tool life, due to its damping capacity;
- For the range of damper sphere diameter tested here, as this diameter increases, the performance of the tool damper improves and, consequently, even longer holes can be machined.

ACKNOWLEDGEMENT

The described article/presentation/study was carried out as part of the EFOP-3.6.1-16-2016-00011 *Younger and Renewing University – Innovative Knowledge City – institutional development of the University of Miskolc aiming at intelligent specialisation* project implemented in the framework of the Szechenyi 2020 program. The realization of this project is supported by the European Union, co-financed by the European Social Fund.

References

- [1] Suyama, D. I., Diniz, A. E., Pederiva, R. (2016). The use of carbide and particle-damped bars to increase tool overhang in the internal turning of hardened steel. *Intern. J. of Advan. Manuf. Tech.*, (86), pp. 2083–2092., doi: 10.1007/s00170-015-8328-z.
- [2] Schneider, G.: Cutting tool applications chapter 10: boring operations and machines. *American Machinist. Modern Machine Shop*, <http://www.opensource-machinetools.org/archive-manuals/Cutting-Tool-Applications.pdf>; (accessed: 12. 02. 2020).

-
- [3] Smith, G. T. (2008). *Cutting Tool Technology: Industrial handbook*. Southampton, Springer-Verlag.
 - [4] Dimarogonas, A. (1996). *Vibration for Engineers*. 2nd ed., New Jersey, Prentice Hall.
 - [5] Liu, X., Liu, Q., Wu, S., Liu, L., Gao, H. (2017). Research on the performance of damping boring bar with a variable stiffness dynamic vibration absorber. *Inter. J. of Adv. Manuf. Tech.*, (89), pp. 2893–2906.
 - [6] Bavastri C. A. (1997). *Redução de Vibrações de Banda Larga em Estruturas Complexas por Neutralizadores Viscoelásticos (Wide band vibration reduction in complex structures by viscoelastic neutralizers)*. PhD thesis, UFSC, Florianópolis Santa Catarina, Brazil.
 - [7] Sandvik. Silent tool for turning: overcome vibrations in internal turning, http://www.sandvik.coromant.com/en-us/products/silent_tools_turning (accessed: 15. 02. 2020).
 - [8] Hahn, R. S. (1951). Design of Lanchester damper for elimination of metal-cutting chatter, *Trans ASME*, 73, 3, pp. 331–335.
 - [9] Biju, C. V., Shunmugam, M. S. (2014). Investigation into effect of particle impact damping (PID) on surface topography in boring operation. *Int. J. of Adv. Manuf. Tech.*, (75), pp. 1219–1231.

EVALUATING CBN TOOL LIFE IN HARDENED BORING OPERATIONS IN LONG OVERHANGS

THOMAS WALLYSON – ZSOMBOR FÜLÖP – ATTILA SZILÁGYI

University of Miskolc, Department of Machine Tools and Informatics
3515 Miskolc-Egyetemváros
szmwally@uni-miskolc.hu

Abstract: This work aims to monitor the tool wear process using optical microscopy, so that the lifespan of the tool could be verified. The tool overhang was varied until it reached a limit (the deepest hole it could machine). The results show that, when the tool overhang is within its stability range, the flank wear of the tool is accentuated when the tool overhang outreaches its stability limit.

Keywords: *tool wear, lifespan, tool overhang*

1. REVIEW OF LITERATURE

Under ideal conditions, the surface roughness profile is formed by the replication of the tool tip profile at regular intervals of feed per revolution. However, many other factors like the dynamics of the metal cutting operation, elastic recovery of the cut region of the work material, ploughing, spindle rotational error and tool vibration, leading to the relative displacement of the tool and work material contribute to the modification of surface profile. In hard turning, theoretically tool vibration is likely to play a significant role in surface generation. Also, tool vibration is significantly influenced by tool wear [1].

It is convenient to calculate the material removal of the machining process, its important parameter that determinates the productivity of the process and quite fundamental for the calculation of the machine power. Therefore, the method of obtaining the volume values should be well calculated such as feed, cut depth, cutting speed and part diameter. The latter should be resized when the diameters of the part are very close to the depth of cut (small diameters), to avoid very large errors on the material removal rate with a variation of 4 to 25% [2].

One of the initial assumptions of machining is that the insert must have a higher hardness than the material that is machined. However, in general, the greater its hardness, the more brittle the material turns to [3].

In the turning of hardened materials operation, due to the high hardness of the cBN, the monitoring of the wear is a fundamental procedure to avoid chipping and breaking of the inserts [3].

Previous work has already indicated the possibility of the use of cBN inserts in the machining of hardened materials and in facing operation, even during the occurrence of interrupted cutting. In the work of Oliveira et al., (2009) [4] the interruptions generated by the geometry of the test specimens promoted excitations in the cut around 184 Hz and more recently, Godoy and Diniz (2011) [5], again turning hardened steels with interruptions promoted excitations at the tip of the tool. The results of this work prove that the cBN insert also resists to higher frequency excitations, as is the case of boring bar operations [3].

2. MATERIALS AND METHODS

All the internal turning experiments of this work were performed using a CNC lathe with 20 CV of power in the main motor and maximum spindle rotation of 4,500 rpm. One 16 mm diameter boring bar of high hardenability ANSI 4140 steel (ISO code A16R SCLCR 09-R) were chosen.

As for the tool insert, an adequate insert for finishing operations on smooth surfaces of hardened steels was chosen. It was composed of CBN (50% wt) and a ceramic phase of TiCN and Al₂O₃; it is ISO code is CCGW09T308S01020F 7015 (class ISO H10). The advantage of the chosen tool insert, when compared to others with a greater CBN content, is its chemical stability in relation to iron. Besides, its toughness is enough to preserve its cutting edge, even though it is reduced when compared to other inserts with a greater CBN content.

The 4340 steel used in the fabrication of the test specimens is a widely employed material in the metal mechanical industry. It presents high hardenability, bad weldability and reasonable machinability, as well as a good resistance to torsion and fatigue – its hardness after quenching varies from 54 to 59 HRC.

The cutting conditions and the machine setup (tool overhang) were tested in two distinct machining tests. The first measured the tool lifespan, where a maximum flank wear (VB_{max}) of 0.2 mm according to ISO 3685 [6] for operations without coolant was considered as the end of tool life criterion. The second measured the radial and tangential components of tool acceleration during the cutting process, in the beginning and in the end of tool life.

For the tool life tests, we defined a complete experimental factorial matrix, composed of 2 factors in 2 levels of variation, resulting in 4 conditions. Each condition was replicated once and led to 8 tests. Thus, the 4 conditions were set below on *Table 1*.

Table 1
Cutting conditions for tool life test with an overhang of 70 mm

Condition	Feed rate [mm/rev]	Cutting speed [m/min]
C1	0.08	360
C2	0.08	300
C3	0.06	300
C4	0.06	360

3. RESULTS

The *Table 2* reports the cutting conditions tested until the end of life, evidencing the results of metal removal rate, surface finish (R_a and R_z) and flank wear (VB_{max}). The results show that the tool at the end of life does not generate significant changes in the roughness of the part, but it generates transformations in the geometric profile of the tool, mainly in the rake plane of the insert, after the removal of a large volume of chips, limited by the flank wear values of the tool.

It is known that the end of tool life was reached when tool flank wear reached 0.2 mm (ISO 3685). The parameter of material removal rate allows a better comparison of the tool life than the time of cutting, especially in cases where there are variations of the cutting speed. It is possible to observe that the increase of the cutting speed causes a decrease in the tool life due to the higher cutting temperatures. The increase in feed rate permits an increase in life. This results carried out to check the significant contribution of each input factor (cutting speed and feed rate) showing the results for surface roughness. It can be observed that the feed rate has significant contribution whereas the cutting speed has less contribution and thus is of less importance.

Table 2
Machining parameters employed in the lifespan test of the CBN insert with constant depth of cut equal to $a_p = 0.1$ mm

Condition	v_c [m/min]	f [mm/rev]	End of tool life			
			Material removal rate Q [10^4 mm ³ /min]	R_a [μ m]	R_z [μ m]	VB_{max} [μ m]
C1	360	0.08	6.05	0.58	2.9	201.6
C2	300	0.08	7.2	0.83	3.4	234.6
C3	300	0.06	7.56	0.5	2.72	220.8
C4	360	0.06	6.48	0.78	3.12	212.5

This experimental study is also to analyse the impact of tool wear on the quality of surface generated in hard turning. *Table 2* shows the roughness parameters R_a , as a function of the flank wear land. The bar graph indicates a gradual increase in the surface roughness as the flank wear land of the tool increases. It can also be observed that, even at the point when the flank wear land was about 0.2 mm, the R_a the value of the surface roughness is less than 0.8 μ m for almost conditions. It is an example showing that the uniform flank wear up to 0.2 does not matter from the standpoint of surface finish. This shows that as a manufacturing process, hard turning can be employed for finish machining as an alternative to grinding. The deterioration in the surface roughness becomes very steep as the wear land crosses the critical value of 0.2 mm.

Figure 1 shows the evolution of tool flank wear during the lifespan test for the 4 tested conditions and an of $L/D = 4.4$. The gradual evolution of the maximum flank

wear (VB_{max}) indicates the absence of malfunctions leading to an abrupt change in the slope of the curve and to the sudden end of the life of the insert.

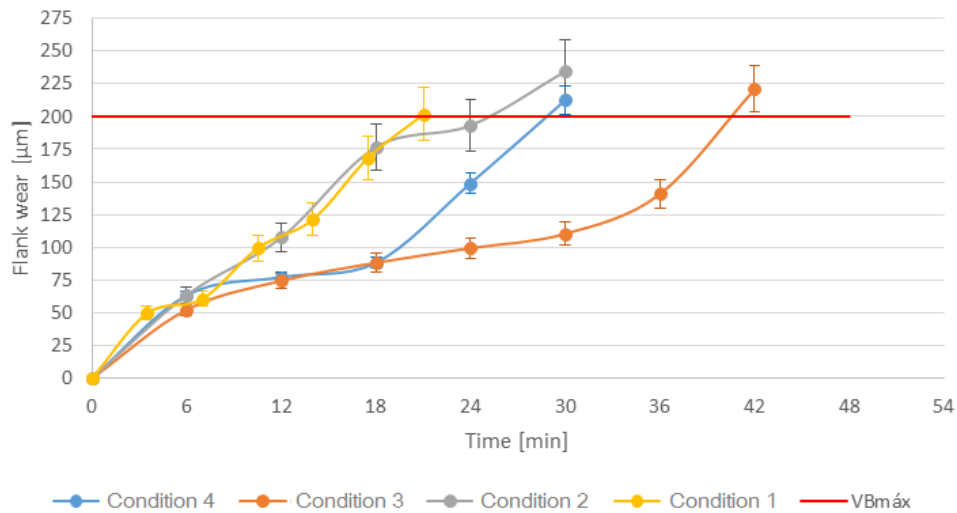


Figure 1
Evolution of tool wear in the 4 machining conditions (Table 1)
for an end of tool life criterion of $VB_{max} = 200 \mu m$

4. CONCLUSION

It can be concluded for internal turning operations of hardened steels, in conditions similar to those used here, that:

- In boring bar operation in hardened materials with continuous cutting, the flank wear of the tool insert is mainly caused by the abrasion of cBN particles originated from it.
- Even at the point when the flank wear land was about 0.2 mm, the Ra the value of the surface roughness is less than $0.8 \mu m$ due to the stability of the cutting condition.

ACKNOWLEDGEMENT

The described article/presentation/study was carried out as part of the EFOP-3.6.1-16-2016-00011 *Younger and Renewing University – Innovative Knowledge City – institutional development of the University of Miskolc aiming at intelligent specialisation* project implemented in the framework of the Szechenyi 2020 program. The realization of this project is supported by the European Union, co-financed by the European Social Fund.

REFERENCES

- [1] Bhaskaran, J. (2011). *Process monitoring of hard turning using acoustic emission technique*. Doctoral Thesis, Faculty of Mechanical Engineering, Anna University, Chennai – 600 025.
- [2] Isakov, Edmund (2009). *Cutting Data for Turning of Steel*. New York, NY, 10018, Industrial Press, Inc., p.179, Table 4.2.
- [3] Suyama, Daniel Iwao. (2014). *Uma contribuição ao estudo do torneamento interno em aços endurecidos*. Doctoral Thesis, UNICAMP, Campinas, São Paulo, Brazil.
- [4] De Oliveira, Adilson José, Anselmo Eduardo Diniz, Ursolino, Davi Janini (2009). Hard turning in continuous and interrupted cut with PCBN and whisker-reinforced cutting tools. *Journal of Materials Processing Technology*, 209, 12, pp. 5262–5270.
- [5] De Godoy, Vitor Augusto A., Diniz, Anselmo Eduardo (2011). Turning of interrupted and continuous hardened steel surfaces using ceramic and CBN cutting tools. *Journal of Materials processing technology*, 211, 6, pp. 1014–1025.
- [6] ISO 3685. *Tool-life testing with single-point turning tools*.

INTRODUCTION OF ACTIVE AND PASSIVE CONTROL OPTIONS FOR HYDROSTATIC PRESSURE CHAMBERS

SÁNDOR GERGŐ TÓTH – GYÖRGY TAKÁCS

University of Miskolc, Department of Machine Tools
3515 Miskolc-Egyetemváros
toth.sandorgergo@uni-miskolc.hu

Abstract: One of the critical points in the design of hydrostatic bearings is the proper selection of the pressure control of the bearing recess, yet the design methods do not pay much attention to this. In addition to conventional solutions, the control of the pressure recesses can be accomplished by the use of volumetric and pressure-sensitive valves in the hydraulics to achieve greater bearing stiffness. A new way of regulating can also be the regulation of the recess with proportional valves.

Keywords: *hydrostatic bearings, recess pressure control, bearing stiffness*

1. INTRODUCTION

Hydrostatic bearings are a special type of fluid-lubricated bearings, where the fluid film layer separating the shaft and inner journal bearing surface and the supporting force is built in the pressure chambers supplied with an external power supply instead of a hydrodynamic force due to the wedge effect between the surfaces. Hydrostatic bearings therefore have much better starting conditions and static stiffness than hydrodynamic bearings, but their design is more complicated, because the pressure of the oil film in the pressure chambers has to be regulated.

The control of the pressure chambers is necessary because the centralized shaft deviates with a given eccentricity in the direction of the pressure chambers due to the load. Due to the bypass shaft pin, the gap size in the direction of eccentricity decreases, which causes a decrease in the volume flow of the pressure chambers, as a result of which the pressure in the pressure chambers increases. Due to the deflected axis, the gap size in the direction of eccentricity decreases, which causes a decrease in the volume flow of the pressure chambers, as a result of the pressure in the hydrostatic chambers increases. In contrast, in the pressure chambers from which the shaft moves, there is an increase in volume flow and a pressure drop. The resulting pressure difference is necessary to return the shaft to its centralized position close to the unloaded position [1], [2]. To ensure shaft aligning, the pressure ratio (β) between the supply pressure and the chamber pressure must be maintained independently of by means of a pressure control element. The control can be done with the help of conventional passive elements (capillary and permanent throttle element)

or with active valves (2-way flow control valves, pressure-sensitive valves, and proportional flow volume/directional valves) [3].

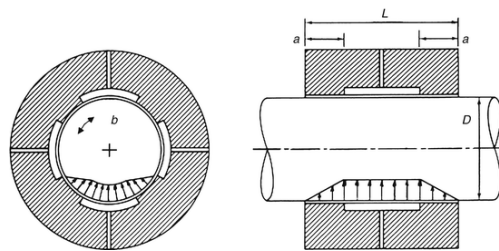


Figure 1

Unloaded pressure field distribution of the hydrostatic journal bearing [1]

2. CONVENTIONAL PRESSURE CHAMBER CONTROL METHODS

The simplest chamber control can be achieved with passive throttles, in which the fluid flow can be laminar or turbulent. Laminar control elements are mostly capillary tubes with a high L/D (tube length / inner diameter) ratio. The advantage of using a capillary tube is that the pressure drop is uniform, so that no heat loss due to a sudden pressure change occurs (however heat is generated from friction). Main drawback is that the control is dependent of the viscosity of the fluid.

Volume flow of oil in the capillary line [2]:

$$Q = \frac{(p_s - p_r) \pi d_k^4}{128 \nu l_k} \quad (1)$$

where:

- p_s – supply pressure;
- p_r – pressure chamber pressure;
- d_k – inner diameter of the capillary tube;
- l_k – length of the capillary tube;
- ν – kinematic viscosity of the film fluid.

It can be seen from *Equation (1)* that the inner diameter of the capillary tube can only be increased slightly because it can greatly increase the volume flow (in other words, the fluid demand), which causes an undesirable friction loss. A further disadvantage is that it can only be used at low speeds due to the size limitations of the installation, as the oil film flow must remain laminar, which is lower ($Re \sim 1000$) for fluids flowing between eccentric cylinders than for fluids flowing in a circular cross-section pipeline.

Turbulent, passive pressure chamber control is possible by incorporating a constant throttle. With a low L/D ratio, greater stiffness can be achieved than with capillary tubes, furthermore the flow is independent on the viscosity of the oil. The main drawback is the higher risk of clogging due to the narrow throttle cross section.

With the traditional control technique, the static bearing stiffness of hydrostatic bearings can be optimized for the size of the bearing gap and the pressure ratio. The highest bearing stiffness can be achieved in capillary control ($\beta = 0.5$), in throttle elements ($\beta = 0.67$) by setting the pressure ratio [3].

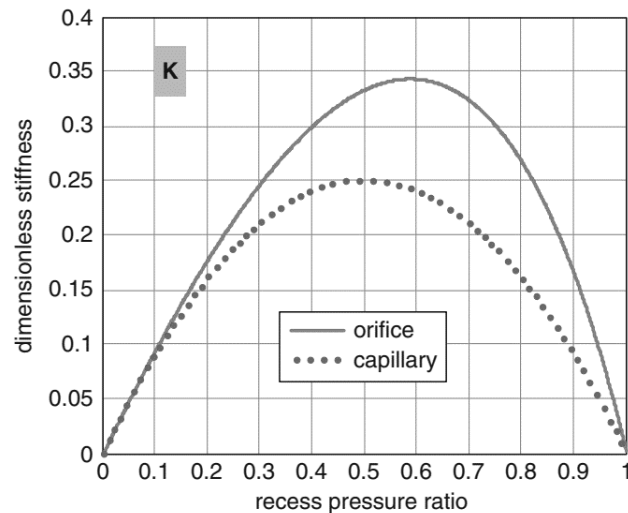


Figure 2

The dimensionless static stiffness of a hydrostatic bearing on a given pressure ratio at different passive flow control units [5]

3. PRESSURE CHAMBER CONTROL OPTIONS WITH ACTIVE VALVES

It can also be used to control pressure chambers with volume flow units, which are also often used in hydraulics, which can be realized by means of a valve or by means of constant flow pumps connected to pressure chambers separately, serving several circuits at the same time. By stabilizing the volume flow, the bearing stiffness and load capacity can be further improved compared to the passive control elements. In this case, the bearing stiffness and the maximum load can be set directly by controlling the supply pressure. For control, a pressure relief valve must be installed for each branch. In practical application, there is always a minimum pressure difference between the bearing pad pressure and the supply pressure due to flow losses, which is at least 2 bar [4].

To control the volume flow, the development of pressure-sensitive valves was also started. With these valves the gap size can be stabilized in a certain load force range and the “infinite bearing stiffness” can be achieved with them. Currently, two main control modes are known: slide-valve and diaphragm valve control. The design of a slide valve is almost identical to a pre-controlled two-way flow control valve, in which the chamber pressure is halved compared to the supply pressure due to the surface ratio of the valve plates. Infinite bearing stiffness is achieved with the valve, but it responds slowly to load changes.

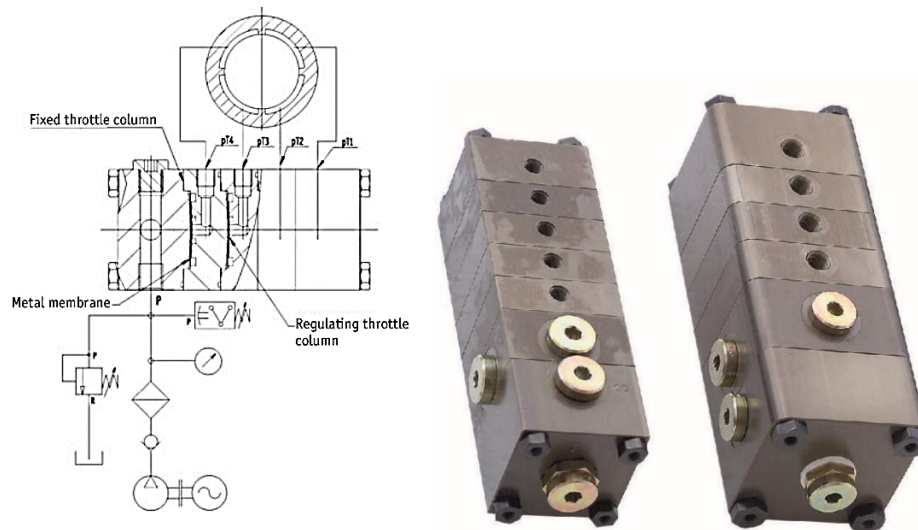


Figure 3
*Progressive diaphragm (PM) flow control valve block
 for hydrostatic pressure chamber control (Hyprostatik) [5]*

Currently, one of the best controls can be achieved by installing diaphragm valves. It controls the volume flow in the diaphragm valve under the influence of the load force. The progressive diaphragm (PM) valve manufactured by Hyprostatik has a fixed and adjustable control part [5]. The first regulator is turbulent throttle, allowing viscosity and temperature-independent control. The fluid flow is then controlled by the elastic deformation of the membrane plate, so the PM flow regulator operates without wear or hysteresis. Due to the low weight of the steel diaphragm disc and the high control forces, the PM flow controller quickly follows the pressure change. Thanks to the automation of today's machines, it is increasingly possible to have a more direct connection between electrical and hydraulic systems. Previously, only discrete-operated directional valves were available, which in turn only provided a switching function, so they are not suitable for steeples volume flow variation. Hydraulic proportional devices generate an output signal, pressure or volume flow proportional to the input signal, which depends on the operation. The regulation of hydrostatic bearings by proportional valves was addressed by Yang X. [6].

With the help of displacement sensors, the size of the bearing gap – i.e. the thickness of the oil film layer – can be measured in real time. By processing the signal in a PID controller, the electric current acts on the torque motor coil of the servo valve and moves the spindle so that the proportional valve opening can be controlled. By controlling proportional valves, a constant bearing gap size can be set, similar to a diaphragm valve.

4. SUMMARY

Hydrostatic bearings can be controlled by capillary tubes, throttles, flow control valves or pressure-sensitive valves. Capillary control can only be used at low speeds, because of the limited allowed Reynolds number the turbulent flow may appear earlier in the bearing than in the capillary tube.

With pressure-sensitive valves, a constant bearing clearance can be ensured, which provides greater and more stable stiffness compared to capillary control. Permanent bearing clearance can also be achieved by controlling proportional directional valves.

ACKNOWLEDGEMENT

The described article was carried out as part of the EFOP-3.6.1-16-00011 *Younger and Renewing University – Innovative Knowledge City – institutional development of the University of Miskolc aiming at intelligent specialisation* project implemented in the framework of the Szechenyi 2020 program.

REFERENCES

- [1] Wang, Q. Jane, Chung, Yip-Wah (2013). *Encyclopedia of Tribology*. Boston, Springer US, ISBN 9780387928975.
- [2] Bassani R., Piccigallo B. (1992). *Hydrostatic Lubrication*. Tribology Series, Volume 22, Amsterdam, Elsevier, ISBN 9780444884985.
- [3] Rowe, W. (1983). *Hydrostatic and Hybrid Bearing Design*. London/Boston, Butterworths, ISBN 9780408013246.
- [4] Perovic' B. (2012). *Hydrostatische Führungen und Lager*. Berlin, Springer, ISBN 9783642202971.
- [5] <https://hyprostatik.de/en/products-service/pm-flow-controller-for-guides/>
- [6] Yang X., Wang Y., Jiang G. (2015). Dynamic characteristics of hydrostatic active journal bearing of four oil recesses. *Tribol T.*, Vol. 58, pp. 7–17.

EXAMINATION OF MACHINE TOOL SLIDEWAY COMBINED WITH PRESSURE CHAMBERS

SÁNDOR GERGŐ TÓTH – GYÖRGY TAKÁCS

University of Miskolc, Department of Machine Tools
3515 Miskolc-Egyetemváros
toth.sandorgergo@uni-miskolc.hu

Abstract: This paper deals with the preliminary functional testing of a novel combined slideway type. In order to improve the accuracy of a portal-type milling machine to be designed as part of a departmental project, special unloaded guideway designs have been investigated, resulting in a slideway structure relieved with hydraulic pressure chambers. A measuring bench was set up to check the amount of the relief. Based on the primary measurements performed, it is proven, that the pressure chambers relieves the load by providing a suitable sliding surface.

Keywords: *hydraulic, slideways, machine tool, pressure chamber, load relief*

1. INTRODUCTION

The departmental consortium partner has repeatedly proposed several horizontal and vertical slideway designs in which the slideway surfaces is supplemented with hydraulic pressure chambers. The design, location and function of the hydraulic pressure chamber are different for each version. A common feature of the solutions is that the resulting gap oil is collected and drained within the pipeline structure. According to the consortium partner, during operation, a fluid flow is created in the narrow gap formed between the beam and the guide surface of the pressure chamber guide ring at the sealing surfaces defining the pressure chambers, the gap flow providing a constant gap size in a self-regulating manner. Because the beam moves on a lubricant film, there will be minimal feed force. The leak oil is collected by an outer ring and conducted through a manifold into the tank. A low (few bar), constant pressure in the chambers would be provided by a hydro-pneumatic unit.

This type of guideway is referred to in the literature as partially unloaded slideways [1]. A partially unloaded slideway is a construction in which a pressurized lubricant, such as air or lubricant fluid, is placed between the sliding surfaces to reduce the load on the sliding surface, thereby moving a heavy body smoothly with minimal friction loss. High-precision machining of parts is required to prevent air leakage and to avoid a drop in compressed air pressure. Furthermore, the surfaces of air-relieved slideways tend to float when the surface pressure is relieved. For this reason, oil-relieved slideways came to the fore in the early stages of development [2].

With the incompressible fluid, the lubrication of the sliding lines is as good as with the compressed air version, while the stiffness of the construction is much higher. The hydrostatic effect is much easier to obtain with oil, since the manufacturing accuracy of these slideways surfaces, does not have to be as strict as when compressed air is used. *Figure 1* represents a perspective view of an oil-lifted guideway. The pockets used to reduce the load are not simple pressure pockets, but hydrostatic chambers with a pressure-reducing function. At high speed feed motion, these hydrostatic pockets eliminate the phenomenon of floating due to hydrostatic action. In this way, it is possible to compensate for the excessive movement that occurs at high speed feeds, which is the biggest problem with partially floating guideways.

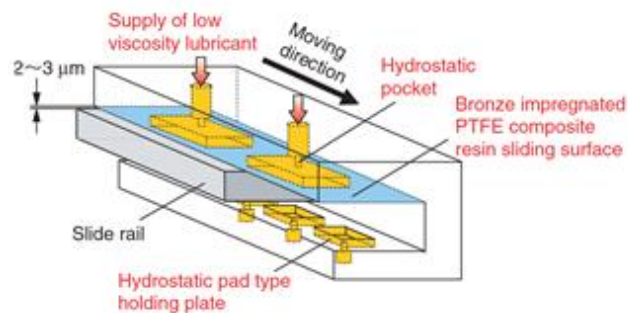


Figure 1
Operating principle of the oil-lifted guideway

2. SETTING UP THE MEASURING BENCH

To perform the measurements, an earlier device developed for testing rolling blocks was modified. With this device it was possible to inspect 8 rolling blocks at same time. Leaving the test frame, block clamping and loading system, the pressure chamber specimens can be inspected to determine the pressure at which the force required to move the beam decreases under a pre-set load, and during measurements the operation of the oil drainage channels can be checked. The specimens are located on the polished side surfaces of a central rectangular beam with 2-2 blocks on each conductive surface (*Figure 2*). The 4-4 specimens were mounted on a motherboard in a “V” shape (negative prism shape). One base plate is attached to the stand, the other is placed on a beam placed on the lower base. The motherboards are surrounded by load rings.

Test specimens are supplied from a common hydraulic circuit, so that the same pressure will be applied in each pressure chamber and the same hydraulic force will be generated in each test specimen. The leakage fluid collecting channels are discharged separately for each block, so it is easy to observe if a leakage starts in one of the slippers. The force exerted on the slippers facing each other in pairs can be

created by tensioning a steel ring supported in the nest at the load center of the specimens.

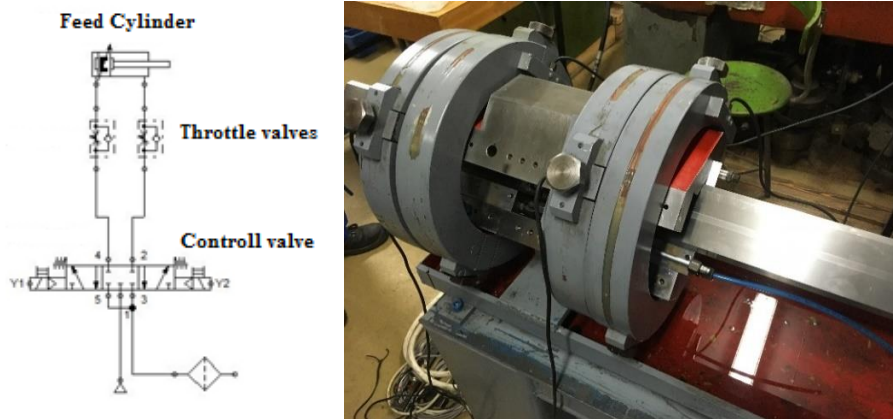


Figure 2
*Hydraulic circuit of the test equipment feed cylinder
and the assembled test equipment*

3. RESULTS OF THE MEASUREMENTS

The purpose of the test is to determine, if the load on the pressure chamber specimens gradually increases, at what chamber pressure is there a more significant decrease in the force in the feed force. The chamber pressure of the feed cylinder can be read with pressure transmitters connected to the hydraulic connections of the cylinder.

The load can be adjusted by the tightening torque of the support bolts of the load ring enclosing the specimens carrying the specimens, from which the magnitude of the preload can be recalculated by knowing the thread diameter and pitch of the support bolt. Expectable gap flow effects can also be evaluated later. But certain principles can be taken into consideration.

During the measurements, the unloaded state and the behavior under three tightening torques (5 Nm, 10 Nm and 15 Nm) were examined for the structure. As the chamber pressure was increased, it was visually inspected for oil leaks in the outlet pipes of the pressure chambers and, if so, to what extent. As a result of the increase in pressure, the load rings suffer an elastic deformation, which results in an increase in the slideway gap and thus in the start-up of the leakage oil. This leakage oil appears on the oil drain pipes as the pressure increases.

At chamber pressures of 0 and 5 bar, the starting pressure was not measured because both the cylinder and the line unit receiving element were significantly deformed even at a pressure of 20 bar. There was a risk of permanent damage to the equipment with higher forces. When checking the tightness of the slipper body sliding surface, it was observed that as long as there was a maximum dripping on the

leaking line, there was no dripping on the side surface of the specimens, but when there is oil leakage on the leaking line, oil leakage also appears on the side surface.

Table 1
Measurement results and observations at a tightening torque of 15 Nm
(4,9 kN preload)

Chamber pressure [bar]	Cylinder pressure [bar]				Leakage	Observation
	+ direction		- direction			
	p ₁	p ₂	p ₁	p ₂		
0	20.2	2	2.5	19.7	Leakage did not appear.	Beam did not move.
5	20.2	2	2.5	19.7		
10	20.2	2	2.5	19.7		
15	20.2	2	2.5	19.7		
20	2.5	3.5	3.5	6.5	Before starting, some leakage outputs dripped. After starting, the drip was more intense, some outputs also showed flow on the cylinder side.	It started with stick-slip and then moved smoothly.
25	2.2	2.2	3.5	6	Intense flow on the cylinder side and a output on the other side, the rest were dripping.	Moved smoothly.

4. SUMMARY

Partially unloaded combined guideway system was tested, with the help of a slideway structure unloaded with hydraulic pressure chambers. A measuring bench was set up to check the magnitude of the unloading. Based on the measurements, it can be seen that the counterforce can be created with hydraulic pressure chambers, which is suitable for relieving the friction guideway.

The system is very sensitive to the parallelism errors of the conductive surfaces, a few μm error already results in the appearance of the oil leakage. If the elastic deformation of the machine causes a parallelism error of a few μm , it will result in the early appearance of the oil leakage.

The amount of leakage oil increases with increasing chamber pressure. This is partly due to the fact that the higher pressure occurs a larger volume flow through

the existing gap, and partly due to the higher loading force owing to the higher pressure, the load rings are more deformed and therefore the size of the gap increases. It takes significantly more force to start the carriage than to keep it moving.

ACKNOWLEDGEMENT

The described article was carried out as part of the EFOP-3.6.1-16-00011 *Younger and Renewing University – Innovative Knowledge City – institutional development of the University of Miskolc aiming at intelligent specialisation* project implemented in the framework of the Szechenyi 2020 program.

REFERENCES

- [1] Saito, T. (2006). Development of Machine Tool's Guideways-Dynamically pressurized, Statically Pressurized and Partially Floated Guideways. *JTEKT Engineering Journal*, No. 1001E, pp. 57–64.
- [2] Mehta, N. K. (1996). *Machine tool Design and Numerical Control*. 2nd edition, New Delhi, McGraw-Hill Publishing Company, pp. 220–221., ISBN 0074622 374.
- [3] Rowe, W. B. (2014). *Hydrostatic, Aerostatic, and Hybrid Bearing Design*. Oxford, Elsevier, ISBN 978012396994.
- [4] Bassani, R., Piccigallo, B. (1992). *Hydrostatic Lubrication*. Tribology Series 22, Amsterdam, Elsevier, ISBN 044488498.

A NEW METHOD FOR PRODUCTION DEVELOPMENT

**LAURA TRAUTMANN¹ – ATTILA PIROS² – JÁNOS PÉTER RÁDICS³ –
IVETT JAKAB⁴ – KATALIN BADA-KERTI⁵**

^{1,2,3}Department of Machine and Product Design
Faculty of Mechanical Engineering
Budapest University of Technology and Economics
Műegyetem rkp. 3., Budapest, H-1111, Hungary
e-mail: @gt3.bme.hu

^{4,5}Dep. of Grain and Industrial Plant Processing
Faculty of Food Science
Szent István University
Villányi street 29., Budapest, H-1118, Hungary
e-mail: @etk.szie.hu

Abstract: This paper introduces a new method for production development with the usage of process observation, fuzzy logic, and sensoring. In collaboration with experts in the field of food science, design, a program was developed that can simulate the behaviour of a semi-finished product during preparation. A factory producing bakery products applied sensors in order to gain real-time data that can be integrated into the program. Because of all the uncertainty of a preparation process, the optimal baking temperature and time are different in each package of the product. With the previously mentioned program, it is possible to provide the optimal values for each package.

Keywords: *Bakery product, production development, programming, fuzzy logic*

1. INTRODUCTION

This article is dealing with production development in the field of semi-finished bakery products. Several factors influence the dough quality. Bakeries sometimes achieve poor dough quality during mixing, which can be caused by biological (yeast), chemical (enzyme reactions, oxidation/reduction) and physical (water movement) process as well [1].

Because of the possibility of the variable semi-finished product, the goal of the system developed by us is to equalize the mistakes by the optimal baking temperature and time that will set by the user. If the production lines are fully examined by sensors, the exact values are known, and it is possible to conclude to other values. Similarly to an equation, if we know the perfect cake shape, taste, etc. as an output, and the input parameters (temperature, time and mass data of the ingredients) except for the final baking time and temperature, the missing parameters can be defined. For the background operation, a fuzzy logic-based system was developed that

contains the rules between the input and output parameters. Fuzzy logic is one of the Artificial Intelligence (AI) tools [2]. By applying AI to model the process and develop the system is nowadays a viable solution in the baking sector [1] [3].

In this study, the goal is to create the best-prepared products with the help of sensors and mathematical programming. The hypothesis states that it is possible to model the behaviour of the preparation process with a mathematical method that could provide the required data – for the finishing phase – for end-users. With this data – optimal beaking temperature and time – the consumer is able to finish his product in the best way.

2. MATERIAL AND METHOD

During the test, products with different parameters were baked, and later the participants were rating the products in five categories (Shape, Shell, Inner structure, Smell, Taste) from 0–5, where zero meant “not appropriate at all”, and five was considered “excellent”. Some of the baked cakes (scones) are shown in *Figure 1*. These had to be evaluated by the participants.

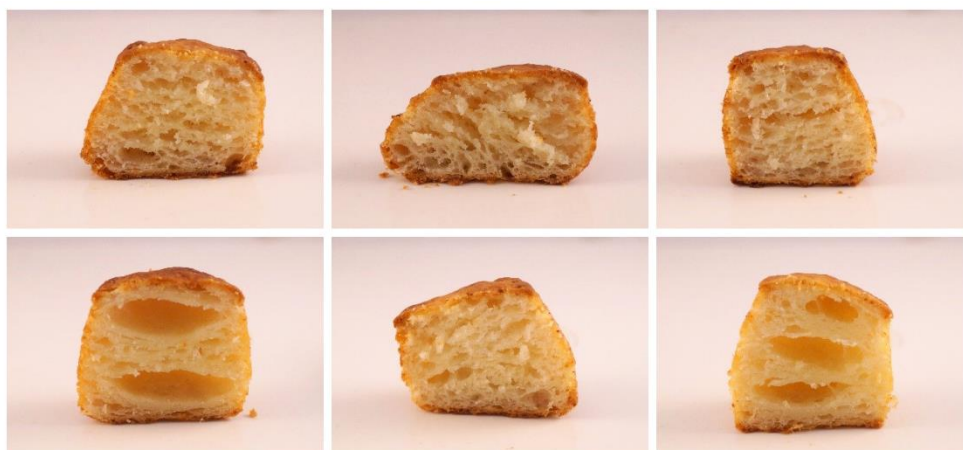


Figure 1
Different baked cakes

In total, 20 participants contributed to the examination as reviewers: 16 women, 4 men. The average age is 27.6 years old. From the members, 15% is a smoker, 85% is a non-smoker. The highest education level for 60% of the people is graduation, 30% have finished a university, and 10% have a Ph.D. degree. 65% of the participants are live in the countryside, 35% of them in the capital.

The program’s validation happened by the valuation of test bakings results, which is presented in the “Results” section. With this test, it can be proved that the result of the baked product is predictable according to the input parameters (such as the temperature of the commodity, the mass of the product in different stages, and so on).

Figure 2 shows the detailed workflow of this research. This article is mainly dealing with the 1 and 2 tasks of the workflow. The 3 and 4 parts will be introduced in detail in the near future.

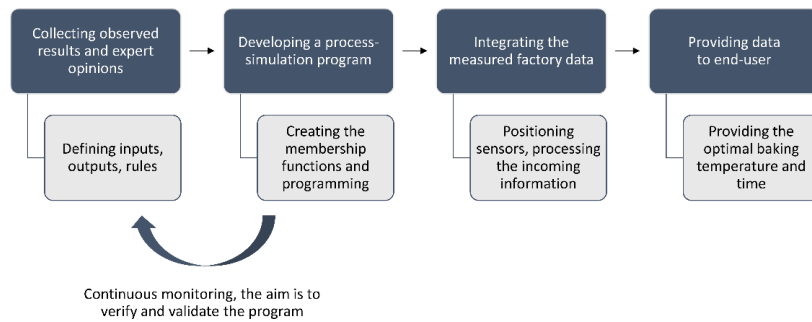


Figure 2

The workflow of the new method for production development

1. Collecting observed results and expert options:
Continuous data gaining process was applied while the experts provide information about the input and output parameters, and also about the rules that define the effect of inputs or combination of inputs on the outputs.
2. Developing a process-simulation program:
In the previous phases of this project, considerable mathematical methods were examined; for instance, neural network, genetic algorithm, and fuzzy logic. It turned out that fuzzy logic is the most suitable method for this task [4]. We used Matlab software in order to develop a fuzzy system.
3. Integrating the measured factory data:
In collaboration, a semi-finished bakery product factory has applied sensors to all the important states of the production line. (For example to the storage area as visible on Figure 3.) The sensors are sending measured values that could be integrated into the program as inputs. Since the rules are already set, the software can automatically provide the required data regarding the baking temperature and time.
4. Providing data to end-user:
The consumer will get this information on the package of the product.

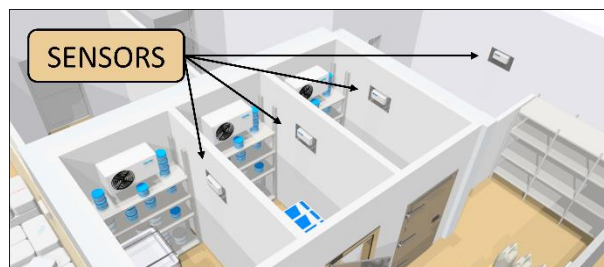


Figure 3

Model of a storage part with sensors

The input parameters are all of those parameters that have an impact on the quality of the final product. All parameters can have low, medium, and high values, that were defined according to measurements in the factory and also by the opinion of experts. The input parameters were already published in a paper by the authors [4]. Defining the output values is a much more complicated task because there is no exact data that can help. Since in “scoring sensory judgment and rating” [5] the researchers use five groups: Shape, Shell, Inner structure, Smell, Taste, we distinguished these categories as well. Since the evaluation of these categories ranges from 0–5 during the study the same ranking was also applied in the mathematical model, as shown in *Table 1*.

Table 1
Output data

	Parameters on 0–5 scale		
Shape	0–1 Flat	3–4 Deformed	5 Correct
Shell	0–1 Burned / Raw	2–3 Vesicular	4–5 Correct
Inner structure	0–1 Hollowed / Solid	2–3 Friable	4–5 Correct
Smell	0–1 Not appropriate	4–5 Correct	
Taste	0–1 Raw / Foreign taste / Salty	4–5 Correct	

The membership functions were created by *Table 1*. As an example of that, *Figure 4*. presents the membership functions of Shape, where the blue function represents the parameter of flat, red is the deformed and yellow represents the correct value.

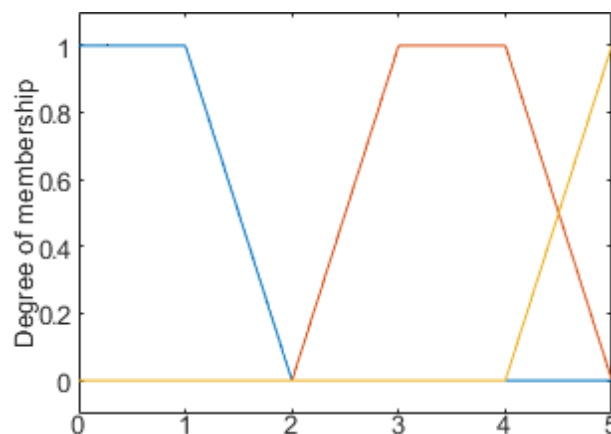


Figure 4
Membership functions of Shape

3. RESULTS

The validation of the program happened by the valuation of test bakings results. The following input parameters were defined as variables, while the others were fixed in the measurement:

- Rising Temperature [°C]
- Time of Rising [min]
- Baking temperature [°C]
- Baking time [min]

Table 2
Introduction of one of the test results

Shape					Shell					Inner structure					Smell					Taste					Cumulative value	Evaluation							
0	1	2	3	4	5	0	1	2	3	4	5	0	1	2	3	4	5	0	1	2	3	4	5	0	1	2	3	4	5	0–20	*		
					15						15	1					6	8							15						15	18.64	Excellent

Table 2 shows the table that helped to collect the data, and there is an example as well. At this specific example, the following variable inputs were used:

- Rising Temperature 40 [°C]
- Time of Rising 20 [min]
- Baking temperature 215 [°C]
- Baking time 6 [min]

During the testing procedure, the following weighting factors were applied. These factors were defined by the expert of this project.

- Shape 0.6
- Shell 0.6
- Inner structure 1.2
- Smell 0.6
- Taste 1.0

The calculation procedure:

1. A given score multiplied by the corresponding number of pieces.
2. E.g., at Inner structure:

$$0 \cdot 1 + 3 \cdot 6 + 5 \cdot 8 \quad (1)$$

3. A given category multiplied by a weighting factor. E.g., at Inner structure:

$$(0 \cdot 1 + 3 \cdot 6 + 5 \cdot 8) \cdot 1.2 \quad (2)$$

4. Sum up of the numbers above.
5. Divide by the number of samples (here 15) due to averaging.

The number in the cumulative value column is used to compare the results of the mathematical model, where we also weighted the values with the same weighting factors.

The evaluation section used the following states. (*Table 2* * sign)

- 0–11 Not appropriate at all
- 11–13 Not appropriate
- 13–15 Medium
- 15–18 Good
- 18–20 Excellent

The mathematical model was built up with the input parameters, with the output parameters (*Table 1*) and with the rules that define the behaviour of the product in different levels of the preparation process. During the validation process, the mathematical model and the actual test had the same input parameters, and if the cumulative values were mainly close, we could say that our hypothesis is correct.

In total, 16 input parameters (12 fixes and 4 variable), 5 output parameters, and 34 rules were defined in this experiment. In the baking process, 15 cakes were baked at a time, all in all on 13 occasions. The cakes were rated according to their shape, smell, inner structure, smell and taste. The test results were compared to the Matlab model, that showed the same group (not appropriate at all, not appropriate, medium, good, perfect) in all cases. (*Table 3*)

Table 3
Comparison of Experiment and Matlab results

Rising Temp. [°C]	Time of Rising [min]	Baking temp. [°C]	Baking time [min]	Evaluation EXPERIMENT	Evaluation MATLAB
40	20	200	5	Excellent	Excellent
40	20	200	7	Excellent	Excellent
40	20	230	5	Good	Good
40	20	230	7	Good	Good
40	20	180	2	Good	Good
40	20	180	12	Good	Good
40	20	250	2	Good	Good
40	20	250	12	Not appropriate	Not appropriate
40	20	215	6	Excellent	Excellent
20	5	215	6	Medium	Medium
20	35	215	6	Good	Good
50	5	215	6	Excellent	Excellent
50	35	215	6	Excellent	Excellent

It means that a fuzzy system could estimate the output of the baking process, that saves a lot of time and resources.

4. CONCLUSIONS AND FURTHER RESEARCH

The goal of this research was to create a fuzzy logic based Matlab model that can simulate a baking process of cakes. In the first step, we gained data from experts in order to define the input, output parameters, and the rules between them. With the first test round, the model resulted in very near values, and all of the evaluation groups were the same. The results of this research prove that the fuzzy system could estimate the baking process's output, which means it could replace tests in different situations. It is easily can be adapted to other environments by change the inputs and outputs parameters.

In the near future, information about the factory process will be collected. These data will be integrated into the model, that is why it will be possible to estimate the semi-finish product's optimal baking time and temperature, that will be placed on the package by label, as shown in Figure 5. This information will automatically be updated based on the collected sensor information analyzed by the fuzzy system.



Figure 5
Model of a product package

ACKNOWLEDGMENT

The research reported in this paper was supported by the National Research, Development and Innovation Fund (2020-4.1.1.-TKP2020), Thematic Excellence Program.

Project no. 2017-1.3.1-VKE-2017-00018 has been implemented with the support provided from the National Research, Development and Innovation Fund of Hungary, financed under the VKE funding scheme.

Moreover, authors would like to express their gratitude to Hanieh Amani for the photographs of pastries.

REFERENCES

- [1] Tucker, G., Adams, M. (2020). *Intelligent dough mixing using AI*. UK, Campden BRI, <https://www.campdenbri.co.uk/blogs/intelligent-dough-mixing.php>.
- [2] Klement, E. P., Slany, W. (1993). *Fuzzy Logic in Artificial Intelligence*. Berlin–Heidelberg, Springer-Verlag.
- [3] Müller, R., Spielvogel, M., Xu, X. (2019). *Semi-Supervised Labeling of Data with Varying Distributions*. Technische Universität München.
- [4] Trautmann, L., Piros, A., Rádics, J. P., Badak-Kerti, K., Berényi, R., Héber, G. (2019). Mathematical Background of the Development of Bakery Product Production. *GÉP*, Vol. 70, No. 4, pp. 57–60.
- [5] Lásztity, R., Törley, D. (1987). *Alkalmazott élelmiszer-analítika II*. Budapest, Mezőgazdasági Könyvkiadó Vállalat.

REVIEWING COMMITTEE

- B. BOLLÓ
Department of Fluid and Heat Engineering
Institute of Energy Engineering and Chemical
Machinery
H-3515 Miskolc-Egyetemváros, Hungary
aramzb@uni-miskolc.hu
- L. CZÉGÉ
Department of Mechanical Engineering
Faculty of Engineering
University of Debrecen
H-4028 Ótemető street 2–4, Debrecen
czege.levente@eng.unideb.hu
- CS. DÖMÖTÖR
Institute of Machine and Product Design
University of Miskolc
H-3515 Miskolc-Egyetemváros, Hungary
machdcs@uni-miskolc.hu
- ZS. FÜLÖP
Institute of Machine Tools and Mechatronics
University of Miskolc
H-3515 Miskolc-Egyetemváros, Hungary
fulop.zsombor@uni-miskolc.hu
- GY. HEGEDŰS
Institute of Machine Tools and Mechatronics
University of Miskolc
H-3515 Miskolc-Egyetemváros, Hungary
hegedus.gyorgy@uni-miskolc.hu
- D. KISS
Institute of Machine Tools and Mechatronics
University of Miskolc
H-3515 Miskolc-Egyetemváros, Hungary
kiss.daniel@uni-miskolc.hu
- T. MANKOVITS
Department of Mechanical Engineering
Faculty of Engineering
University of Debrecen
H-4028 Ótemető street 2–4, Debrecen
tamas.mankovits@eng.unideb.hu
- T. POÓS
Department of Building Services and Process
Engineering
Budapest University of Technology and Economics
H-1111 Budapest, Bertalan Lajos str. 4–6. Build. D. 110.
poos@mail.bme.hu

G. PSZOTA	Institute of Physics University of Miskolc H-3515 Miskolc-Egyetemváros, Hungary pszotag@gmail.com
L. RÓNAI	Institute of Machine Tools and Mechatronics University of Miskolc H-3515 Miskolc-Egyetemváros, Hungary ronai.laszlo@uni-miskolc.hu
F. SARKA	Institute of Machine and Product Design University of Miskolc H-3515 Miskolc-Egyetemváros, Hungary machsf@uni-miskolc.hu
T. SZABÓ	Institute of Machine Tools and Mechatronics University of Miskolc H-3515 Miskolc-Egyetemváros, Hungary mrbszabo@uni-miskolc.hu
A. SZILÁGYI	Institute of Machine Tools and Mechatronics University of Miskolc H-3515 Miskolc-Egyetemváros, Hungary szilagyi.attila@uni-miskolc.hu
Á. TAKÁCS	Institute of Machine and Product Design University of Miskolc H-3515 Miskolc-Egyetemváros, Hungary takacs.agnes@uni-miskolc.hu
GY. TAKÁCS	Institute of Machine Tools and Mechatronics University of Miskolc H-3515 Miskolc-Egyetemváros, Hungary takacs.gyorgy@uni-miskolc.hu
D. TÓTH	Institute of Machine Tools and Mechatronics University of Miskolc H-3515 Miskolc-Egyetemváros, Hungary toth.daniel@uni-miskolc.hu
S. G. TÓTH	Institute of Machine Tools and Mechatronics University of Miskolc H-3515 Miskolc-Egyetemváros, Hungary toth.sandorgergo@uni-miskolc.hu
Á. TÖRÖK	KTI – Institute for Transport Sciences H-1119 Budapest, Than Karoly street 3–5, Hungary torok.adam@kti.hu

Responsible for the Publication: Prof. dr. Zita Horváth
Published by the Miskolc University Press under leadership of Attila Szendi
Responsible for duplication: Works manager: Erzsébet Pásztor
Editor: Dr. Ágnes Takács
Technical editor: Csilla Gramantik
Proofreader: Zoltán Juhász
Number of copies printed:
Put the Press in 2020
Number of permission: TNRT – 2020 – 225 – ME
HU ISSN 1785-6892 in print
HU ISSN 2064-7522 online